AD-A077 052 FLORIDA UNIV GAINESVILLE F/G 6/5
AN INVESTIGATION OF BONDING MECHANISMS AT THE INTERFACE OF A PR--ETC(U)
DEC 78 L L HENCH , R W PETTY , G PIOTROWSKI DAMD17-76-C-6033
UNCLASSIFIED NL

2 OF 3
AD
A077052

Figure 31 A higher magnification of Fig. 30 showing the periodontal membrane (PM) between the mineralized tissue (M) on the implant (I) on the right and alveolar bone (B) on the left. (100X).

Based on the results of the six month screening study a two year program using the 45S5 and 45S5F bioglass compositions was initiated and is in progress. Several of the implants fractured coronally producing an open wound in the oral cavity. Subsequently osseous tissue filled in over the remaining root portion of the implant and epithelial tissue overgrowth sealed the site. The resulting buried roots remained in place for a total implantation period of 2 years. Electron microprobe profiles across the bone - implant interface show a Si-rich layer 120 μm thick on the surface of the bulk glass and a Ca, P rich transition layer 70 μm thick between the Si-rich layer and bone (31).

When harvesting the single tooth bioglass implants the animal is anesthetized and a block section of the maxilla or mandible including the implanted tooth and adjacent natural teeth is removed without sacrificing the animal. The resulting defect produced in the anterior mandible or maxilla can be filled with an appropriately shaped bioglass implant. One 45S5 bioglass block implant has been in place for 6 years. Clinical examination reveals normal mucosa over the implant with no signs of gross inflammation. Radiographic evaluation after 4 years shown in Fig. 32 shows bone directly adjacent to the implant.

Smith has conducted a preliminary investigation to study the effect of orthodontic loading on the bond which develops between bioglass and bone (32). Aluminum oxide implants coated with 45S5 bioglass were placed bilaterally in the mandibular first molar region of rhesus monkeys. The implants were loaded by a lingual arch appliance delivering a continuous, lingually directed force which was varied from 425 to 925 grams for six and nine week loading periods.

Histological evaluation of the implant tissue interface revealed direct fusion of bone to the bioglass in five of the six implants. Interestingly it was noted that the areas of attachment were randomly located on both the buccal and lingual surfaces of the implants with no apparent response to the stress developed by the arch appliance (see Fig. 33). Figure 34 is a plot of the net change of interimplant or intermolar distance as a function of loading time. There is no change in the interimplant distance for the bioglass coated implants during the first six weeks when a force of 425 grams was applied (solid line). In contrast note the changes which occurred with tantalum implants (dashed line) and the intermolar distance of the maxillary 1st permanent molars (dotted line) under the same loading conditions. Increasing the force to 925 grams for three additional weeks produced a decrease of 0.3 mm in the interimplant distance.

The bioactive glass-ceramic material Ceravital developed by the Leitz Instrument Group has been implanted in the mandible and zygomatic arch of swine for implant periods of up to 1 year (11). Gross observation has shown bone growing up to and around the implants. Light microscopy has revealed bone containing healthy osteocytes in direct contact with the implants.

The Leitz group has conducted limited clinical trials using Ceravital for augmentation of the anterior region of the alveolar ridge (33). Clinical examination after six months revealed no apparent complications. Tooth root implants and ossicular chain replacements of Ceravital also have shown initial success.

Figure 32 X-radiograph of 45S5 bioglass implant in anterior region of mandible of a baboon after 4 years.

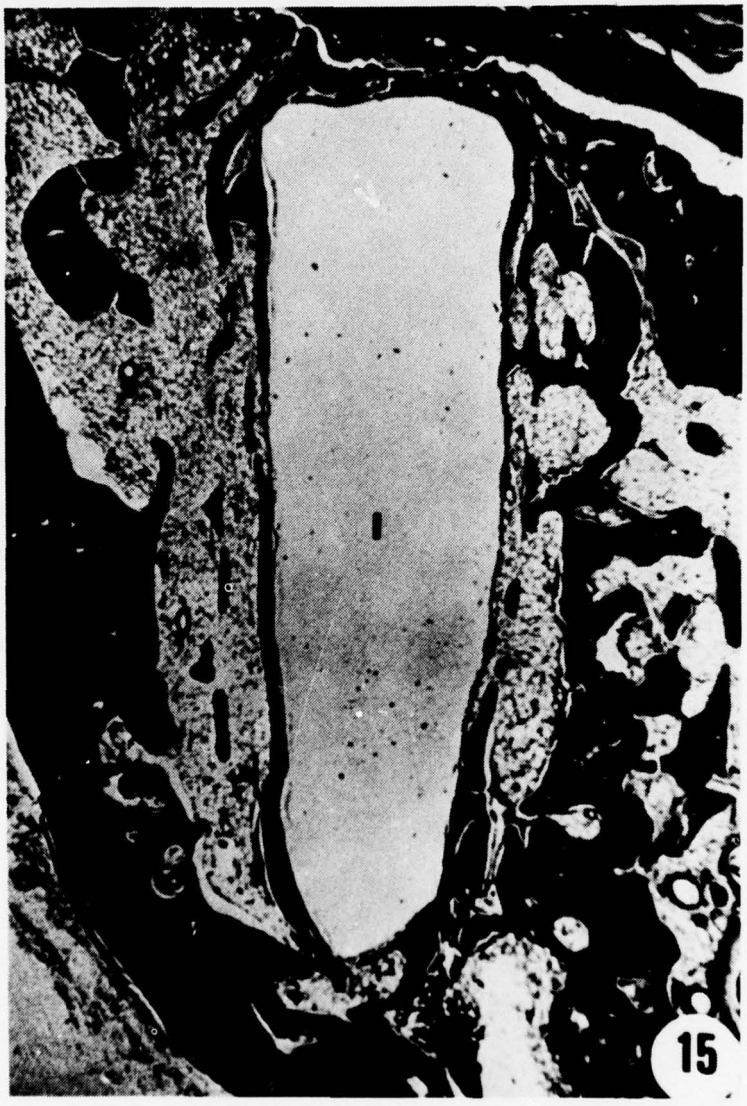

Figure 33 Light micrograph demonstrating bony approximation to bioglass coated alumina implant in monkey mandible. Implant was loaded by a lingual arch appliance for 5 weeks.

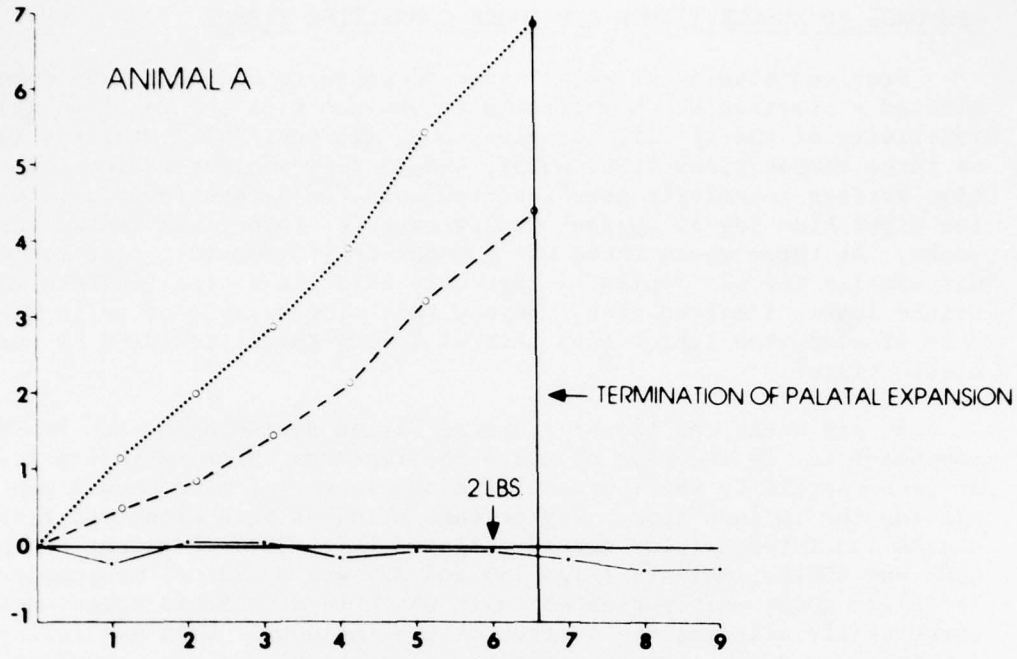

Figure 34 Net change from initial interimplant and intermolar distance in millimeters as a function of loading time (weeks).

MEDULLARY CANAL RESPONSE

While the reactions between bioglass and osseous tissue have been discussed extensively, little has been said concerning the interface between bioglass implants and bone marrow. A recent study conducted by Harrell et al. (32) in which bioglass specimens were placed in rat tibiae for time periods up to 28 months gave no indication of any adverse reactions between the bone marrow tissue and the implant surface. In fact examination revealed bone in contact with the implant surface extending across the entire width of the tibia which in effect isolated the implant from direct contact with the marrow tissue. Bioglass having less surface reactivity than the 45S5 composition will be more resistant to any surface modifications induced by marrow tissue and as long as they fall within the bone bonding boundary will maintain their ability to bond to osseous tissue.

Blencke et al. (34) have reported on the bioactive glass-ceramic material Ceravital which is similar in composition to the bioglass system. When Ceravital was implanted in the tibia or femur of several animal species (rats, rabbits, dogs) for time periods of up to 30 months no signs of destruction of the implant surface not in direct contact with osseous tissue were noted. Areas of the implants not in direct contact with bone were covered by a thin layer of connective tissue. Their experiments revealed no evidence of long term inflammation or the development of giant cells.

RESPONSE TO MUSCLE TENDON AND LOOSE CONNECTIVE TISSUE

Previous studies of soft tissue response to bioglass have demonstrated a reaction which varies in accordance with the in vitro surface reactivity of the specific bioglass compositions (35). Bioglass implants of three compositions 45S5, 45S5F, $45B_5S5$ representing medium low and high surface reactivity were inserted into the biceps femoris muscle of the right hind leg of Sprague Dawley rats for three, six and sixteen weeks. At three weeks there was a moderate inflammatory reaction which was similar for all implants. Directly adjacent to the implants was a single layer of macrophages. Beyond this single layer of cells was a zone of elongated fibroblasts several layers thick, followed by normal muscle tissue.

At six weeks the tissue response varied depending on the implant composition. In the case of the 45S5F implants which exhibited low surface reactivity there was still a single row of macrophages separating the implant from a region consisting of thin elongated fibroblasts and intercellular mature collagen (Fig. 35). Adjacent to the 45S5 and $45B_5S5$ implants (Figs. 36 and 37) was a zone of macrophages and large irregular multinucleated cells which in some areas appeared to be structurally altering the surface of the implants. This was followed by a multilayered zone with much larger fibroblasts and more abundant collagen than in the case of the 45S5F implants. These features are characteristic of a more severe foreign body response as might be expected from a more surface active material.

At 16 weeks all implants were surrounded by a synovial membrane. There was evidence of continued alteration of the implants by synovial cells and phagocytosis of the glass particles. The severity of the reaction again correlated with the relative surface reactivity of the three compositions.

Light microscopic examination of soft tissue removed from an area adjacent to a hip prosthesis coated with 45S5F bioglass after 14 months in a stumptailed monkey revealed regular connective tissue with an absence of acute inflammation (Fig. 38). The cellular morphology consisted of fibroblasts and mature fibrocytes enclosed in dense collagen (Figs. 39 and 40).

Figures 38-40 show that the cellular morphology of the tissue adjacent to the bioglass coated femoral head prosthesis is undisturbed after 14 months implantation. The cells are all typical of fibroblasts actively producing collagen or fibrocytes which are mature and enclosed in a very dense collagen matrix. In none of these sections of this tissue were there any inclusions within the cytoplasm containing inorganic debris suggesting deterioration of the bioglass coating or corrosion of the metal undercoating. In contrast, it has been shown (36) that uncoated stainless steel implants give rise to metallic debris particles enclosed in vacuoles in the cellular cytoplasm after the same time period in humans. Thus while bonding as occurs between bioglass and bone was not achieved between bioglass and soft tissues, gross deterioration of the tissues or destruction of the implant was not observed within the 14 month time period. These findings are not

Figure 35 Soft tissue interface of a 45S5F bioglass implant (C) after six weeks in rat muscle. Note the mononucleated cells (M) at the interface. Note also the fibroblasts (F) surrounding the implant. (1000X).

Figure 36 Soft tissue interface of a 45S5 bioglass implant after six weeks in rat muscle. Multinucleated cells (MP) are shown adjacent to pieces of the implant (C). (1240X).

Figure 37 Soft tissue interface of a $45B_5S5$ bioglass implant after six weeks in rat muscle. Multinucleated cells (MP) are adjacent to pieces of the implant (C). (1240X).

Figure 38 Light micrograph of area adjacent to 45SF-coated monkey hip prothesis after fourteen months. The tissue appears normal in all respects. (1,300X).

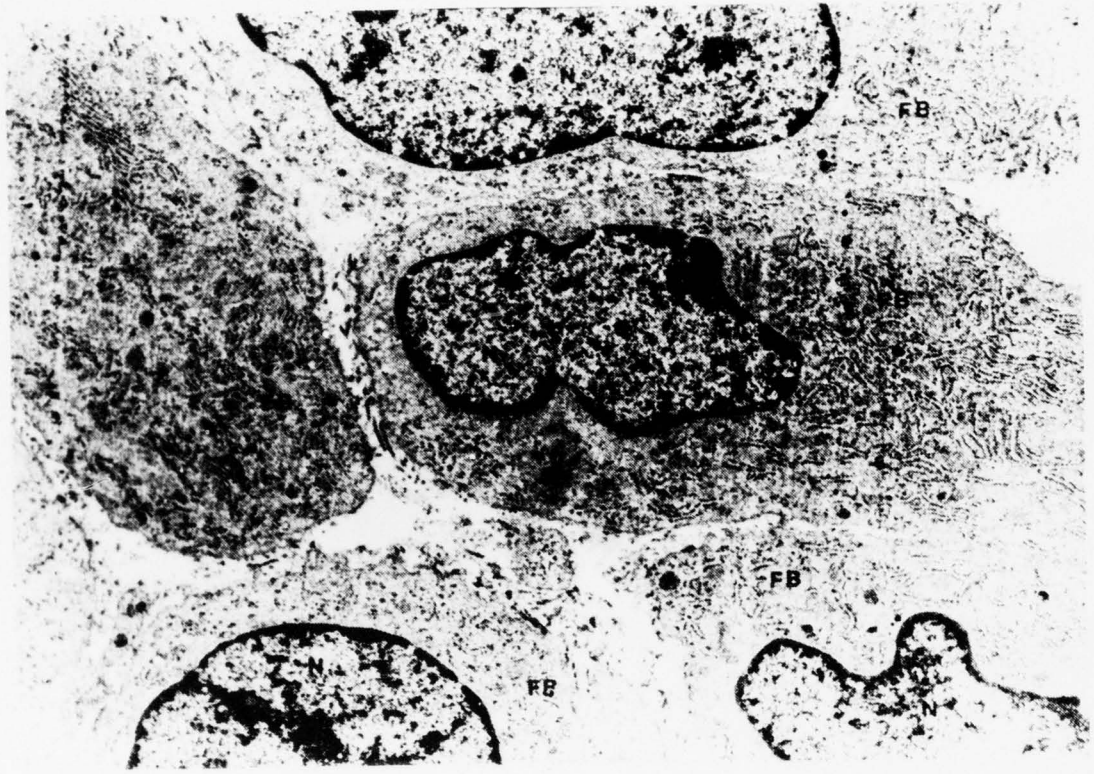

Figure 39 Representative field from tissue surrounding bioglass-coated implant seen in Fig. 38. Note the absence of cytoplasmic vacuoles containing inorganic material. (12,600X).

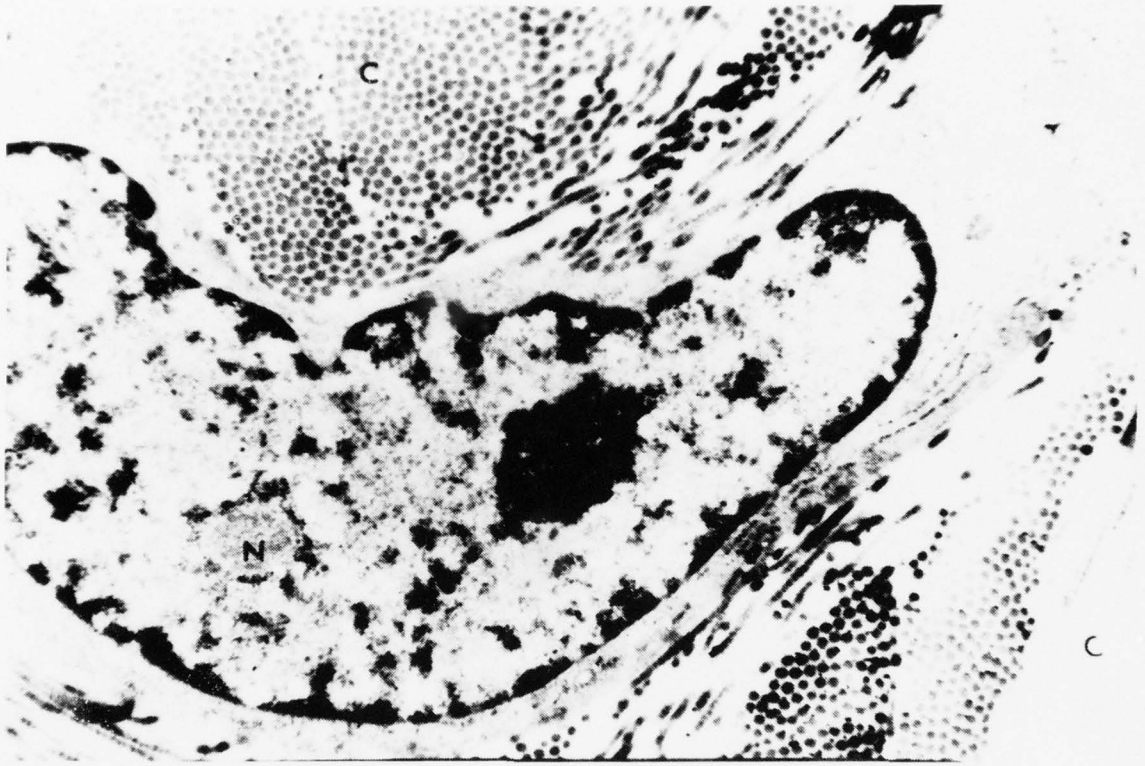

Figure 40 Transmission electron micrograph of soft tissue from around a bioglass coated monkey hip prosthesis, after fourteen months implantation. Mature fibrocyte with large nucleus and scant cytoplasm. Cell is completely surrounded by mature collagen fibers cut both longitudinally and in cross section. (21,700X).

surprising when one considers the totally different set of requirements of hard and soft tissue formation. To design a material system which in effect duplicates certain steps which occur during mineralization would predetermine that this same system would not bond to soft tissues where mineralization is not an integral part of the tissue formation process.

BONDING TO CELLS IN CULTURE

Recent experiments of Dr. Robert Grant and colleagues have shown that osteoblast-like cells derived from the rat calvaria can be grown on 45S5 and 42S4.6 bioglass substrates in culture (37). Growth rates are similar to growth rates on control dishes of inert plastics or inert glasses. However, the cells grown on the controlled surface reactive glasses that bond to bone in vivo also become rigidly attached to the bioglass interface in culture. The attachment appears to be a result of a mineralization process which incorporates the intercellular substances generated by the cells into the active surface as well as providing adhesion of the cell membrane itself as shown in the SEM of Fig. 41.

Figure 41 Scanning electron micrograph shows osteoblasts growing on 45S5 bioglass surface and forming collagen fibrils. (40,000X).

Details of the biological processes involved are still under intensive investigation but the interwoven morphology of the cellular and collagen incorporation within the interface is distinct in the SEM shown in Fig. 41. Transmission electron microscopy of such cell culture-bioglass interfaces show additional evidence of the strong adhesion at the cell membrane-bioglass interface (Fig. 42). EDXA evaluation of the interface derived from the cell cultures using the TEM shows that the bonding zone is a Ca-P rich layer, similar to that found previously for rat post *in vivo* interfaces using the same analytical scanning TEM system (38).

Extended use of the tissue culture models should make it possible to isolate the experimental variables necessary to answer many of the fundamental questions raised in the Introduction.

Figure 42 Transmission electron micrograph of bone cell-bioglass interface.

IN VITRO BONDING MODEL EXPERIMENTS AND SUMMARY OF BONDING MECHANISMS

Even simpler systems than tissue cultures provide evidence of the unique interfacial bonding features of this class of implant materials. In a clever experiment designed by Pantano (39) 45S5 bioglass polished discs were exposed to a weak (.04 g/ℓ) soluble collagen suspension at 37°C for 10 days. Figure 43 shows collagen fibers woven into and out of the hydroxyapatite surface which was formed on the bioglass substrate. Higher magnification SEM, EDXA analysis and electron diffraction shows that collagen is bonded to the surface by means of hydroxyapatite agglomerates comprised of crystallites in the range of 60 nm long.

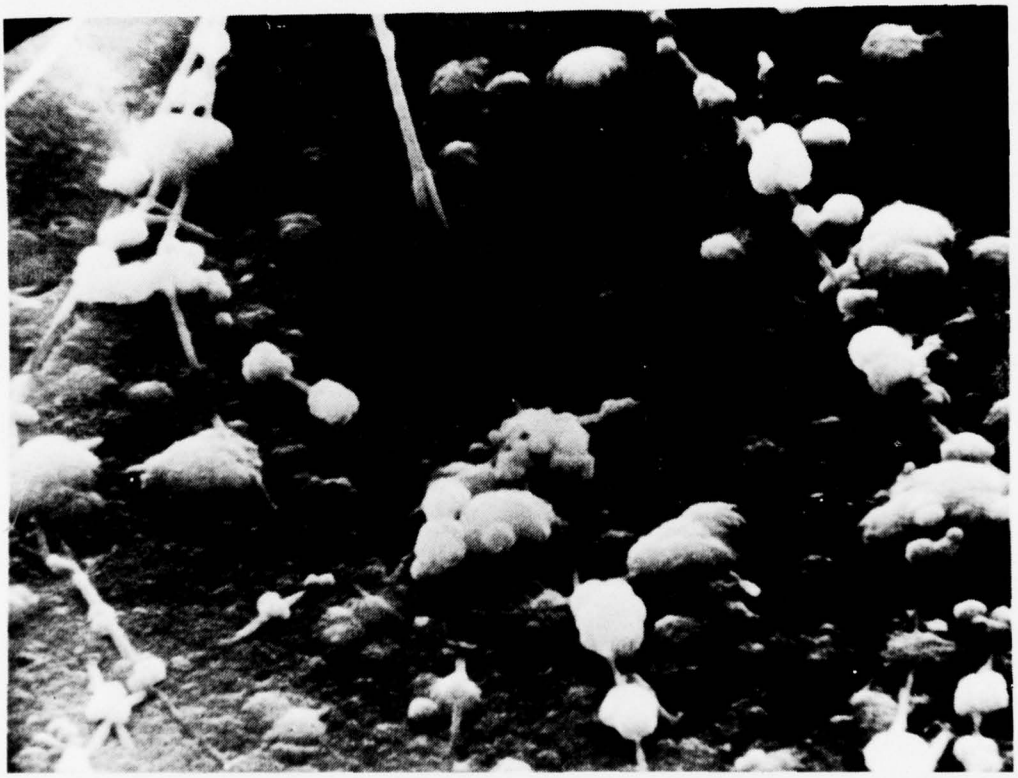

Figure 43 *In vitro* bonding of collagen fibers to bioglass surface.

Of equal importance was the finding that additions of small concentrations of a mucopolyssacharide, (MPS) chrondrotin sulfate, greatly enhanced formation of a strongly adherent organic structure on the bioglass substrate. Figure 44 shows at the same magnification the surface morphology resulting when the collagen, at the same concentration as in Fig. 43, was added in the presence of the MPS. The mutual interaction of collagen-hydroxyapatite and MPS seems to create almost a trabeculated type of morphology even without the presence of cells. The

Figure 44 In vitro bonding of collagen fibers to bioglass surface in the presence of chrondrotin sulfate.

similarity between the bonded collagen-MPS structures of Figs. 43 and 44 to those derived from cell cultures and those obtained from early stage bonded implants in rat tibias are striking. These similarities suggest that the mechanism of stable bonding between bone and the implant surface is a consequence of ionic sites on collagen and MPS molecules becoming cross linked with the high surface area hydroxyapatite film that forms on the implant surface almost immediately after exposure to physiological solutions. The Ca and P from the solutions serve to increase the thickness of the inorganic film forming at the interface. As the Ca-P rich film grows it hydrates and crystallizes to form hydroxyapatite agglomerates incorporating the organic species into an intimately bonded contiguous structure that stabilizes eventually to a thickness of about 25-30 μm merging into the cellular structure of bone. The transition zone between nonliving and living matter thus provides the mechanical strength and the mechanical compliance needed for the interface to transfer stress effectively.

POTENTIAL APPLICATIONS

Bioglass ceramic materials show promise for application in the areas of medicine, dentistry, and veterinary medicine in which repair, modification, or reconstruction of the skeletal system or teeth is required. Based on the results of a two year study in baboons limited clinical trials in humans will soon be initiated with bioglass coated high strength alumina single tooth implants. This area will represent the first of many applications of bioglass bone bonding systems.

Applications still in the animal experiment stage include the stabilization of metallic prostheses coated with bioglass compositions, permanent stabilization of artificial limbs, mandibular ridge augmentation of edentulous patients, maxillo facial reconstruction of the middle ear and spinal fusion using bioglass blocks or screws for the elimination of chronic pain. Suffice it to say that any application requiring permanent and direct bonding of a material to hard tissue in the body would represent a potential application for the bioglass system.

REFERENCES

1. Hench, L.L., Splinter, R.J., Allen, W.C., and Greenlee, T.K. Jr., Bonding Mechanisms at the Interface of Ceramic Prosthetic Materials, J. Biomed. Mats. Res. Symp., No. 2, Interscience, 117, 1972.

2. Beckham, C.A., Greenlee, T.K. Jr., and Crebo, A.R. Jr., Bone Formation at a Ceramic Implant Interface, Calc. Tissue Res., 8, 165, 1971.

3. Hench, L.L. and Paschall, H.A., Direct Chemical Bonding Between Bioactive Glass-Ceramic Materials and Bone, J. Biomed. Mats. Res. Symp., No. 4, 25, 1973.

4. Griss, P., Greenspan, D.C., Heimke, G., Krempien, B., Buchinger, R., Hench, L.L., and Jentschura, G., Evaluation of a Bioglass-coated Al_2O_3 Total Hip Prosthesis in Sheep, J. Biomed. Mats. Res. Symp., No. 4, 10, 511, 1976.

5. Miller, G.J., Greenspan, D.C., Piotrowski, G., Hench, L.L., Mechanical Evaluation of Bone-bioglass Bonding, presented at Second Annual Meeting of the Society for Biomaterials, Philadelphia, Abstract No. 108, 1976, 81.

6. Hench, L.L, Paschall, H.A., Allen, W.C., and Piotrowski, G., Interfacial Behavior of Ceramic Implants, National Bureau of Standards Special Publication 415, May 1975, 19-35.

7. Piotrowski, G., Hench, L.L., Allen, W.C., and Miller, G.J., Mechanical Studies of the Bone-bioglass Interfacial Bond, J. Biomed. Mats. Res. Symp., 9, 47, 1975.

8. Stanley, H.R., Hench, L.L., Going, R., Bennett, C., Chellemi, S.J., King, C., Ingersoll, N., Ethridge, E. and Kreutziger, K., The Implantation of Natural Tooth from Bioglass in Baboons, Oral Surg., Oral Med., Oral Path., 42 No. 3, 339, 1976.

9. Hall, C.W., Mallow, W., Hose, F., Progress Toward a Permanent Skeletal Extension, presented at Second Annual Meeting, Society for Biomaterials, Philadelphia, Abstract No. 158, 1976, 106.

10. Strunz, V., Bunte, M., Stellmach, R., Gross, U.M., Kuhl, K., Bromer, H., and Deutscher, K., Bioaktive Glaskeramik als Implantatmaterial in der Kieferchirurgie, Dtsch. Zahnarztl. Z, 32, 287, 1977.

11. Strunz, V., Gross, U.M., Bromer, H., Deutscher, K., Glaskeramik fur Zahnartzliche and Kieferchirurgische Implantate, Report MT-0250, Ernst Leitz, Gmb H., Wetzler, Germany, January 1975 - July 1976.

12. Hench, L.L. and Ethridge, E.C., Biomaterials--the Interfacial Problem, in Advances in Biomedical Engineering, J.H.U. Brown and J.F. Dickson, Eds., Academic Press, New York, 1975, 36.

13. Lyman, D.J. and Seare, W.J. Jr., Biomedical Materials in Surgery, Am. Rev. Mat. Sci., 4, 415, 1974.

14. Graves, G.A., Hentrich, R.L., Stein, H.G., and Bajpai, P.K., Resorbable Ceramic Implants, J. Biomed. Mats. Res. Symp., 2, 91, 1971.

15. Driskel, T.D., O'Hara, M.J., Sheets, H.D. Jr., Greene, G.W. Jr., Natiella, J.R., and Armitage, J., Development of Ceramic and Ceramic Composite Devices for Maxillofacial Applications, J. Biomed. Mats. Res. Symp., 2, 345, 1972.

16. Andrade, J.D., Interfacial Phenomena and Biomaterials, Med. Instrum., 7, 110, 1973.

17. Hench, L.L., Ceramics, Glass and Composites in Medicine, Med. Instrum., No. 2, 1, 136, 1973.

18. Hench, L.L. and Paschall, H.A., Histo-chemical Responses at a Biomaterials Interface, J. Biomed. Mats. Res. Symp., No. 5 (Part 1), 49, 1974.

19. Greenspan, D.C. and Hench, L.L., Chemical and Mechanical Behavior of Bioglass Coated Alumina, J. Biomed. Mats. Res. Symp., Materials for Reconstructive Surgery, Clemson University, 1975.

20. Clark, A.E., Hench, L.L., and Paschall, H.A., The Influence of Surface Chemistry on Implant Interface Histology: A Theoretical Basis for Implant Materials Selection, J. Biomed. Mats. Res. Symp., No. 2, 10, 161, 1976.

21. Clark, A.E., Paschall, H.A., Hench, L.L., and Harrell, M.S., Compositional Analysis of the Formation of Bone-implant Bone, J. Biomed. Mats. Res. Symp., Materials for Reconstructive Surgery, Clemson University, 1975.

22. Clark, A.E., Paschall, H.A., Hench, L.L., and Harrell, M.S., Surface Chemical Analysis of Bioglass Orthopaedic Implants, J. Biomed. Mats Res. Symp., Materials for Reconstructive Surgery, Clemson University, 1975.

23. Hench, L.L., Development of a New Biomaterial-prosthetic Device, Orthopaedic Mechanics, D. Ghista, Ed., Academic Press, (1978).

24. Miller, G.J., Greenspan, D.C., Piotrowski, G., and Hench, L.L., Mechanical Evaluation of Bone-bioglass Bonding, in Report No. 7, An Investigation of Bonding Mechanisms at the Interface of a Prosthetic Material, U.S. Army Medical Research and Development Command, Contract No. DAMD 17-76-C-6033, 1976, 24.

25. Ferrari, M.G., Carr, T. and Piotrowski, G., Standard Method of Test for Ability of a Biomaterial to Bond to Bone, in Report No. 7, An Investigation of Bonding Mechanisms at the Interface of a Prosthetic Material, U.S. Army Medical Research and Development Command, Contract No. DAMD 17-76-C-6033, 1976, 39.

26. Nilles, J.L., Colletti, J.M. Jr., Wilson, C., Biomechanical Evaluation of Bone-porous Material Interfaces, J. Biomed. Mats. Res. Symp., 7, 231, 1973.

27. Nilles, J.L., Lapitsky, M., Biomechanical Investigations of Bone Porous Carbon and Porous Metal Interfaces, J. Biomed. Mats. Res. Symp., No. 4, 63, 1973.

28. Burstein, A.H., Frankel, V.H., A Standard Test for Laboratory Animal Bone, J. Biomech., 4, 155, 1971.

29. Piotrowski, G., Ferrari, M., and Petty, W., Bioglass Coated Monkey Hip Prostheses--A Progress Report, in Report No. 8, An Investigation of Bonding Mechanisms at the Interface of a Prosthetic Material, U.S. Army Medical Research and Development Command, Contract No. DAMD 17-76-C-6033, 1977, 78.

30. Hench, L.L., The Promise and Problems of Bioceramics in Total Joint Replacement, Proceedings of American Academy of Orthopedic Surgeons Workshop in Total Joint Replacement, Atlanta, Georgia, 1978.

31. Harrell, M.S., Keane, M.A., Acree, W.A., Bates, S.R., Clark, A.E., and Hench, L.L., Thickness of Bioglass Bonding Layers, 4th Annual Meeting of the Society for Biomaterials, San Antonio, Texas, Abstract No. 80, 1978, 111.

32. Smith, J.R., Bone Dynamics Associated with the Controlled Loading of Bioglass Coated Aluminum Oxide Endosteal Implants, Masters Thesis, University of Washington, 1977.

33. Strunz, V., Gross, U.M., Bromer, H., Deutscher, K., Glaskeramik fur Zahnartzliche and Kieferchirurgische Implantate, Report MT-0250, Ernst Leitz, Gmb H., Wetzler, Germany, January 1976 - August 1976.

34. Blencke, B.A., Bromer, H., and Deutscher, K.K., Compatibility and Long-term Stability of Glass-ceramic Implants, J. Biomed. Mat. Res. Symp., 12, 307, 1978.

35. Hench, L.L. and Paschall, H.A., Direct Chemical Bond of Bioactive Glass-ceramic Materials to Bone and Muscle, in Report No. 3, An Investigation of Bonding Mechanisms at the Interface of a Prosthetic Material, U.S. Army Research and Development Command, Contract No. DADA 17-70-L-0001, 1972.

36. Paschall, H.A., Rodebush, M., and McVey, J.T., A Comparison of Soft Tissue Reaction to a Bioglass Flame Spray Coated Hip Prosthesis and Metallic Screws, in Report No. 3, An Investigation of Bonding Mechanisms at the Interface of Prosthetic Materials, U.S. Army Medical Research and Development Command, Contract No. DADA 17-70-C-0001, 1972.

37. Grant, R., Pfizer, Inc. Research Laboratory, Maywood, New Jersey, To be published.

38. Hench, L.L., Johnson, P.F., Jenkins, E.J., Grant, R., Stevens, R., Transmission Electron Microscopy of Bone Cell Culture Samples on Bioglass, in Report No. 8, An Investigation of Bonding Mechanisms at the Interface of a Prosthetic Material, U.S. Army Medical Research and Development Command, Contract No. DAMD 17-76-C-6033, 1977, 90.

39. Pantano, C.G. and Hench, L.L., Surface reactions mediating the formation of a bone-bioglass bond, To be Published.

C. MECHANICAL TESTS OF THE BONE-BIOGLASS BOND

by

G. Piotrowski

INTRODUCTION

Bioglass has, over the years, been shown to adhere to living osseous tissue. The bond has been thoroughly documented and characterized by many in vivo and in vitro ultrastructural studies including scanning electron microscopy, transmission electron microscopy, Auger electron analysis, etc. Such techniques have provided much detail on the structure of the bond on a microscopic level and on the time-history of the bond formation. These studies, however, are not able to answer the question "How strong is the bond between bone and bioglass?" A wide variety of models and test procedures have been used to determine the strength of the bone-bioglass bond. It is the purpose of this paper to summarize these studies and to assess their contribution to the total knowledge of the strength of the bone-bioglass bond and of its application to clinical orthopaedics.

TESTING MODELS

The interface between two materials can be loaded in two primary ways: by a normal stress, or by a shear stress as shown in Figure 1.

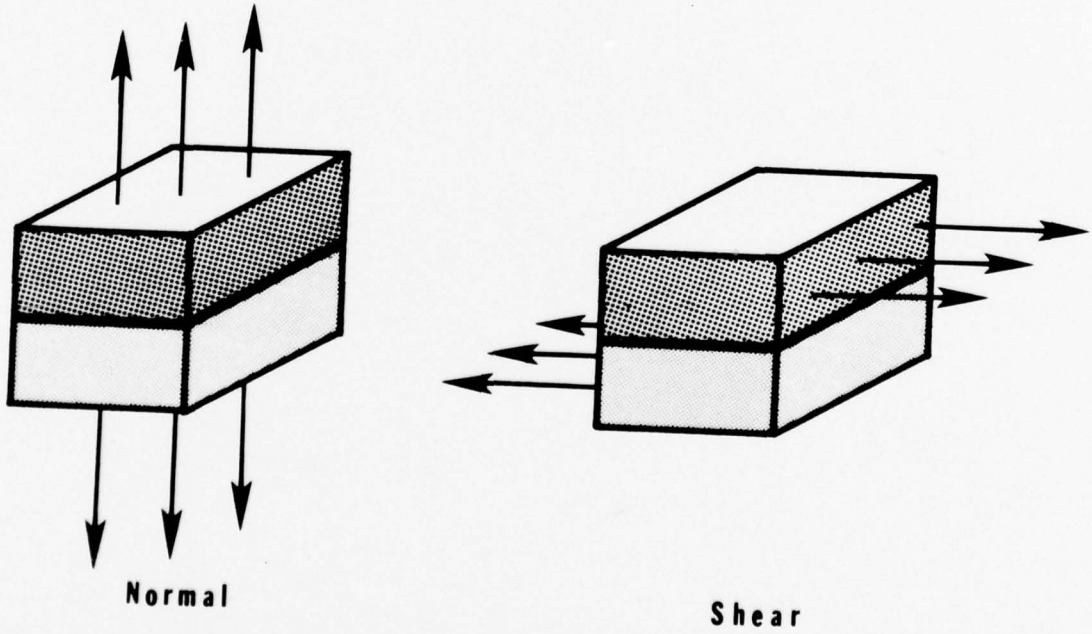

Fig. 1 Mechanical testing can involve normal loading of an interface, which tends to separate the surfaces, or shear loading, which tends to slide the surfaces relative to each other, or a combination of both.

The most severe of these testing modes is the application of a normal tensile stress, since that literally tends to split the surfaces apart. However, this loading is not one that would be normally encountered in an application of a bioglass or bioglass-coated implant. The type of loading that is much more likely in this case is one where the two surfaces are sheared relative to each other. For this reason all the test protocols involved surgical implantation of a specimen into or against a bone, and subjecting the "healed" bone-bioglass interface to a shear load. Where possible, shear stresses were calculated in order to eliminate variations in geometry from the data and allow conclusions based on intensive (stress) rather than extensive (force) quantities.

TEST MODELS

Over the span of this project, eight different models, illustrated in Figures 2-9, were used to assess the strength of the bone-bioglass interface. The assessment ranged from a qualitative description (was the implant stuck in the bone?) to a quantitative determination of the interface stress at the time of fracture of the specimem during a test.

The first specimens were rectangular chips of bioglass (Figure 2), 1 x 2 x 2 mm, implanted into a defect machined in the lateral cortex of rat femurs (1,2). These were allowed to heal for six weeks at which time the animals were sacrificed and the implant and the surrounding host bone examined. No quantitative attempts were made to extract the implant.

A second model involved the creation of a transverse midshaft osteotomy in the right femur of a rat, interposing a washer made of bioglass and reassembling the bone using a wire as an intramedullary rod for fixation, as illustrated in Figure 3 (3,4). The washers were made of 45S5 bioglass with a 6 mm outer diameter, 1 mm inner diameter, and a thickness of 0.5 mm. The femurs were harvested at periods ranging from 6 to 28 weeks and both the healed bone and the opposite, intact, femur subjected to torsional loading to failure, and the fracture torques recorded. Stresses at the fracture and at the interface were estimated for some of the specimens using a precursor version of the SCADS computer program (5,6).

A series of monkey femurs received midshafts segmental replacements of bioglass (4,7), as shown in Figure 4. Two sets of implants were used, one made of a solid piece of bioglass-ceramic and the other a stainless steel implant flame-sprayed with bioglass. Small Schneider intramedullary nails were used for fixation, and the duration ranged from 23 to 50 weeks. As was the case with the rat femurs, these specimens (with the nail removed) were twisted to failure and the stresses at the interface calculated using the SCADS computer program (6).

An attempt to replace canine fibulas with artificial substitutes, consisting of rods of either alumina covered with bioglass, or stainless steel coated with bioglass, proved unsuccessful. This model, illustrated in Figure 5, was derived from one used by Enneking, et al. (8) to

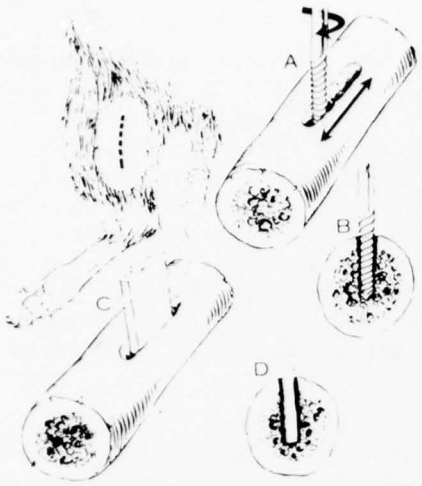

Fig. 2 The initial studies were done with small blocks of bioglass inserted into defects in rat femurs.

Fig. 3 The bioglass washer, seen at the femur's midshaft, completely separates the two parts of the rat's femur.

Fig. 4 The segmental replacement in this monkey femur also completely separates the two parts of the bone.

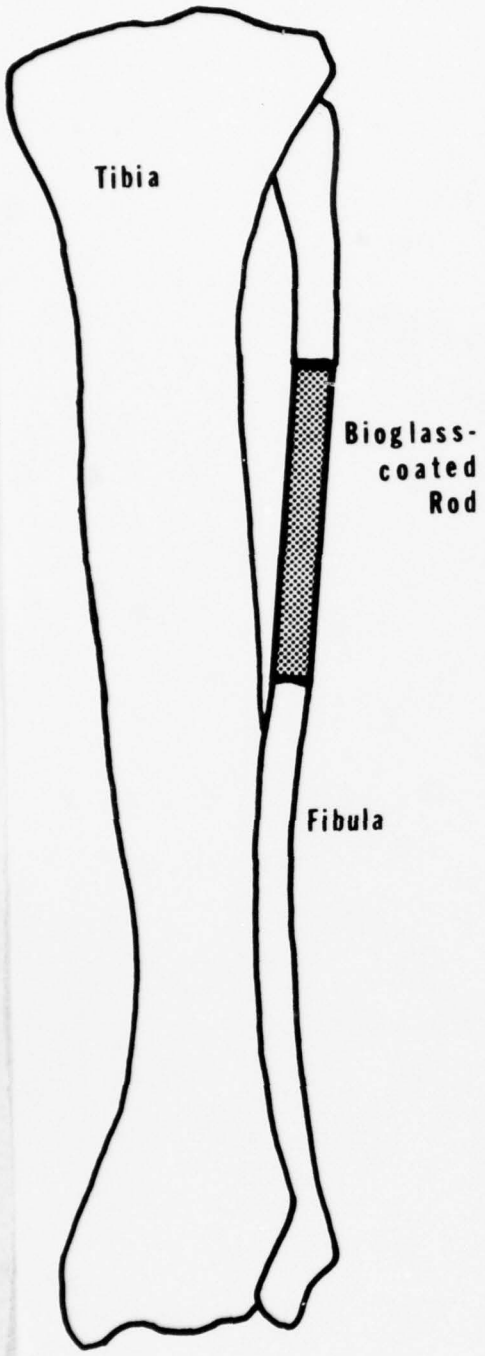

Fig. 5 A four centimeter long segment of canine fibula was replaced by a bioglass-coated cylindrical replacement. Fixation was provided be surrounding soft tissue.

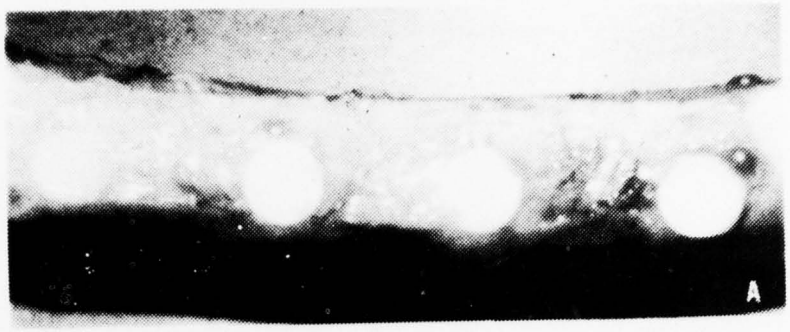

Fig. 6 Right circular cylinders of bioglass, bioglass-ceramic, and alumina coated with bioglass were installed into holes drilled into the femoral cortex of a dog.

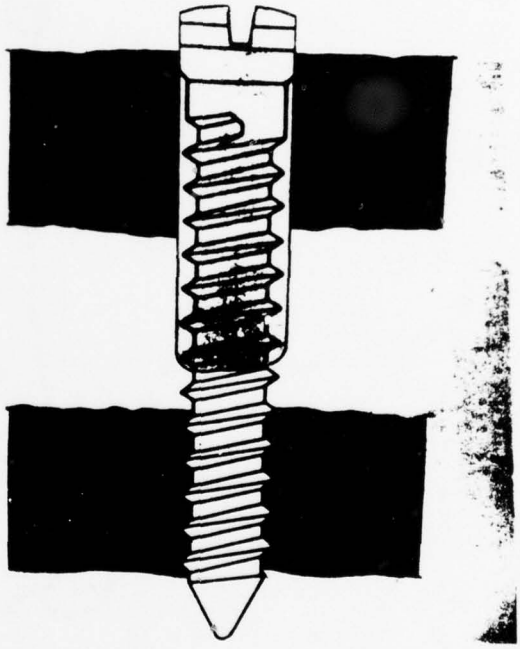

Fig. 7 The bioglass coating around the upper end of bone screw has been machined into a circular cylinder, which is well fixed in one cortex by the screw's uncoated threads screwed into the opposite cortex.

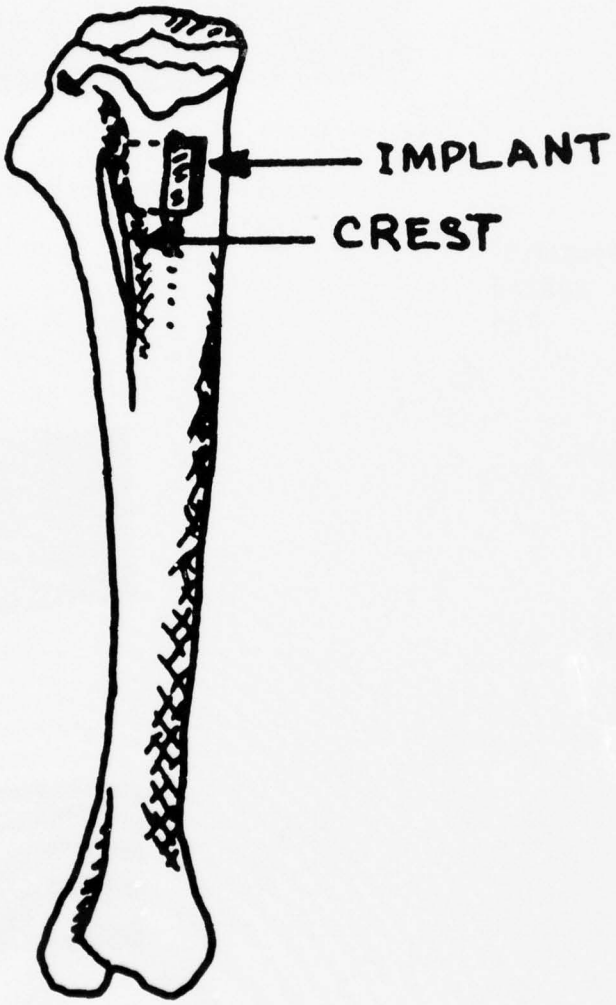

Fig. 8 The bioglass specimen to be tested with the in vivo proof test is implanted across the anterior crest of the rat's tibia.

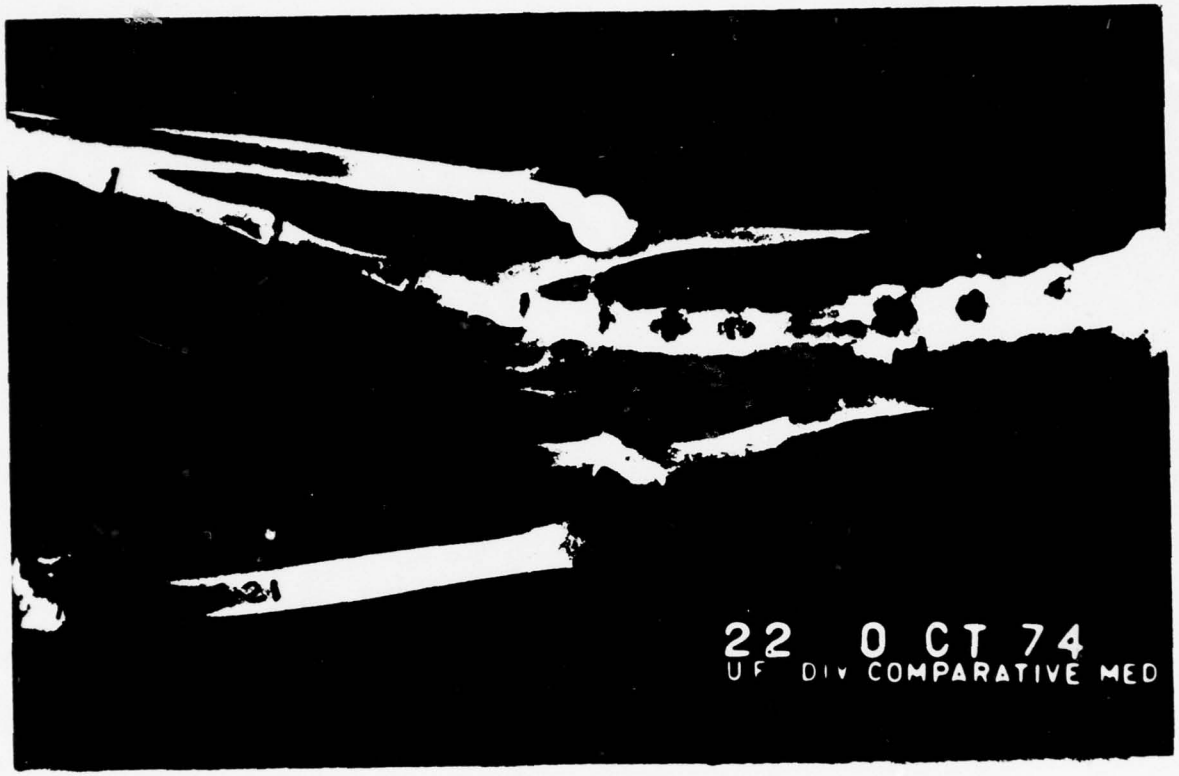

Fig. 9 This femoral head replacement is made of 316 stainless steel coated with bioglass.

study autogenous bone grafts. No internal fixation devices were used in that series, and the implants were intended to be held in place simply by the surrounding soft tissues.

Many of the problems encountered in developing a viable test model for measuring the strength of the interface revolved around the lack of fixation between bone fragments and implants. Thus, two series of experiments employed a hole drilled transversely through the cortex of dog femurs, and insertion of a circular cylinder of bioglass or some inert material, such as steel, cobalt-chromium alloy, or alumina. In the first series, right circular cylinders of 6.3 mm diameter were inserted in the drill holes, as shown in Figure 6, allowed to heal for 16 weeks, and the force required to push the cylinders through the cortex was measured (9). Due to the difficulty of assessing or measuring the actual contact area between bone and implant, no stress calculations of the interfacial shear stress were made. Figure 7 illustrates a second series of similar implants involving the implantation of bone screws coated near the head with a bioglass coating (10) and installed through both cortices of canine long bones. This model provided for secure fixation of the implant relative to the bone, and the fixation was independent of the clearance between bone and implant. Thus variations in bonding between tightly and loosely fitted implants could readily be studied. The torque required to extract the specimen was measured directly, and again no attempt was made to calculate the interfacial shear stresses due to the difficulty of determining the actual contact area.

The canine push-out model led to the development of an in vivo proof test for bonding ability of various compositions of bioglass (9,11). A specimem 4 x 4 x 1 mm is inserted into a defect milled across the anterior ridge of a proximal rat tibia as shown in Figure 8. At sacrifice, 10 or 30 days post-operatively, a force of 30 newtons is applied to push the implant out. If the implant is not dislodged by this force, it is considered to have bonded to the bone.

The final model to be described here was not developed for the purpose of assessing the interfacial strength, but to assess the clinical viability of a bioglass-based materials system for orthopaedic implants (4,12). Femoral head replacements for monkey femurs were designed, fabricated, coated with bioglass, implanted as in Figure 9 for various durations, and at sacrifice forcibly extracted from the femur by use of a testing machine. Thus, the force required to extract the stem of the prosthesis was measured directly; again no stresses were computed due to the difficulty of establishing the "true contact area."

RESULTS

The first series of implants, implanted into defects in the rat femurs, were found to be firmly held by the bone surrrounding the implant. The bond was secure enough that fragments of glass remained attached to bone even after the bone-implant specimen was sawed through

the implant, or sectioned with a diamond knife. Typically, as illustrated by Figure 10 (taken from Ref. 1) the bioglass is fragmented and near the interface fractures in the glass appear normal to the interface and terminate there.

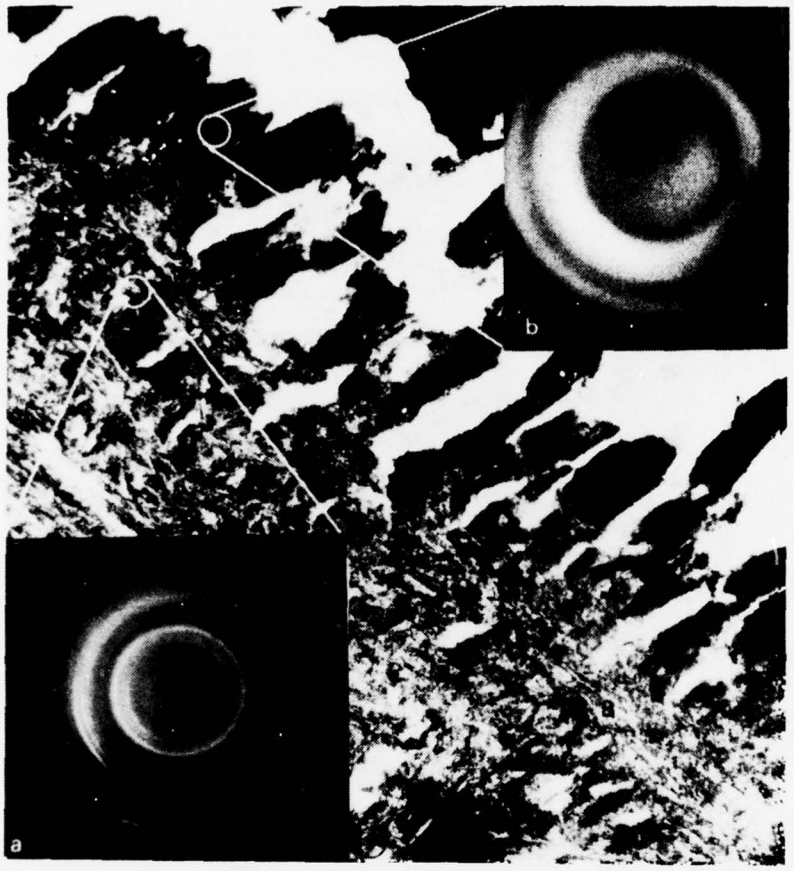

Fig. 10 The bioglass was fragmented by the machining operations used to produce this section. Note that the fractures are perpendicular to the interface, and that the fragments of bioglass (C) are still attached to the bone (B).

Six of the 16 rat femurs containing 45S5 bioglass washers united, while 11 of 13 rat femurs undergoing a sham operation (osteotomy and internal fixation, but no washer) united. The fractional difference between the strengths of the two femurs of an animal, with one femur having been operated on and the other being a normal femur, was defined as

$$d = (T_H - T_N)/(T_H + T_N)$$

where T_H was the fracture torque for the osteotomized and healed femur, (with or without washer), and T_N the fracture torque for the normal femur. These differences are summarized in Figure 11. Note that those

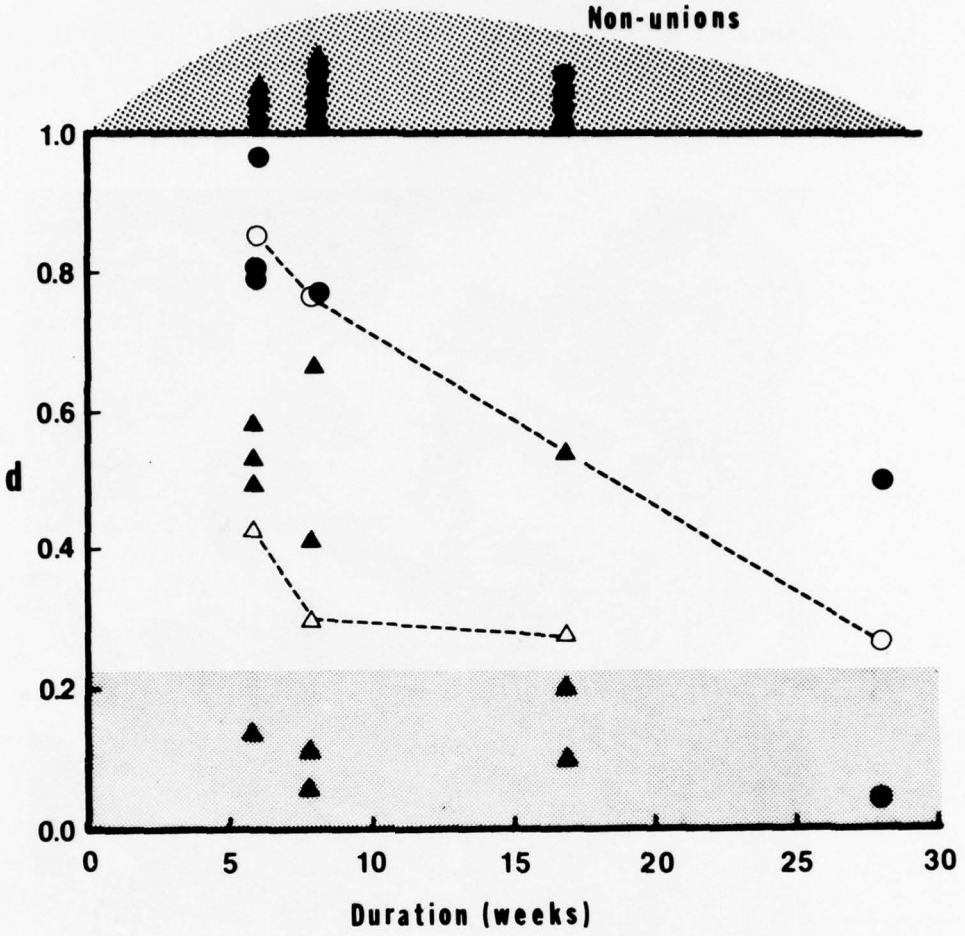

Fig. 11 The differences in fracture torques of healed osteotomized rat femurs vs. intact femurs are plotted against time post-operatively. The circles denote bones containing a bioglass washer separating the fragments, while the triangles represent osteotomized bones which did not receive an implant. The solid symbols represent individual pairs of bones, while the open symbols and the dashed lines indicate averages. The shaded region at the bottom represents normal side-to-side variation (2 std. deviations) of fracture torques of paired intact rat femurs (13).

washer-containing femurs that united attained appreciable strength levels, particularly at long implantation times. Fracture stresses for normal rat femurs were found to average 102 MPa, with a standard deviation of 39 MPa. For one femur containing a bioglass washer the shear stress at the fracture site, which was not adjacent to the washer, was computed to be 50 MPa, while the interface withstood a stress of at least 14.6 MPa without fracturing.

Of the monkey femurs receiving segmental replacements, most went on to union but in several instances a solid bioglass-ceramic implant fractured while implanted in the body. As before, those specimens that bonded to bone, bonded very well, with the strength of the healed bone approaching the strength of the normal bone on the other side. The differences in torsional strengths between femurs with implants and contralateral, intact, femurs are summarized in Figure 12, and show that much of the femur's structural integrity has been recovered in the case of femurs containing solid bioglass-ceramic implants. The flame-sprayed specimens tolerated much lower loads (larger differences) and lower stress levels; closer examination of the fractured specimens revealed that the fractures occurred at the interfaces between the bioglass coating and the metal substrate, not between the bone and the bioglass. Fracture stresses for intact bones (tibias and contralateral femurs)

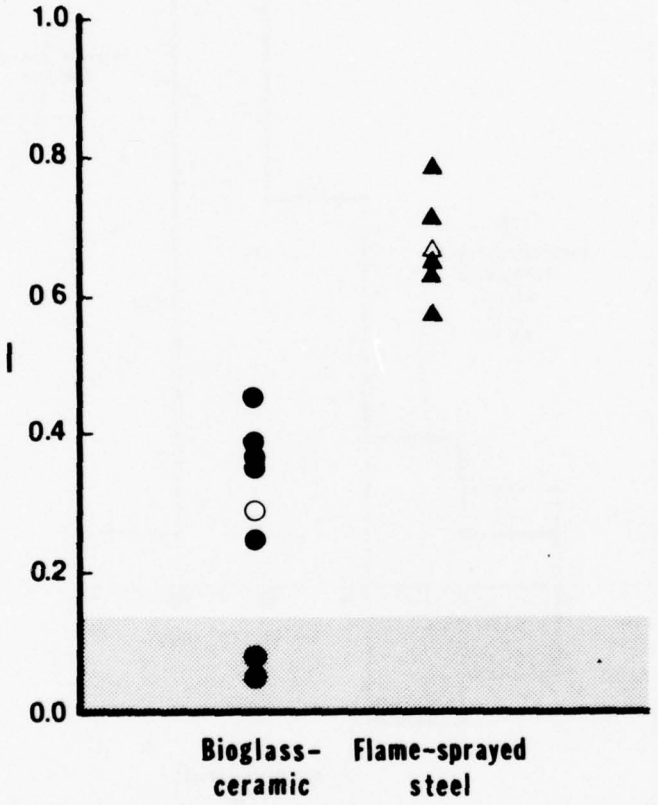

Fig. 12 The differences in fracture torques of monkey femurs containing segmental replacements vs. intact femurs are illustrated for implants of bulk bioglass-ceramic and for stainless steel implants flame-sprayed with bioglass. Each solid symbol represents a pair of bones, and the open symbols the average values. The shaded region at the bottom indicates normal side-to-side variation (2 std. deviations) of fracture torques of paired monkey tibias from the same animals (14).

were found to average 152 MPa, with a standard deviation of 29 MPa (see Fig. 13). Stresses at the fracture sites of bones containing solid bioglass implants averaged 86 MPa, while the interfaces between bone and bioglass withstood, on the average, a stress of 83 MPa. The shear stress on one interface was computed to be 117 MPa; this fracture (like most fractures) traversed both bone and bioglass and did not preferentially follow the interface.

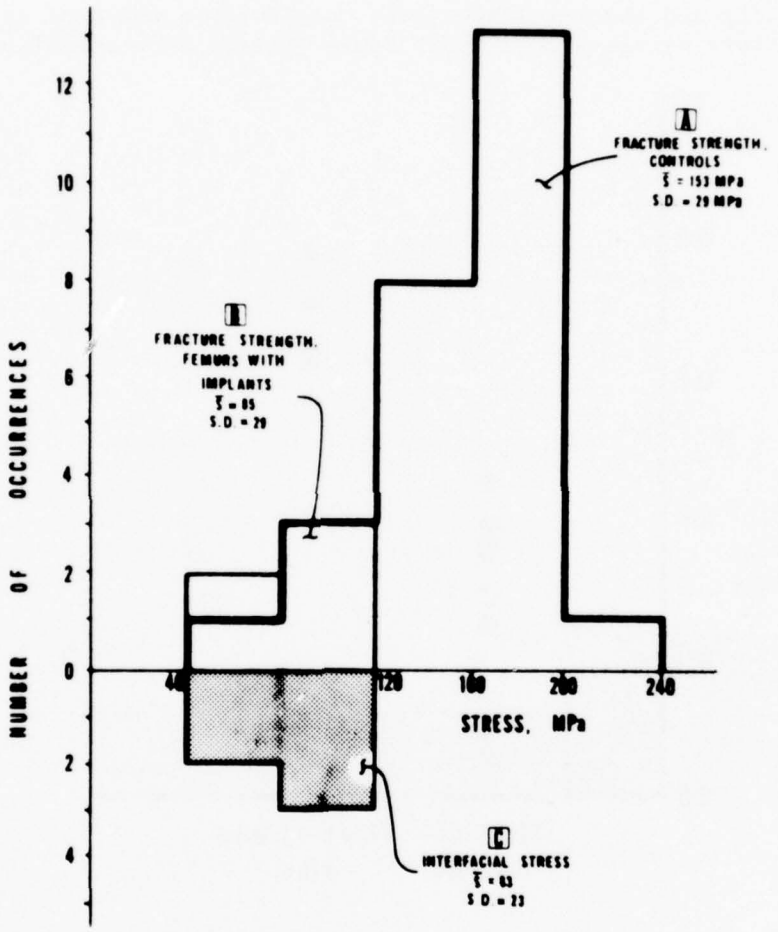

Fig. 13 Torsional shear stresses were calculated at the fracture sites of controls [A] (normal monkey tibias and the intact femurs), at the fracture sites of femurs containing bulk bioglass-ceramic segmental replacements [B], and at the interfaces between bone and those implants [C].

The test specimens involving cylinders of bioglass transversely located in the cortices of dog femurs illustrated with great clarity the fact that bioglass implants required substantially more force to dislodge them from healing bone than was the case with inert materials such as steel, cobalt chromium alloys, and alumina. Figure 14 summarizes the forces required to push out the cylinders made of various materials.* The inert materials required an average of 15 N to push out, while the bioglass and bioglass-ceramic cylinders required an average of 250 N. In one instance in the processing of the specimen, a piece of bioglass broke off from one of the implants at the point where the bioglass touched the far cortex. The strength of the glass was of the order of 40 MPa, strongly suggesting that the interface between bioglass and bone was about that strong.

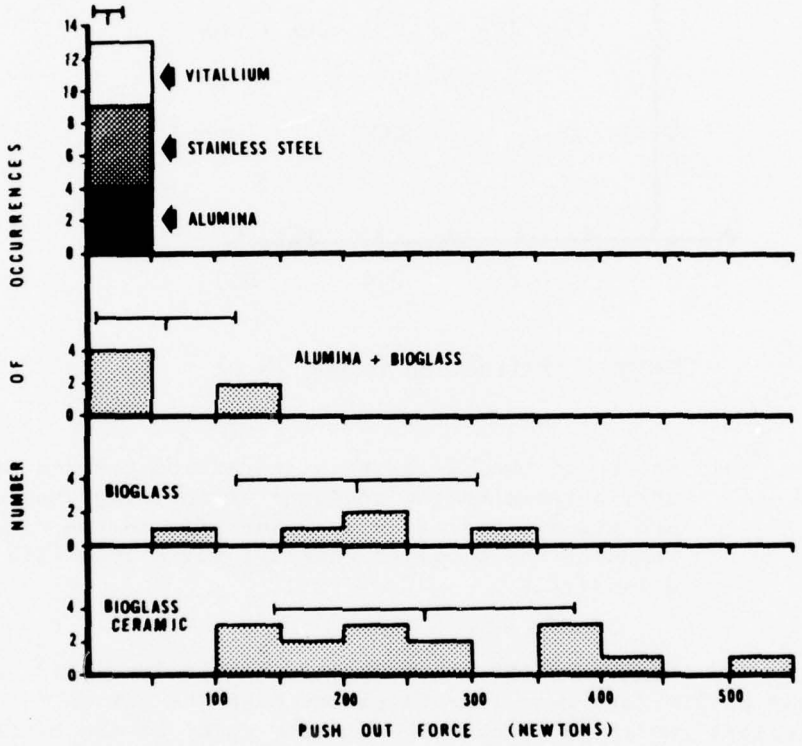

Fig. 14 Summary of forces required to push out cylinders of various materials implanted in canine femur cortices.

*The "alumina + bioglass" specimens were made of solid alumina covered with a thin fused coating of bioglass, which was subsequently found to include alumina migrated to the surface during the fusing process. The presence of alumina at the surface seems to interfere with the bonding process.

Similar kinds of results were noted for the extraction torques for the coated screws. Figure 15 illustrates the portion of the extraction torque attributable to the presence of the coating. Some of the screws inserted with a loose fit between the bioglass and the clearance hole did not appear to bond, while all of the screws with a snug fit in the clearance hole required two to three times as much extraction torque as uncoated screws (average extraction torque for uncoated screws was 0.19 N·m).

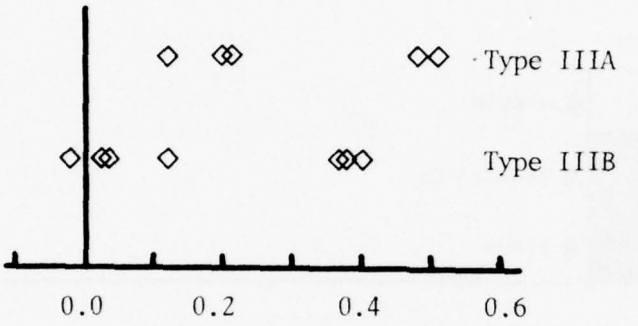

Fig. 15 Values of the increase in extraction torques of coated screws attributable to the presence of the bioglass coating. Type IIIA are screws inserted with a snug fit in the clearance hole surrounding the bioglass coating, while Type IIIB were inserted with a loose fit.

The results of the canine push out test described above, as well as some preliminary measurements of the push out forces for small blocks of bioglass implanted across the anterior spine of the tibia in rats suggested that a shear stress level of 1.0 MPa could easily be withstood by a bonded bone-bioglass interface. This led to the development of the "mini-push out" test. Thirty samples of 45S5 bioglass were tested at 10 and 30 days, with 73% of the implants passing the test at 10 days and all at 30 days. While this mini-push out test does not measure the strength of the bond but simply demonstrates its existence, it also serves to point out that the bond forms very quickly.

· The results of the trials of the monkey femoral head prostheses emphasized the importance of initial fixation of bioglass implants. When immediate post-operative fixation of bioglass-coated femoral head prostheses was poor, the implant would not bond to the femur. However, when carefully installed, the implants required about 270 N to pull the

stem out of the femur after only two months' duration. This 270 N force is roughly four times as great as the weight of the animal itself, and it is inconceivable for that kind of a pull-out load to be subjected to the implant in vivo. Thus it appears that the degree of fixation shown between the bioglass and the bone in the case of this functioning prosthetic implant is more than adequate for clinical application of such material systems.

DISCUSSION

The most striking feature about the overall range of test results is the observation that if a bioglass implant bonds to bone, it bonds extremely well, and if it does bond it will do so very quickly. Of the non-unions encountered, all of them can be explained by the excessive movement of the implant relative to the bone during the healing process. This indicates that it is critical that a bioglass implant be held immobile relative to the host bone for a duration of about two weeks, during which time the bonding process will be initiated and carried far enough for the attachment between bone and bioglass to form. If the process is disrupted during this time span, the chemical reactions necessary for bond formation are not completed and no bond forms.

If a specimen of bioglass within the host bone is held fixed during this critical time period and the bond does form, the bond becomes very strong, and appears to equal the strength of normally healed fractured bone. Fractures of long bones typically take several months before healing is completed, despite the fact that union will occur fairly rapidly. Similarly, autogenous bone grafts require about a year to recover their structural integrity fully. A similar sequence can be seen for the formation of the bond between bioglass and bone; union occurs relatively rapidly, in about two weeks, and this bond matures and increases in strength over a period of the next few months.

The maximum stress level sustained by an implant loaded in shear was calculated to be 117 MPa. This stress level is one standard deviation below the average shear strength of normal intact cortical bone when loaded to failure in torsion. This suggests that the strength of the interface at 42 weeks in nearly equal to the strength of intact cortical bone. The fact that bone remodeling will take place to relieve stress concentrations at the junction between bone and implant suggests that even if the bond is only as strong as the bone, it will be quite adequate and that failure will not occur at the interface between a well-bonded implant and bone, but will always occur away from it. This has been demonstrated on many occasions during the mechanical testing of the bone-bioglass interface.

Due to difficulties in establishing the true contact area between the bioglass cylinders and the host bone, shear stresses have not been calculated for these data. If one assumes a nominal contact area extending over 4 mm of the cylinder and an average force of about 250 N, an average shear stress of 3.2 MPa is calculated. This is quite a bit

smaller than the average interfacial stress of 83 MPa computed for the segmental implants in the monkey femurs, and suggests that the bond forms over only a small portion of the bone-bioglass interface in the cylindrical model. This may be due to the fact that the cylinders are not fully loaded during the time of healing and the bonds may not have developed fully as a result.

For a cylinder being pushed out of a bone's cortex, the average shear stress, s_{ave}, is given by

$$s_{ave} = F/\pi dL$$

where F is the push-out force, d is the diameter of the cylinder, and L is the length of the apparent contact area between bone and bioglass implant. For the coated screw implants, the average shear stress is given by

$$s_{ave} = (T/r)/2\pi rL$$

where T is the portion of the extraction torque attributable to the bioglass coating and r the radius of the cylindrical coating surface. Similar size dogs were used for both the push-out tests and the coated screw studies, and thus L can be taken to be the same for both specimens as a first approximation. Then it can be shown that

$$T = F \cdot 2r^2/d,$$

if the bond strength is the same in both cases. Substituting 1.5 and 6.25 mm for r and d respectively, the average value of 250 N for the push-out force yields an expected average value of T of 0.18 N·m. In fact, the average value of T for all snug-fitting screws represented by Type IIIA in Figure 15 is 0.30 N·m (10); the higher torque value may be due to the better fixation inherent in the coated screw model, leading to more rapid bonding and maturing of the bond.

Since implants can be designed quite readily to allow large interfaces between implant and bone, one can conclude that a bioglass coating on a metallic device, as exemplified by the monkey femoral head replacements, is a viable materials system which holds much promise in the development and application of permanent orthopaedic implant devices.

SUMMARY

Over the past nine years a large number of devices made of bioglass or with bioglass coatings have been installed in eight different animal models. Bonding occurred more or less consistently, with the primary interference to bonding being poor fixation of the implant during the critical immediate post-operative period. When bonding did occur, it occurred within a few weeks, and eventually the interfaces became extremely strong, resisting attempts at fracture at the interface; in almost all cases the fracture did not occur at the interface between

bone and bioglass. The maximum stress recorded at a mature bone-bioglass interface was of the order of the strength of the healing bone around it. This indicates that the bond between bone and bioglass is as strong as the bone itself, and that this phenomena will lead to the development of clinically useful permanent orthopaedic devices held in place by the chemcial bond between bone and bioglass.

REFERENCES

1. L.L. Hench, R.J. Splinter, W.C. Allen, and T.K. Greenlee, Jr. "Bonding Mechanisms at the Interface of Ceramic Prosthetic Materials," J. Biomed. Res. Symposium, No. 2, Interscience, N.Y., 1972, pp. 117-143.

2. C.A. Beckham, T.K. Greenlee, Jr. and A.R. Crebo, "Comparisons of Morphological Techniques Used in Evaluating a Ceramic-Bone Implant," J. Calcified Tissue Res., Vol. 8, 1971.

3. G. Piotrowski, R. del Valle, and B.D. Miller, "The Mechanical Strength of the Bone-Ceramic Bond," in Report No. 2, An Investigation of Bonding Mechanisms at the Interface of a Prosthetic Material, U.S. Army Medical Research and Development Command, Contract No. DADA 17-70-C-0001, August 1971, pp. 15-25.

4. L.L. Hench, H.A. Paschall, W.C. Allen, and G. Piotrowski, "Interfacial Behavior of Ceramic Implants," in Biomaterials, ed. by E. Horowitz and J.L. Torgesen, National Bureau of Standards Special Publication No. 415, pp. 19-35, May 1975.

5. G. Piotrowski and G.A. Wilcox, "The STRESS Program: A Computer Program for the Analysis of Stresses in Long Bones," J. Biomechanics, 4:497-506, 1971.

6. G. Piotrowski and G.I. Kellman, "A Stress Calculator for Arbitrarily Drawn Sections - the S.C.A.D.S. Computer Programme," in Orthopaedic Mechanics: Procedures and Devices, ed. by D.N. Ghista and R. Roaf, Academic Press, 1978, pp. 317-340.

7. G. Piotrowski, L.L. Hench, W.C. Allen, and G.J. Miller, "Mechanical Studies of the Bone Bioglass Interfacial Bond," J. Biomed. Mater. Res. Symposium No. 6, pp. 47-61, 1975.

8. W.F. Enneking, H. Burchardt, J.J. Puhl, and G. Piotrowski, "Physical and Biological Aspects of Repair in Dog Cortical-Bone Transplants," J. Bone Jt. Surg. 57-A:237-252, 1975.

9. G.J. Miller, D.C. Greenspan, G. Piotrowski, and L.L. Hench, "Mechanical Evaluation of Bone-Bioglass Bonding," in Report No. 7, An Investigation of Bonding Mechanisms at the Interface of a Prosthetic Material, U.S. Army Medical Research and Development Command, Contract No. DAMD 17-76-C-6033, October 1976, pp. 24-39.

10. G. Piotrowski, R. Parker, M. Madden, "Bonding of Bioglass to Canine Cortical Bone," in Report No. 9, An Investigation of Bonding Mechanisms at the Interface of a Prosthetic Material, U.S. Army Medical Research and Development Command, Contract No. DAMD 17-76-C-6033.

11. M.G. Ferrari, T. Carr, and G. Piotrowski, "Standard Method of Test for Ability of a Biomaterial to Bond to Bone," in Report No. 7, An Investigation of Bonding Mechanisms at the Interface of a Prosthetic Material, U.S. Army Medical Research and Development Command, Contract No. DAMD 17-76-C-6033, October 1976, pp. 40-49.

12. G. Piotrowski, M.G. Ferrari, and R.W. Petty, "Bioglass Coated Monkey Hip Prostheses - A Progress Report" in Report No. 8, An Investigation of Bonding Mechanisms at the Interface of a Prosthetic Material, U.S. Army Medical Research and Development Command, Contract No. DAMD 17-76-C-6033, December 1977, pp. 78-89.

13. G.J. Howell and G. Piotrowski, "Biomechanical Properties of Paired Rat Femurs," in Report No. 3, An Investigation of Bonding Mechanisms at the Interface of a Prosthetic Material, U.S. Army Medical Research and Development Command, Contract No. DADA 17-70-C-0001, August 1972, pp. 123-136

14. G.J. Miller and G. Piotrowski, "A Brief Note on the Variability of the Torsional Strength of Paired Bones," J. Biomechanics, 7:247-248, 1974.

D. BONDING OF BIOGLASS TO CANINE CORTICAL BONE

by

G. Piotrowski, R. Parker, and M. Madden

INTRODUCTION

The effect of the type of host bone on the bonding of bioglass to that bone is not clearly understood. The in vivo "proof test" for bonding ability, involving the cancellous bone of the proximal rat tibia, has shown consistent bonding by most samples of various batches of bioglass, (see Paper "Rate of Bond Formation of Bioglass and Dense Hydroxyl Apatite). However, 45S5 bioglass implants failed to bond when used to replace a segment of canine fibula, which is almost totally cortical bone (1). Two hypotheses to explain this discrepancy in bonding behavior were proposed: a) motion between implant and bone interferes with the bonding process, and b) cancellous bone, being metabolically more active than cortical bone, must be present for the bond to form. The experiment described in this paper was designed to test the latter hypothesis.

Cobalt-chromium alloy bone screws were partially coated with bioglass, the bioglass machined to a cylindrical surface, and the screws implanted transversely in long canine bones for nine weeks, using the uncoated threads for fixation. At sacrifice the extraction torque of the screws was measured to assess the degree of bonding.

A comparison of the extraction torques of coated and uncoated screws shows that coated screws required more, up to three times as much, torque for extraction than uncoated screws. However, some coated screws inserted with relatively large clearance between bioglass and bone did not appear to bond. This implies that excessive space between bone and bioglass is an important factor in the inhibition of the bonding process.

MATERIALS AND METHODS

Three types of implants were prepared as shown in Figure 1: Type I, short (10 mm) uncoated screws; Type II, long (22 mm) uncoated screws; and Type III, long (22 mm) screws with a portion of the threads near the head coated with bioglass. All screws* were made of a cobalt-chromium alloy**, and had a major outer thread diameter of 3.5 mm. The coating of 52S4.6 bioglass was applied by the immersion coating process (2), the glass surface ground into a cylindrical shape, and the driving recess re-established. Part of the screw head was removed during the machining of the bioglass cylinder.

*provided by Howmedica, Inc.
**Vitallium®

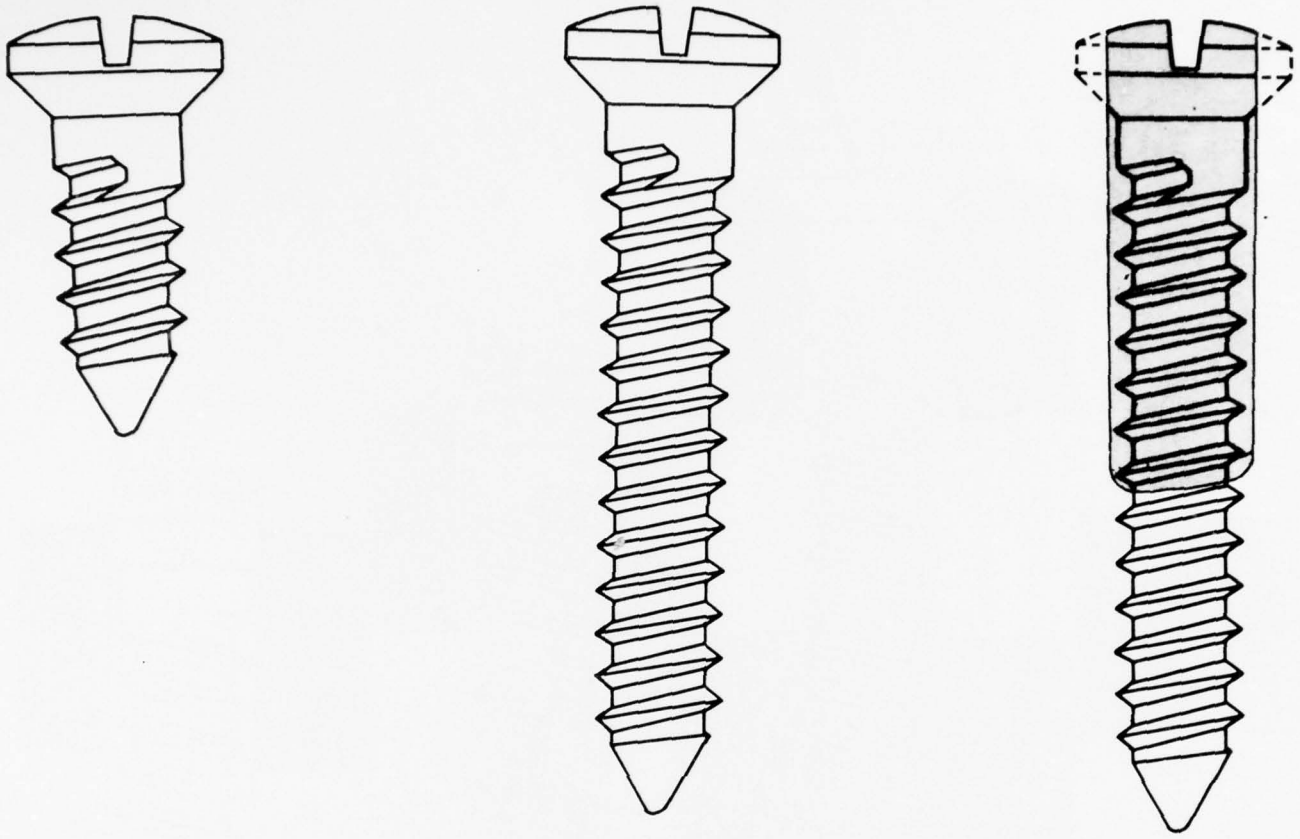

Fig. 1 Three types of Co-Cr screws were used in this study. Type I and II are uncoated, while the Type III screws were immersion-coated with bioglass.

Twenty-two screws were implanted into the humeri, femora, and tibiae of one mongrel dog. The middle 3/4 of each bone was used for implantation sites, and the periosteum stripped off the bone prior to drilling. For Type I screws, only a pilot hole was drilled in the near cortex and the screw inserted, as shown in Figure 2. Type II screws were inserted after the pilot hole was drilled through both cortices, and a clearance hole made in the near cortex. Two types of installations were used with Type III screws in order to assess the effects of bone-bioglass spacing. Type IIIA screws were installed into holes identical to those for Type II screws, i.e., a pilot hole through both cortices and a pilot hole to provide a snug fit for the bioglass cylinder. The clearance holes for Type IIIB screw installations were enlarged, so that the hole was up to 0.5 mm larger than the implant. Figure 3 illustrates the relative locations of each of the four types of screw installations.

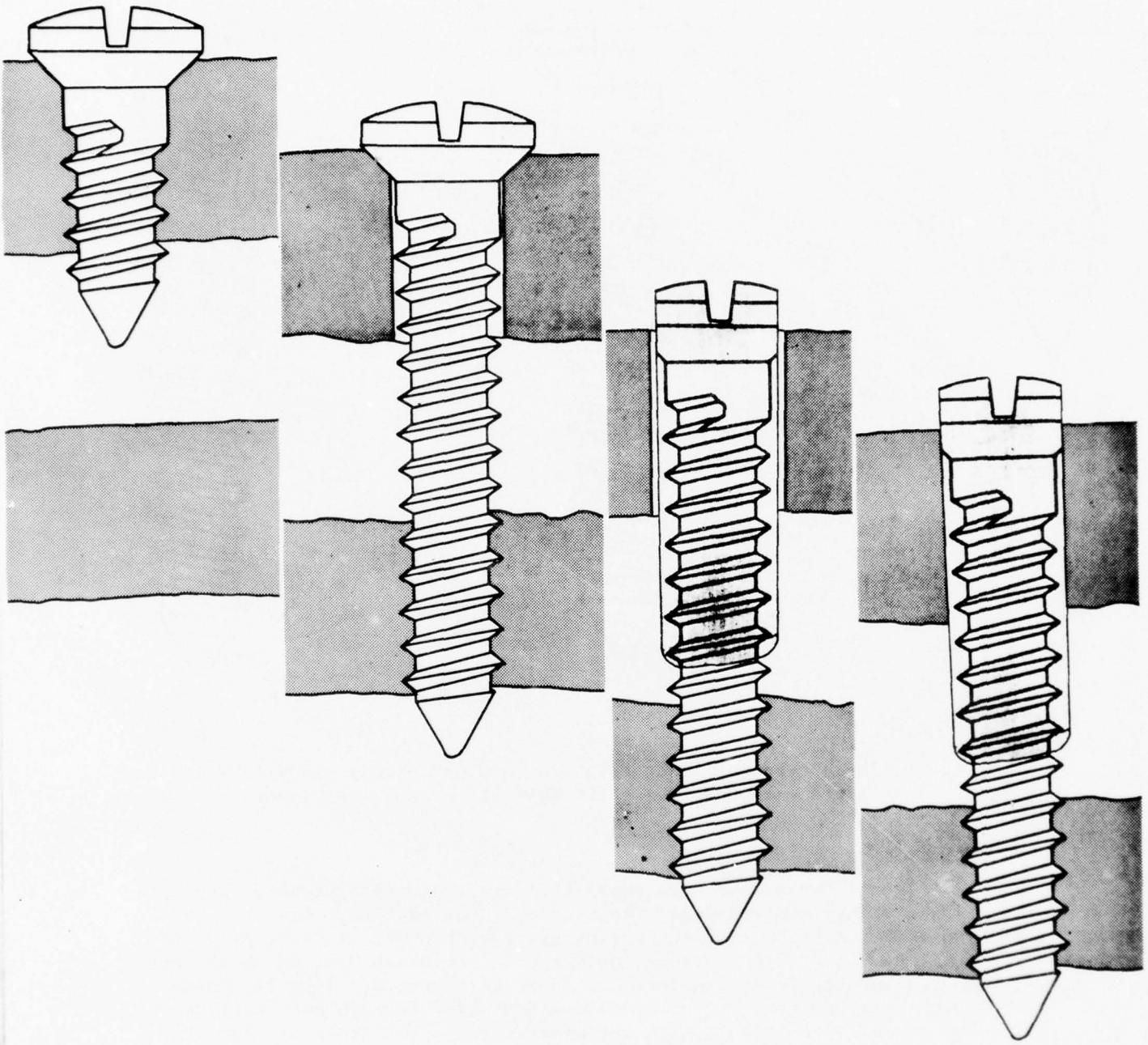

Fig. 2 Four types of installations were used. Type I and Type II installations use uncoated screws. Coated screws installed with minimal clearance between bioglass and bone are labelled Type IIIA, while coated screws installed in oversize clearance holes are referred to as Type IIIB.

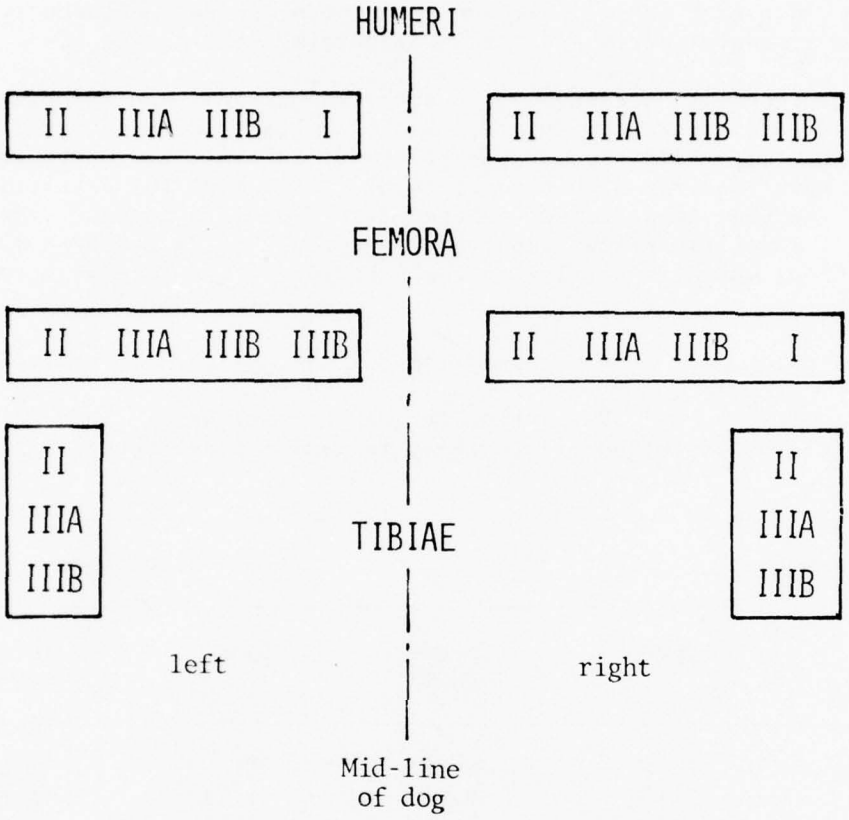

Fig. 3 Schematic of the six long bones of the dog serving as implantation sites for the 22 implants used.

Post-operatively the dog was allowed to move about in his run. Tetracycline was administered for one week prior to sacrifice to label new bone being formed at the time.

The dog was sacrificed at 9 weeks post-operatively, and all six implanted bones excised. The periosteum and other soft tissue surrounding the heads and the points of all screws were removed. The bones were immediately placed on a torsional load cell and the screws extracted while the load cell recorded the torque required to extract each screw.

RESULTS

The maximum torques required to extract each of the screws are listed in Table 1, and grouped by installation type in Figure 4. The extraction torques of all uncoated screws, Type I and Type II, was less than 0.3 N·m (2.6 in·lb), with no apparent difference between screws through a single cortex and screws traversing both cortices.

All Type IIIA screws, with a snug fit between bone and bioglass, required torques greater than 0.3 N·m to extract, with an average of 0.49 N·m. Type IIIB screws appeared to divide into two distinct groups. Some screws required high torques (0.57 ± 0.02 N·m) for extraction, suggesting that these screws behaved like Type IIIA screws. The other group of Type IIIB screws required low torques (0.24 ± 0.07 N·m) for extraction, which is similar to the behavior of the Type II screws.

TABLE 1

Extraction Torques For Screws
Installed Transversely in Canine Long Bones*

Bone	Left Side		Right Side	
	Type	Torque (N·m)	Type	Torque (N·m)
Humerus	I	0.28	II	0.25
	IIIB	0.56	IIIA	N.R.
	IIIA	0.39	IIIB	0.59
	II	0.14	IIIB	0.56
Femur	IIIB	0.17	II	N.R.
	IIIB	N.R.	IIIA	0.40
	IIIA	0.70	IIIB	0.22
	II	0.22	I	0.06
Tibia	II	0.19	II	0.22
	IIIA	0.67	IIIA	0.31
	IIIB	0.31	IIIB	0.22

*Screws listed in proximal-to-distal order. N.R. - no readings were obtained for this screw.

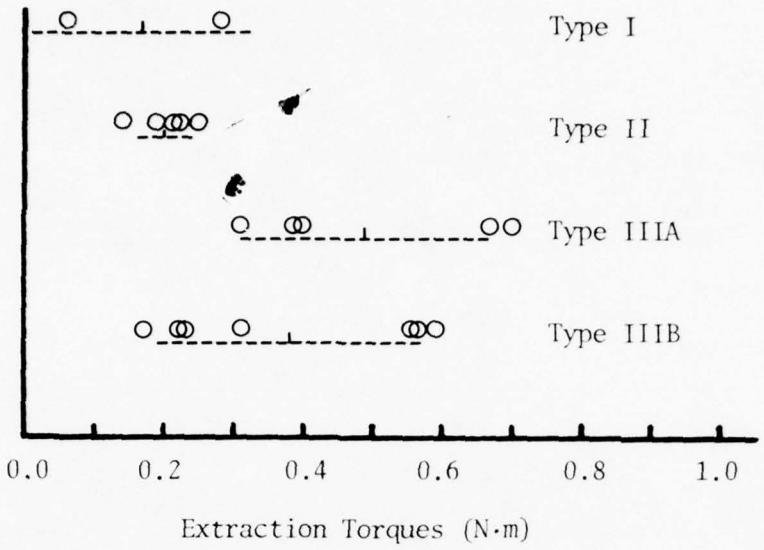

Fig. 4 Summary of the extraction torques for the screws, grouped by type of installation. The mean ± one standard deviation are indicated by the vertical and horizontal dashed lines.

For purposes of comparison, the results from Type I and Type II screws were combined into one group, with a sample size of 7, a mean extraction torque of 0.19 N·m, and a best estimate of the standard deviation of 0.075 N·m. The student's t - test was used to test the significance of difference between mean torques for various groups, and these results summarized in Table 2.

Coated screws inserted with a snug fit clearly required higher extraction torques than uncoated screws. Coated screws inserted into holes of varying degrees of fit did not demonstrate, on the average, a statistically significant higher extraction torque, implying that more data points need to be acquired. No statistically significant difference was established between the two groups of coated screws, again suggesting more data points are needed.

Examination of the patterns of bone labelled by tetracycline is still in progress. The clearance holes show evidence of vigorous repair, while the treaded holes in the opposing cortex show relatively little labelled bone. Coated screws with low extraction torques (Type IIIB) appear to show less fluroescence in the adjacent bone than firmly fixed screws, indicating a lower level of osteogenic activity.

TABLE 2

Summary of Statistical Comparison
of Average Extraction Torques

Comparison	Student's t-test	Difference between Mean Extraction Torques
Uncoated vs. Type IIIA	t=3.1, P<0.01	statistically significant
Uncoated vs. Type IIIB	t=2.3, P$\sim$0.05	significance not demonstrated
Type IIIA vs. Type IIIB	t=0.9, P~0.4	not significant

DISCUSSION

The overlap of the distributions for the extraction torques of Type I and Type II screws suggests that the primary contribution to the extraction torque in all screws comes from the part of the screw threaded into the cortex, and that the portion of the screw passing through the clearance hole in the near cortex is not mechanically held firmly in the bone. Burstein, et al. (3), and Schatzker, et al. (4) have shown that a screw hole fills in with woven bone, which remains radioluscent for a considerable time. This new bone does not appear to grip the screw threads in the clearance hole very tightly, and apparently offers no resistance to the extraction of the screws.

The effect of the glass coating on the extraction torque can be found by subtracting the average extraction torque for uncoated screws, 0.19 N·m, from the torques measured for the coated screws. These values are summarized in Figure 5, which illustrates the component of the extraction torque attributable to bone-bioglass bonding. Three of the screws, all Type IIIB, appear to be totally unaffected by the bioglass coating. Four others seem to be lightly bonded to the bone, while the remaining five screws appear to be well bonded to the bone. All the bioglass used in this study comes from a lot which has passed the "proof test" for bonding ability (2), and thus the failure to bond must be

attributed to some feature of the installation. The relatively low level of tetracycline labelling indicates little bone apposition is occurring, and that the bonding process has been inhibited. The relatively large clearance between bone and bioglass is implicated in the inhibition of bonding, but more data points are needed.

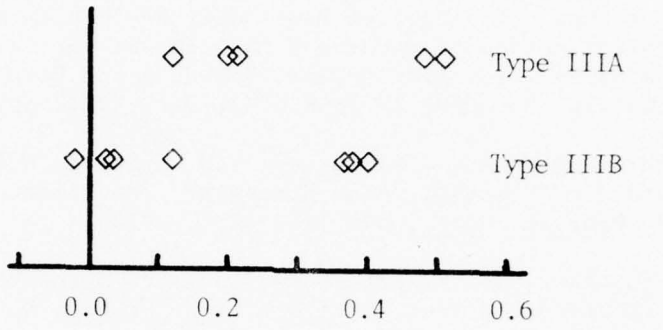

Fig. 5 Summary of the contributions of the bioglass coatings to the extraction torques.

SUMMARY AND CONCLUSIONS

Cobalt-chromium screws, some uncoated and some partially coated with bioglass, were implanted transversely in long bones of a dog, with a pilot hole in one cortex and a clearance hole in the other. At sacrifice nine weeks post-operatively, the screws were extracted and the peak extraction torque recorded. The main findings were:

1. The resistance to extraction for uncoated screws originated in the part of the screw threaded into the bone, not in the portion of the screw passing through the clearance hole. Average extraction torque for uncoated screws was 0.19 N·m.

2. A bioglass coating around the portion of the screw passing through the clearance hole more than doubled the extraction torque, if the coating was in close apposition to the cortical bone post-operatively. Average extraction torque for such screws was 0.49 N·m.

3. If bioglass is not in close apposition to cortical bone initially, the formation of the bone-bioglass bond may be delayed or inhibited.

4. Bioglass will bond to cortical bone, if the bioglass surface is in close apposition to the bone and no motion between bone and implant takes place.

REFERENCES

1. Piotrowski, G., T. Carr, M. Ferrarri and R.W. Petty, "Evaluation of Bioglass Canine Fibula Grafts," in Report No. 8, An Investigation of Bonding Mechanisms at the Interface of a Prosthetic Material, U.S. Army Medical Research and Development Command, contract No. DAMD 17-76-C-6033, Dec. 1977, pp. 60-67.

2. Clark, D.E., M.C. Madden, and L.L. Hench, "Development of Bioglass Coatings for Vitallium Prosthetic Devices," in Report No. 8, An Investigation of Bonding Mechanisms at the Interface of a Prosthetic Material, U.S. Army Medical Research and Development Command, Contract No. DAMD 17-76-C-6033, Dec. 1977, pp. 68-77.

3. Burstein, A.H., J.D. Currey, V.H. Frankel, K.G. Heiple, P. Lunseth, and J.C. Vessely, "Bone Strength: The Effect of Screw Holes," J. Bone Jt. Surg., 54A:1143-1156, 1972.

4. Schatzker, J., R. Sanderson, and J.P. Murnagham, "The Holding Power of Orthopaedic Screws In Vivo," Clin. Orthop. No. 108:115-126, May 1975.

E. THE RATE OF BOND FORMATION OF BIOGLASS AND DENSE HYDROXYLAPATITE IMPLANTS IN RATS

by

M. Madden, L.L. Hench and M. Jarcho

INTRODUCTION

Previous studies in this program have shown that the histological and chemical nature of the bioglass-bone bond changes as a function of time. One of the objectives of the present study is to establish the change in strength of the interfacial bone-bioglass bond as a function of time. A minipush-out model developed for the rat is modified to produce quantitative analysis of interfacial failure stresses. Data from the quantitative interfacial failure analysis was used to select a single load of 30 newtons to be applied to the rat tibial implants as a pass-fail criterion for bonding. The time dependence of bonding is measured in terms of the fraction of implants which pass the 30 newtons interfacial loading.

Earlier studies have also showed that the bioglass-bone bond involves the formation of a biologically active hydroxylapatite layer at the interface between the implant and bone. Recent work on dense hydroxylapatite (durapatite) implants reported by one of the authors (MJ) also shows evidence of bone-durapatite bonding (1). Therefore a second objective of this study is to compare the rate of bonding of durapatite with the rate of bioglass using the same rat tibial minipush-out model.

EXPERIMENTAL PROCEDURE

The protocol for the quantitative minipush-out model involved time periods of 2, 4, and 8 weeks with 20 45S5 Bioglass and 20 Durapatite implants per time period. Implants 4mm x 4mm x 1mm were placed in carefully prepared surgical defects in rat tibiae following procedures previously described (2). At sacrifice, the tibiae were removed, cleaned of soft tissue, placed in cold Ringer's solution, and kept refrigerated until the mechanical test was performed.

An accurate measure of the force required to cause failure of the bone was obtained by using an Instron University Testing Machine. The removed tibia was placed in the jig as shown in Fig. 1 with the implanted portion centered between the two semi-circular supports. The ends of the tibia were then secured by the screws. These two supports can be independently rotated to provide optimum orientation for clamping. Once the tibia was mounted, these supports were rotated simultaneously about one axis. The base on which the two supports ride can also be rotated to provide optimum orientation about the second axis, perpendicular to the first. The forces in the jig resulting from testing of the implant occur perpendicular to sliding surfaces so no locking of the movable parts of the jig is necessary. Proper orientation of the implant during testing is important to insure the implant-bone interface is loaded in shear only.

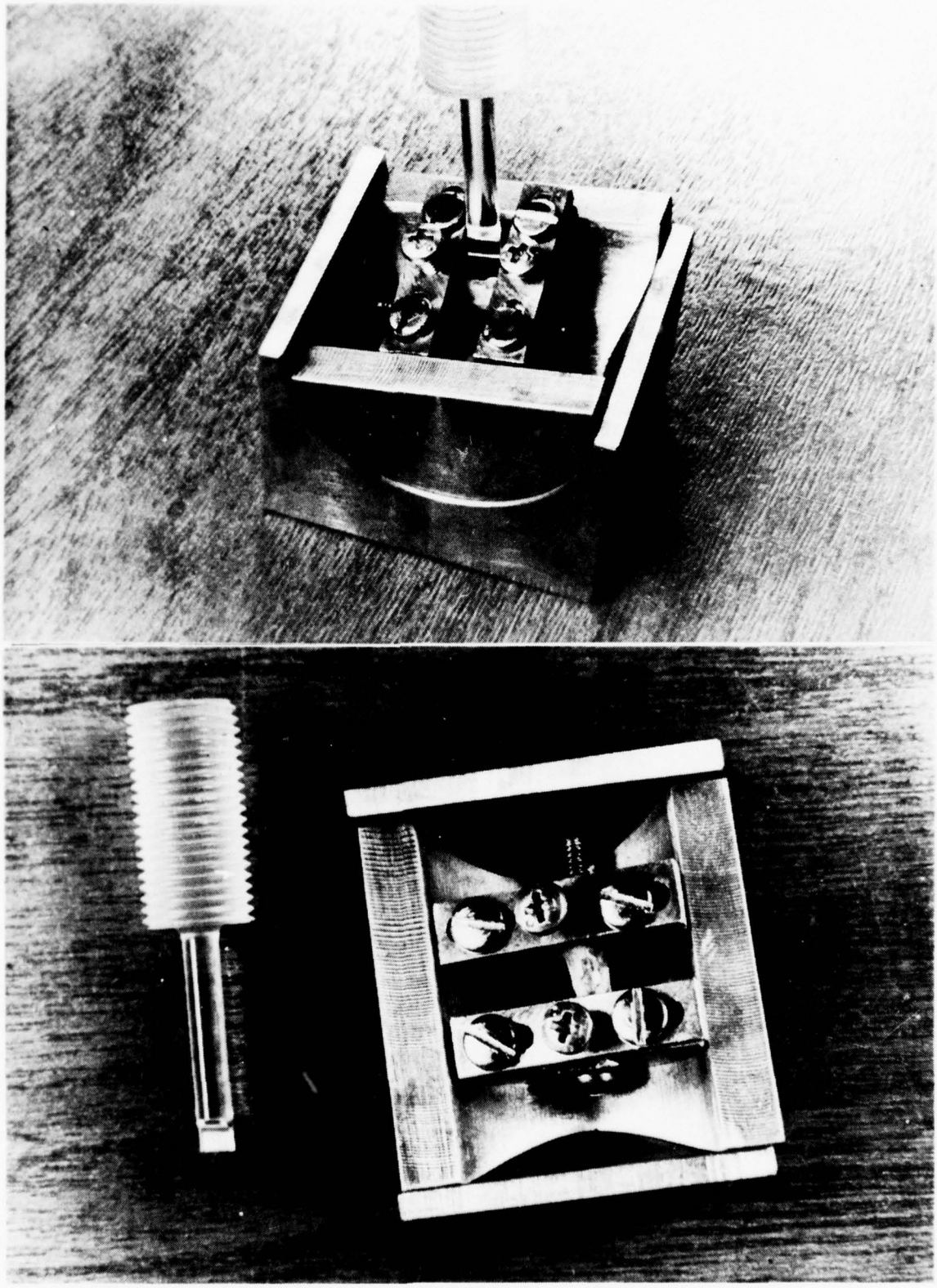

Fig. 1 Mounting jig with tibia containing implant in testing position. Magnification 2X.

The jig containing the mounted tibia is then placed on the bottom compression platen of the Instron. The movable top platen was not used and a test head consisting of a brass rod machined to a .75mm x 3.5mm rectangular end substituted. The test head shown in Fig. 1 is of identical geometry but made of plexiglass, which later proved too weak and had to be replaced with the brass rod. The rectangular end of the test head was covered with a small piece of electrical tape to prevent implant fracture from stress concentrations caused by surface irregularities on either the implant or test head.

The test head was moved close to the implant surface and the implant rotated until the end of the test head was coincident with the end of the implant and the motion of the test head parallel to the surfaces of the implant. Testing was performed at a test head speed of .1" per min. Load was measured continuously using a strip chart recorder. The tibia was loaded until failure occurred. After testing, the tibia was removed from the jig and placed in 10% buffered formalin.

The interfacial area was determined by splitting the tibia with a razor saw in a plane parallel to the 4mm x 4mm faces of the implant and bisecting the 4mm x 1mm face. The interior surfaces, i.e., the ones previously in contact with the implant, were photographed at approximately 4X.

The method of measuring interfacial contact area is illustrated in Fig. 2. The areas of the bone surfaces in contact with the 4mm x 4mm faces were determined by planemetry directly from the photograph. Many times, but not always, one of the surfaces of the implant was in contact with the marrow cavity, as shown in Fig. 2A. The area of the marrow cavity was not included in the interfacial area.

The interfacial areas of the edges were calculated by measuring lengths ℓ_1 - ℓ_6, shown in Fig. 2B, and assuming the trapezoidal geometry with a 1mm altitude, as shown in Fig. 2C. Since the area of a trapezoid is the average of the bases multiplied by the altitude, the angles between the non-parallel edges and the base is immaterial, as shown in Fig. 2D.

The areas were summed and divided into the failure load to obtain the interfacial shear stress.

The failure loads observed in this and a previous study (1) showed that well bonded implants could easily withstand an interfacial load of 30 newtons. Thus a sponge forceps was modified and calibrated to produce in sequence 10N, 20N, and 30N of load to the implant. Details of the instrument are presented in Report #7. The load required to dislodge the implant is recorded. Implants bonded sufficiently to withstand the 30N load without dislodging are reported to have "passed" the qualitative minipush-out test. Several major advantages are inherent in the qualitative minipush-out test: 1) it is simple and quick thus permitting a large number of samples to be evaluated; 2) it can be performed on the animal in the final moments of terminal sedation thus permitting an estimate of the in vivo bond strength; and 3) it is

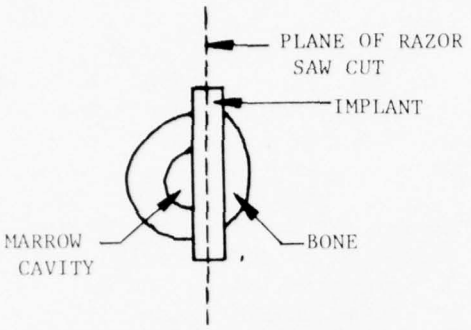

Figure 2A. Implant Configuration.

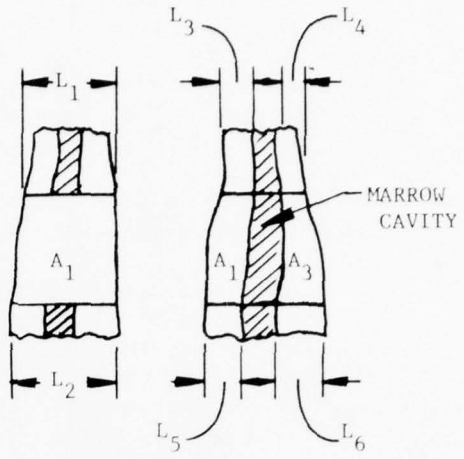

Figure 2B. Areas and Dimensions Determined from Photograph

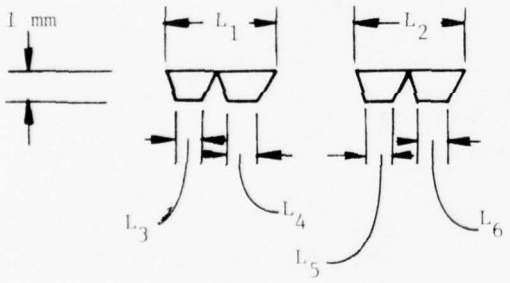

$$\text{AREA} = \frac{L_1 + L_3 + L_4}{2} + \frac{L_2 + L_5 + L_6}{2}$$

Figure 2C. Edge Area Determinations.

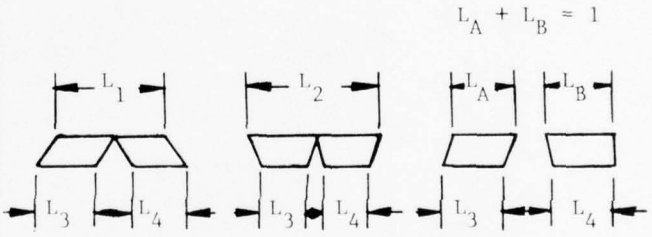

$$\text{AREA} = \frac{L_1 + L_3 + L_4}{2}$$

Figure 2D. All of these Edge Configurations have the Same Area.

Fig. 2 Interfacial area determinations.

inexpensive. The prime disadvantages of the procedure are: a) interfacial areas cannot be measured which prevents calculating failure stresses; and b) misalignment of the implant and loading device may occur which can result in loss of accuracy.

RESULTS AND DISCUSSION

Considerable problems were encountered in the performance of the quantitative minipush-out tests. There was sufficient variation in the geometry of rat tibiae to make mounting time consuming for all and impossible for some. Some bones fractured at failure, making area determination impossible. A majority of the 8 week tests failed through the implant, as shown in Fig. 3. The loads for failure during the 8 week tests were higher than expected (~120N), and this may have overloaded the mounting jig sufficiently to cause failure by bending of the specimen. The entire 8 week series on both materials is dropped from the Table of Results (Table I) for this reason. Because of the high strength of the interface at 8 weeks a different procedure would be required to measure the values accurately.

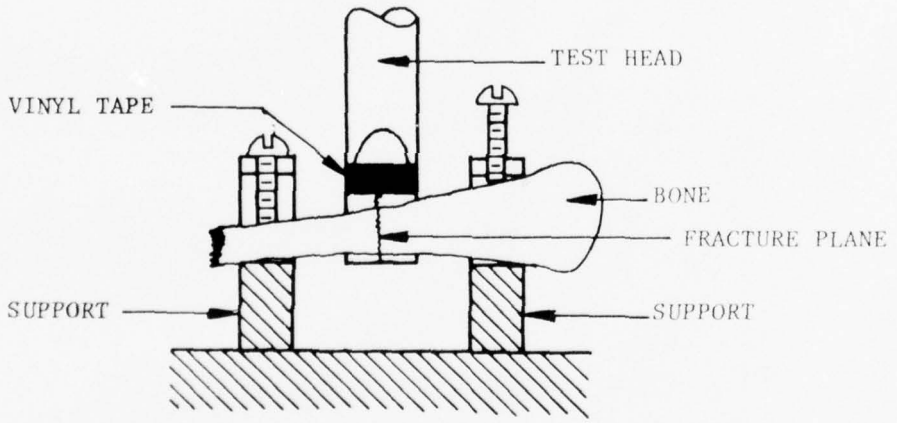

Fig. 3 Typical failure of 8 week implants. Failure occurred by this means for both durapatite and bioglass.

Results for the 2 and 4 week tests on both materials are given in Table I. These results are not as consistent as had been initially hoped. Since the error from the Instron testing machine is less than 1%, the wide variation must be due to other errors, i.e., areas that appeared to be bonded in fact were not, or some unknown biological variable. The possibility of an error in area determination is supported by examples such as animals number 37A and 10A, (Table I), which had a 0 failure load but not a zero interfacial area.

TABLE I

Bioglass								Durapatite							
2 Week				4 Week				2 Week				4 Week			
Animal				Animal				Animal				Animal			
#	Load	Area	Stress	#	Load	Area	Stress	#	Load	Area	Stress	#	Load	Area	Stress
3	72.0	18.5	3.90	24A	42.3	26.5	1.60	56	34.2	26.8	1.28	31A	3.6	29.0	.12
5	20.5	26.4	.78	25A	65.8	29.9	2.20	58	40.5	31.2	1.30	32A	60.5	35.7	1.69
6	62.7	19.7	3.18	26A	62.3	37.2	1.67	59	20.9	31.3	.67	36A	96.1	29.1	3.30
7	20.9	27.1	.77	27A	44.5	26.1	1.70	60	21.4	32.1	.67	37A	0	37.5	0
8	32.0	33.6	.95	28A	75.6	29.6	2.55	61	28.5	27.0	1.06	38A	81.4	28.7	2.84
9	64.1	30.2	2.12	29A	127.7	30.7	4.16	62	36.5	25.6	1.43	40A	38.3	34.2	1.12
10	49.4	30.2	1.64	51A	30.7	37.1	.83	8A	32.5	23.9	1.36	42A	48.9	38.5	1.27
11	24.5	25.0	.98	52A	105.0	20.0	5.25	10A	0	28.9	0	47A	16.5	36.6	.45
13	28.9	29.6	.98	53A	39.6	31.7	1.25	11A	31.1	26.5	1.17	60A	43.6	35.9	1.21
14	48.9	28.1	1.74	54A	59.2	36.6	1.62	12A	14.7	28.1	.52	61A	101.4	22.9	4.43
16	66.7	30.9	2.16	55A	92.5	28.7	3.22	13A	24.9	27.6	.90	63A	95.2	24.0	3.97
18	52.5	22.9	2.29	56A	55.6	30.5	1.82	14A	65.4	22.8	2.87				
19	65.8	25.0	2.63	57A	56.5	36.6	1.54	15A	58.7	17.4	3.37				
				58A	4.45	25.8	.17	17A	19.6	28.6	.69				
				59A	82.3	25.0	3.29	18A	30.3	30.9	.98				
								19A	15.6	25.6	.61				
Aug.		26.71	1.85			30.1	2.19			27.14	1.18			32.0	2.04
Std. Dev.		4.44	.98			5.10	1.31			3.73	.84			5.50	1.49

Areas in mm^2
Loads in newtons
Stresses in newtons/mm^2

Interfacial area is plotted as a function of time in Fig. 4. The Durapatite material has 6% more interfacial area at 4 weeks. This area should be related to the growth rate of bone cells on the material in question, but may also be affected by the presence or absence of the marrow cavity, as shown in Fig. 3A, which is a surgical (exact location of the implant slot) and biological (absolute size at the tibia and relative size of the marrow cavity) variable. Thus the growth rate of the two materials is approximately the same.

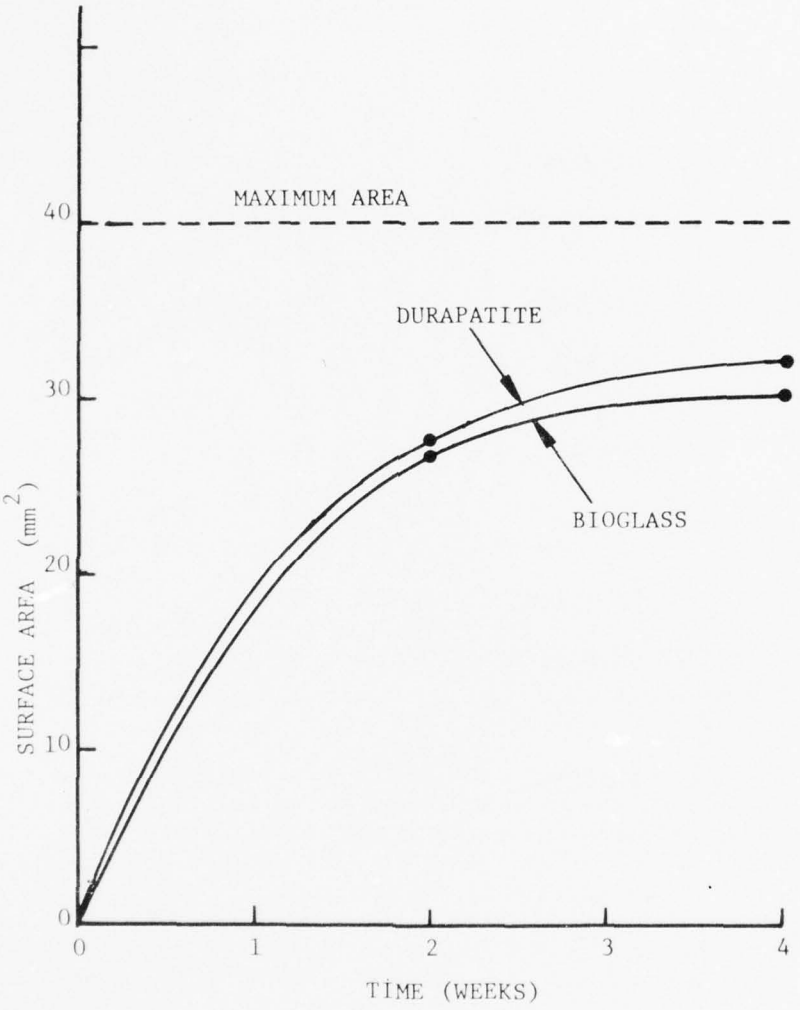

Fig. 4. Area of bone in contact with the implant as a function of time.

Examination of the failure loads in Table I reveals that, at 4 weeks, 93% of the bioglass and 73% of the durapatite implants would pass the 30N qualitative minipush-out test. The number that would pass the same 30N test at 2 weeks is 69% for bioglass and 56% for durapatite. There is a small fraction (<5%) for both materials that did not bond (failure load <5N) which is probably due to motion of the implant in the bone during the first 7 days while the bond is forming.

Results of the time dependence of bonding for both materials using the qualitative minipush-out test are summarized in Table II. It is apparent from these results that reliable bonding, at a 90% level develops by 10 days for both materials. By 30 days 100% reliability at the 30N failure load has been established. Thus, these results confirm the findings of the quantitative tests reported in Table I and establish that the qualitative minipush-out procedure is acceptable for rapid, inexpensive evaluation of reliability of bone bonding implants.

TABLE II

Time Period	Material	Failure load (newtons) 0-10	10-20	20-30	>30	Total # of rats
7 days	bioglass	1	2	--	7	10
	durapatite	4	1	--	4	9
10 days	bioglass	--	--	1	9	10
	durapatite	--	1	--	9	10
21 days	bioglass	--	--	--	9	9
	durapatite	1	1	--	10	12
30 days	bioglass	--	--	--	14	14
	durapatite	--	--	--	12	12

By combining results of both experiments it has been shown that 18 of 23 bioglass implants survive a 30N interfacial load at 10-14 days and 23 of 23 bioglass implants survived a 20N interfacial load at 10-14 days. Also, 37 of 38 bioglass implants survived a 30N interfacial load after a 21-30 day period of implantation. A previous study, Report #7, using the qualitative minipush-out model showed 30 of 30 bioglass implants bonded at the 30N load or higher at 30 days yielding a total of 67 of 68 bioglass implants which have been shown to bond at a 30N load level by 30 days. A total of 90 of 91 45S5 bioglass implants have been shown to withstand at least a 20N load by a 30 day period. This level of confidence in developing an interfacial bond is most encouraging for both purposes of implant quality control and eventual clinical application.

The reliability of bonding of the dense hydroxyapatite material, durapatite, is good but not quite as high as bioglass. Again combining results from the both sets of tests yields: 17 of 26 at a 30N load after 10-14 days; 21 of 26 at a 20N load after 10-14 days; 30 of 35 at a

30N load after 21-30 days. Thus, a total of 51 of 61 durapatite implants have been shown to withstand at least a 20N load by a 30 day period of time. The lower reliability of the durapatite bonding may be related to the expitaxial nature of the mineralization bond to this material. It may be more sensitive to variations in the width separating the implant and the surgical defect than bioglass which develops a very wide, >100μm, bonding zone.

Seven days is the lower time limit for this type of test. We feel that for shorter time periods the accuracy of the initial fit between the defect and the implant has a large effect on the results, i.e., the time required for new bone to grow into close contact with the implant is as important as the time required for the bond to form once contact is made.

In all the samples investigated, the bony tissue around the implant site appeared macroscopically normal for both bioglass and durapatite implants. No inflammation or infection was present. Reaction of the soft tissue surrounding the extremeties of the implants was minimal and slightly less for the durapatite samples than the bioglass implants.

Of the many materials we have tested using this procedure, such as dense alumina, porous hydroxylapatite, calcium phosphate glasses and a variety of nonbonding silicate glasses, durapatite is the only material that has demonstrated bond formation rates and reliability of bonding reasonably comparable to bioglass.

The quantitative minipush-out test procedure was conceived as a rapid and inexpensive extension of the qualitative mini-push out test and hopefully would provide an alternative to the use of dogs or other large animals for quantitative tests. The savings in animal care and surgical costs were more than offset by the increased technician time required to perform the mechanical testing and area determinations. The wide variation in results do not warrant the amount of time spent in the performance of the tests.

CONCLUSIONS

Several conclusions drawn from the data include:

1) Bioglass and durapatite implants have comparable rates of bond formation and bond strengths up to eight weeks implant time in rats.

2) Between 4 and 8 weeks the load required for failure is still increasing. Whether the stress at failure is increasing or the bonding area is increasing at a constant failure stress was undetermined.

3) A small fraction of both materials do not bond (failure load less than 5N). The reliability of bioglass at a 20N level is at 99% (90 of 91) by 30 days. The reliability of durapatite

bonding is somewhat less than bioglass, e.g., 84% (51 of 61) at 20N by 30 days.

4) Results using the quantitative minipush-out test show a slightly lower bond strength and rate of bond formation when compared with the qualitative minipush-out test series.

5) Any future quantitative tests could best be done on larger animals, e.g., dogs, that would allow many samples to be placed in a single animal and thus reduce the biological variables. Testing would be easier, and with properly sized implants stresses should be based on the surface area of the implant and the assumption that all of this area is in contact with cortical bone.

REFERENCES

1. Jarcho, M., Kay, J.F., Gumer, K.I., Doremus, R.H., and Drobeck, H.P. "Tissue, Cellular and Subcellular Events at a Bone-ceramic Hydroxylapatite Interface," J. Bioengineering, 1, 79-92, 1970.

2. Report No. 7, U.S. Army Research and Development Command, Contract No. DAMD 17-76-C-6033.

F. MECHANICAL PROPERTIES OF THE BONE-BIOGLASS INTERFACE

by

D.E. Clark, W.A. Acree and L.L. Hench

The bonding of bioglass to bone has been established in Reports 1-8. Furthermore, the chemical compositional variations that occur at the bone-bioglass interface have been well characterized in this research program. However, the correlation between the interfacial chemical profiles and mechanical properties of the interface has not been evaluated until now. The possibility that the bioglass-bone interface is elastically compliant is raised by the finite element stress analyses of bioglass tooth implants in canine evaluated by Klawitter and Weinstein at Tulane University, New Orleans, LA. The objective of the present investigation is to use microhardness measurements across bonded interfaces of specimens that have been implanted for various periods of time to determine the gradation in mechanical properties.

It is known that during implantation the surface of the bioglass is depleted in Na, Ca and P, thus producing a Si-rich layer. Subsequently, the Ca and P are redeposited onto the implant surface, i.e., over the Si-rich layer. The composition of this Ca, P layer varies over a finite thickness of 10-30 microns. At the Si-rich interface, the concentrations of Ca and P are low whereas at the bone interface the concentration of these elements are much higher and approximately equivalent to their concentrations in the bone. Thus, a smooth compositional gradient is established across the bone-bioglass interface during bonding. As shown in Report #8, the thickness of these layers stabilizes after ~1 year implantation in rat tibia.

It is proposed that since the composition varies across the interface (over a distance of >100 microns), the mechanical properties must also vary. It is extremely difficult, if not impossible, to measure certain mechanical properties such as tensile strength and elastic moduli of this interface with existing technology. However, it is possible to measure the hardness variations across the interface. This important materials parameter is related to the elastic modulus of the material. Although not necessarily a linear relationship, high values of hardness usually correspond to high values of the elastic modulus.

A rat tibia in which a 45S5 bioglass specimen had been implanted for one year was analyzed using the electron microprobe (EMP). The EMP method employed is described in detail in Report #8. The compositional variations that occurred at the cortical bone-bioglass interface are shown in Fig. 1. The thickness of the Si-rich layer that developed during the one year period was ~60 microns and the thickness of the Ca, P layer was ~20 microns.

Hardness values were obtained across this same interface using a Kentron microhardness tester. As with the EMP, the hardness data shown in Fig. 1 represent hardness values at various locations across the

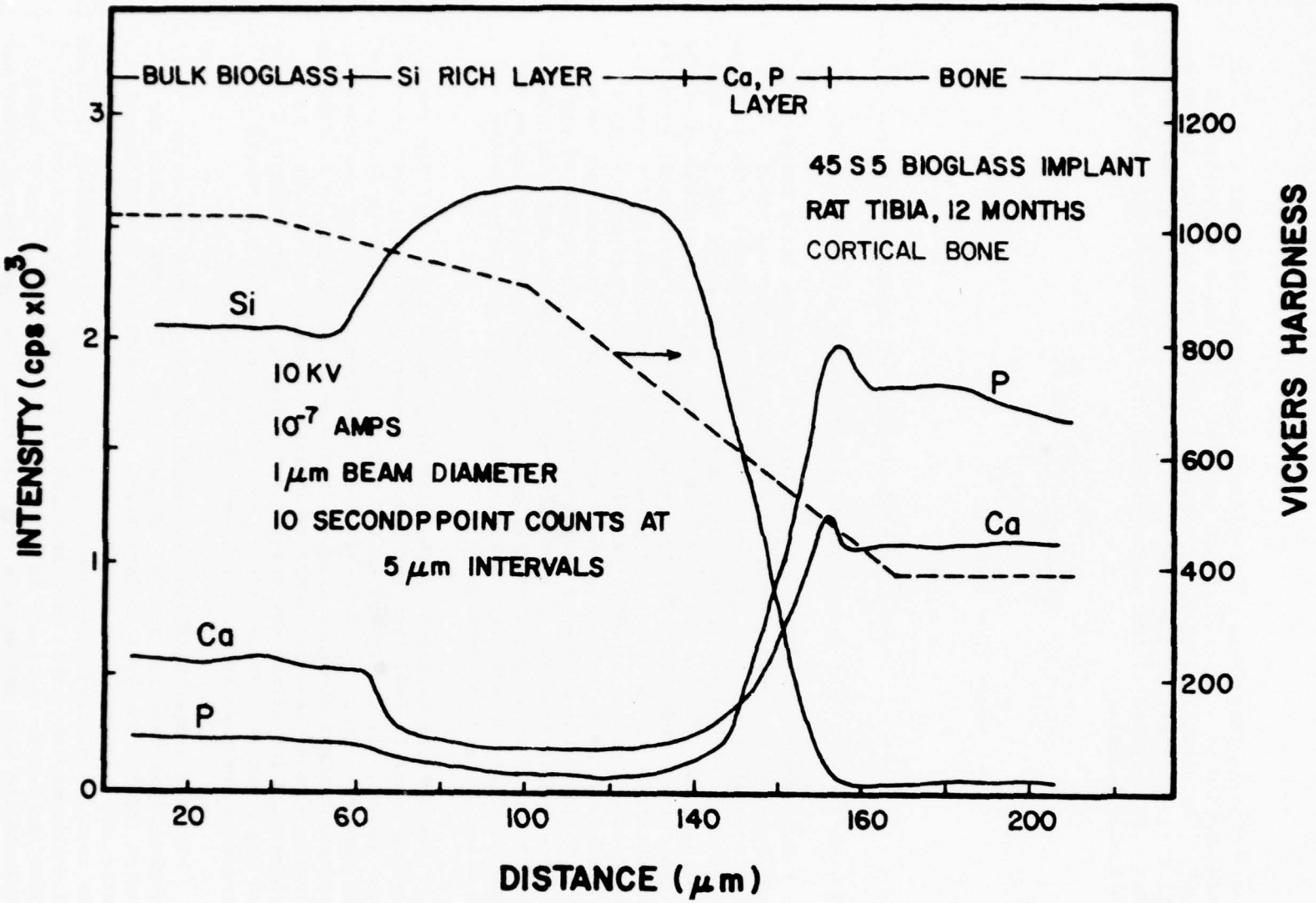

Fig. 1 Electron microprobe analysis and hardness evaluation of the bone-bioglass interface for a one year rat tibial implant.

bone-bioglass interface. This microhardness tester features a constant load applied to a pyramid shaped indentor. The angle of penetration is 136°. The dimensions of the indentation left on the specimen depend on its ability to deform plastically. In order to obtain a hardness measurement, the diagonal of the square indentation is measured and used in the following formula:

$$\text{Hardness} = \frac{2L \sin a/2}{d^2}$$

where L = load

a = 136°

d = length of diagonal of indention measured in microns

Typical values of the dimensions of the diagonals are 1-20 microns.

Hardness values are usually reported in Vickers units which range from 900-1300 for most glasses to 200 for metals such as steel. The magnitude of the load is extremely important when measuring the hardness of glasses. Excessive loads cause cracking of the glass and give spurious hardness values. When the load is too small, the dimensions of the indentation become difficult to measure leading to considerable error in the measurement. A 105 gram load was found to be adequate for measuring the hardness of the bone-bioglass interface. Indentations were made starting in the bulk bioglass near the interface. Measurements were also taken in the middle of the Si-rich layer, in the middle of the Ca, P layer and in the bone near the interface. Two measurments were taken in each position across the interface. The results are plotted on the same graph as the EMP data in Fig. 1 in order to show the relative location of each hardness value.

The average hardness of the bulk bioglass is 1072; that for the Si-rich layer in 884; that for the Ca, P layer is 621; and that for the bone is 403, all in Vickers units. Thus, there is a smooth decrease in the hardness across the bone-bioglass interface. The large decrease in hardness between the bulk bioglass and bone corresponding to a change in elastic modulus and difference in ability to deform plastically, is compensated for within the bonding interface by the intermediate Si-rich and Ca, P layers. These layers provide an incremental and smooth decrease in hardness across the bone-bioglass interface.

Table I summarizes hardness values obtained across the bone-bioglass interface for several implant times. Two sets of data are listed for the one year implant time. These data are from different interfacial locations on the same specimen (see Fig. 2). The data for the second and third specimens listed in Table I, corresponding to 6 and 12 months implantation, were measured in new bone. The data for the first and fourth specimens in Table I corresponding to 1 and 12 months implantation were measured in cortical bone. The same general trend was observed in the hardness values for all specimens; the hardness decreases uniformly from the glass, through the Si-rich and Ca, P layers, into the bone.

TABLE 1

Hardness Values Across the Bioglass-Bone Interface for Various Implant Times. Refer to Figure 2 for Location of Measurement.

Specimen	Location	Bulk Glass	Si-Rich Layer*	Ca, P Layer*	Bone
1 month	2	1339	517	286	
6 months	3	1015	696	355	177
12 months	1	973	498	350	198
12 months	2	1072	884	621	403

*Measurement taken in middle of layer.

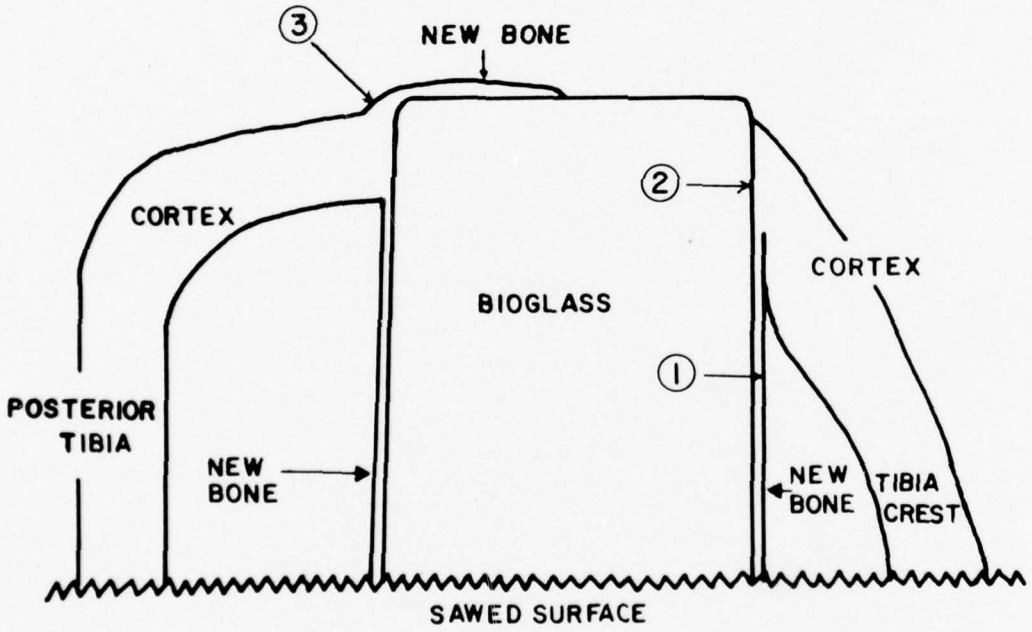

Fig. 2 Schematic drawing showing cross sectional view of bioglass implant in the rat tibia.

Several interesting observations can be made about the results shown in Table I. The continuing decrease with time in microhardness value for the bulk glass near the interface is perhaps a result of continued sodium ion depletion from the glass. The implant interface in close proximity to cortical bone (location #2) shows less change in microhardness with time, assuming the initial value of the bioglass is the same at both locations which is reasonable. The hardness values of the dense cortical bone and Ca, P layer in contact with the bone are also significantly higher in location #2 than in the newly formed bone of location #1 for the 1 year specimen. Apparently the density of the bone in contact with the bioglass and its vascularity affects the mechanical properties of both the bone and the interfacial bond developing between the implant and the bone. Additional evaluation of the microstructural features of the bone and correlation with the mechanical properties of the interface would be desirable. Also, it is important to establish the importance of type of bone on the rate formation of the interfacial bond and the mechanical strength of the bond.

G. THE PROMISE AND PROBLEMS OF BIOCERAMICS IN TOTAL JOINT REPLACEMENT

by

L.L. Hench

I. INTRODUCTION

Bioceramics are defined as ceramic materials designed to achieve a specific biological or physiological behavior. The use of bioceramics, in addition to biopolymers and biometals, provides additional versatility in the materials available for solution of health care problems.

Research objectives for use of bioceramics in total joint replacement include the following:

1. Decrease the presence of metallic corrosion products,

2. Eliminate polymer debris products from wear of articulating surfaces,

3. Minimize friction of articulating surfaces,

4. Minimize rate of wear of articulating surfaces and most importantly,

5. Decrease the incidence of loosening of acetabular and especially femoral components by eliminating use of PMMA by either

   a) achieving a minimal fibrous capsule formation, such as with dense alumina or pyrolytic carbon, or

   b) obtaining a direct chemcial bonding across the bone-implant interface through use of controlled surface active bioglass, or bioglass-ceramic coatings on high strength metallic or ceramic substrates.

It is just within the last 15 years that the interest in bioceramic implants has reached its present level of intensity. The early encouraging results of Smith and studies of a ceramic-polymer composite, Cerosium (1-4), followed by the pioneering efforts of Hulbert and Klawitter in demonstrating controlled growth of tissue into porous ceramics (5,6), the recent clinical successes of Boutin in using high density alumina ceramics for replacement of hips (7) and Bokros' and co-workers development of pyrolytic carbon cardiovascular devices (8,9) have been epochal steps in the generation of the field of bioceramics. The objectives of this paper are: 1) to describe briefly the various approaches taken towards designing bioceramic materials; 2) to review briefly the current status of potential applications of bioceramics in total joint prostheses; and 3) describe the current problems that must be solved

before various bioceramics can be used routinely in joint replacement in humans. The interested reader is referred to other more detailed reviews for additional information of the historical development of bioceramics (5,9), tissue growth in porous ceramics (6), and interfacial problems associated with bioceramic implants (10).

II. GENERAL BIOCERAMIC DESIGN FACTORS

A successful bioceramic material must satisfy a large number of design factors as discussed in a recent paper by the author (11). Among others, it must have suitable mechanical and biological properties and be able to be fabricated into functional devices. These are severe materials design limitations. It is the general lack of toxic components in many ceramic materials that has led to the considerable interest in designing ceramics for medical and dental applications. A number of tests have been developed to examine the biological compatibility of bioceramics and other biomaterials. Such tests usually involve the exposure of small samples of bioceramics to the soft tissues of small animals such as rodents (12,13) or to living tissue cultures in incubators (14,15). Of several dozens of ceramic compositions examined by such means only a few have shown sufficient compatibility with tissues to justify consideration for future medical and dental implants. Additional requirements of sufficient mechanical strength to serve a functional need as an implant and the necessity of fabricating the material into a suitable device further decreases the number of favorable bioceramic compositions. Consequently, at the present time the field of bioceramics can be generally classified into three types of materials.

Figure 1 illustrates the three major types of bioceramics in terms of a relative reactivity index. Nearly inert bioceramics show little chemical change during long term exposure to physiological solutions. Tissue response to this class of bioceramics involves a very thin, several micrometers or less, fibrous membrane surrounding the implant materials. Because fibrous tissues do not chemically bond to nearly inert bioceramics, fixation within the body must be established by a strong mechanical interlock with tissues. High purity alumina and pyrolytic carbons are currently the most acceptable bioceramics of this type. When high strength is required, fully dense alumina or pyrolytic carbon is utilized and the mechanical interlock is provided by large perforations in the implant, threads or steps on the surface (6,16), or use of polymethylmethacrylate grouting agent between the implant and bone to provide short term mechanical frictional fit. When strength requirements are sufficiently low, large pores of 50 to 200 μm cross sectional diameter can be utilized to establish mechanical interlocking by tissue ingrowth (5-8,17). This approach is shown in Fig. 2.

This microradiograph obtained by Klawitter and Hulbert illustrates bone (B) growing into the pores of 200 μm pores of an alumina ceramic implanted in a rabbit femur for 8 weeks.

A very high degree of control over the size and interconnection of the porosity can be achieved by the innovative replamineform process

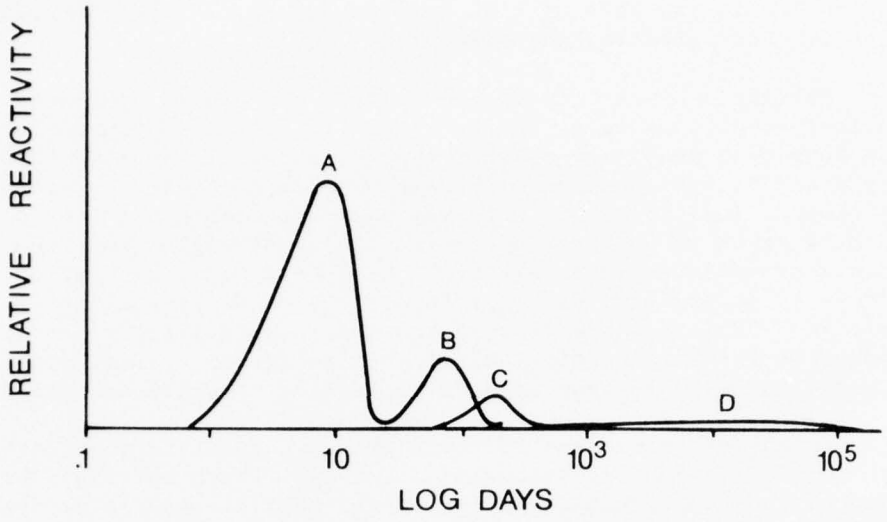

Fig. 1. Bioceramics reactivity spectrum. (A) Resorbable bioceramics, e.g., $Ca_3(PO_4)_2$; (B) Moderate surface reactive bioglass; e.g., Na_2O-CaO-P_2O_5-SiO_4; (C) Low surface reactive bioglass-ceramic; e.g., Na_2O-CaO-CaF_2-P_2O_5-SiO_2; (D) Nearly inert bioceramics, e.g., Al_2O_3 and pyrolytic carbon.

Fig. 2. Bone growth into porous alumina (by J. Klawitter and S. Hulbert).

developed by White, Weber, Roy and co-workers (18). In this process the uniform pore skeletal structures of certain marine invertebrates is replicated in the form of high purity alumina or other materials or directly converted to hydroxyapatite.

Fatigue and wear studies on fully dense alumina exposed to physiological conditions have reported there is little reason for concern for the long term stability of this type of material (18-20). However, aging and fatigue studies of porous alumina conducted by Frakes, Brown and Kenner indicate that there may be considerable concern for the long term strength of porous bioceramics (20). Strength reduction of porous calcium-aluminate bioceramics (21) with load and implantation is particularly severe (20) with fracture stresses decreasing to a range of only 700-900 psi. As will be discussed in detail later, recent fracture mechanics lifetime predictions of even fully dense alumina indicate a severe long term fatigue problem if tensile stresses are present (46).

At the other extreme of the bioceramic reactivity spectrum, Fig. 1, are totally resorbable bioceramics (22-24). Such materials must have compositions that contain only elements that are easily processed through normal metabolic pathways such as Ca and P. With time such reactive bioceramics are totally resorbed by the body and replaced by tissues. Consequently, the function of totally resorbable bioceramics is merely to serve as a scaffolding or filler of space, permitting tissue infiltration and replacement. This is a similar function of that provided by bone grafts from the host. However, a major advantage of the use of resorbable ceramics over host bone grafts is a ready supply, controlled variations in size, and elimination of a second surgical procedure. However, a disadvantage of this type of bioceramic is the serious strength reduction that occurs during the resorbtion process. Consequently, mechanical design factors must be seriously considered to eliminate fracturing of the tissue and resorbable ceramic structure during the intermediate stages of healing. One material, tricalcium phosphate, appears to be the most outstanding success of a bioceramic of this type (23,24). Calcium aluminate-phosphate compositions also show promise in monkey models. Micrographs, courtesy of Graves, et al. (22), Fig. 3, show the resorbtion of the microstructure of a 52 w/o CaO, 48 w/o Al_2O_3, 20 w/o P_2O_5 bioceramic during 16 weeks in a monkey femur. There is a strong compositional dependence of the rate of resorbtion in the various systems of this type.

Bioceramics in the middle of the reactivity spectrum, Fig. 1, are based upon the concept of controlled surface reactivity of the material. In this class of bioceramics the composition is designed such that the surface undergoes a selected chemical reactivity with the physiological system establishing a chemical bond between tissues and the implant surface (25-35). The chemical reactions are such that the bonded interface protects the implant material from further deterioration with time. Thus the potential of this approach is to combine the high strength of nearly inert bioceramics or biometals with surface chemical reactivity favorable to tissue bonding. Since controlled surface reactive implants are not restricted to being stabilized with the tissues only by mechanical interlocking, more flexibility in device design and fabrication can be achieved. Bioglass and bioglass-ceramic compositions developing

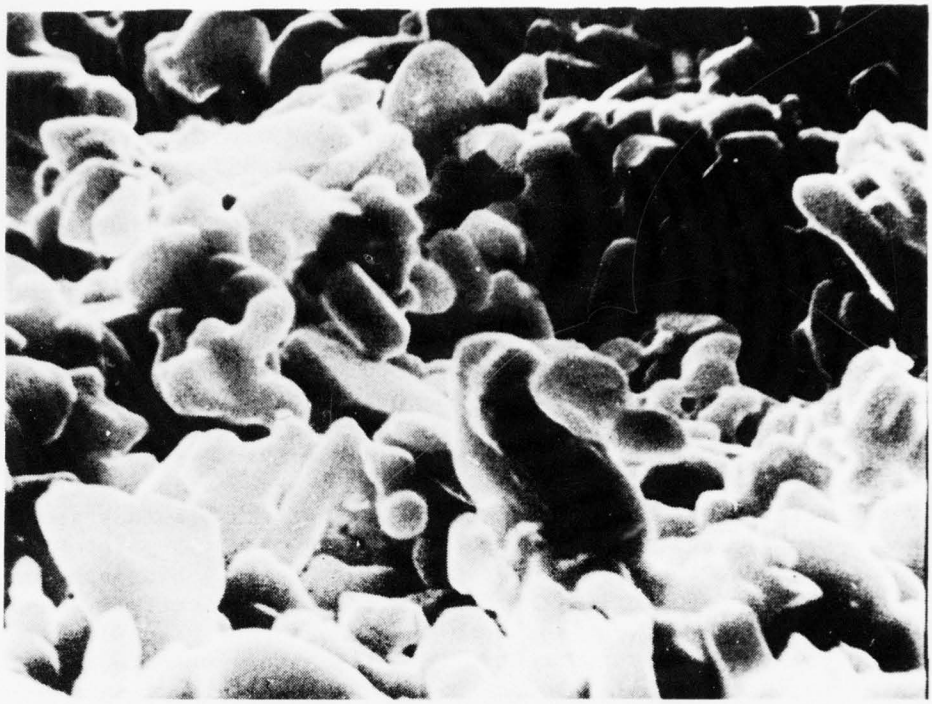

(A)

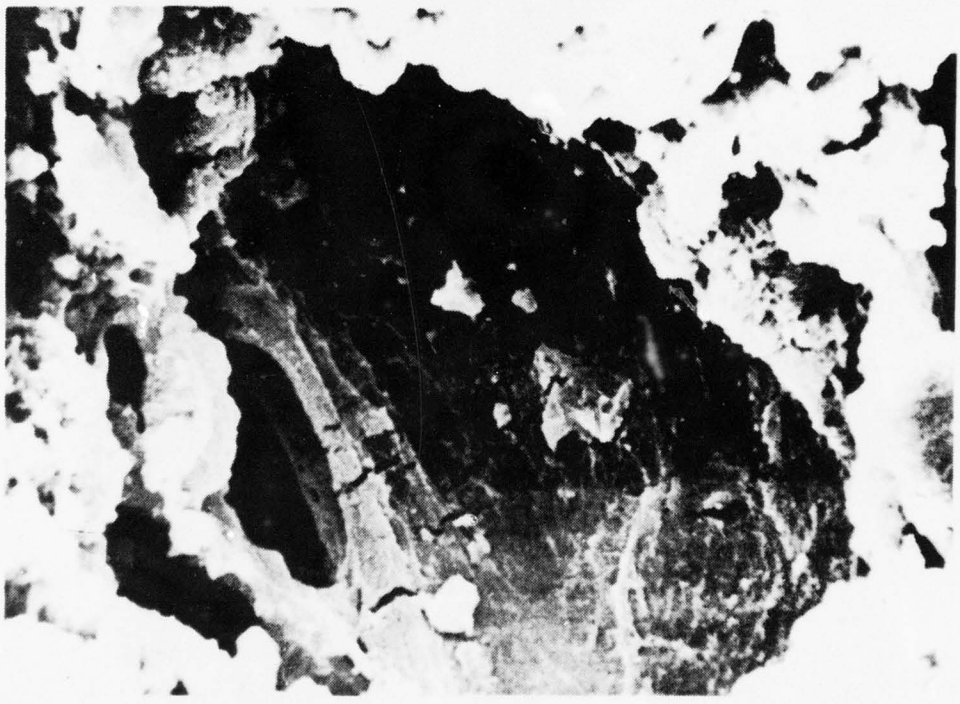

(B)

Fig. 3 Resorbable bioceramics (courtesy G. Graves).

(A) Before resorbtion by bone.
(B) Partial resorbtion after 16 weeks.

a reactive calcium phosphate mineralizing bond with bone are successful examples of this approach towards bioceramics (25-35).

Figure 4 illustrates the structural contiguity that develops at a bone and bioglass interface. A microtomed 700 A thin section of a 45S5 bioglass implant in a rat tibia for 3 weeks is shown in the scanning transmission mode of a Phillips EM 301 microscope (Fig. 4). The dark areas are structural remnants of the interfacial bridges between bone and bioglass after passage of the microtome, which also fractures the section (light areas). In Fig. 5 is shown the results of compositional point counting at 0.1 μm intervals in the thin section at points 1-4 using energy dispersive X-ray analysis in the transmission electron microscope. The Si in the bioglass implant serves as a tracer to identify the interface. There is a transition between bioglass and bone between points 3 and 4. The compositional spectrum at point 4 is characteristic of bone, the spectrum at point 1 is that of bioglass and those in between are characteristic of the interfacial, chemically bonded bridge between the implant and bone. To the author's knowledge, this data represents the first direct proof of the ability of a foreign material to form a stable, compatible bond with living tissues.

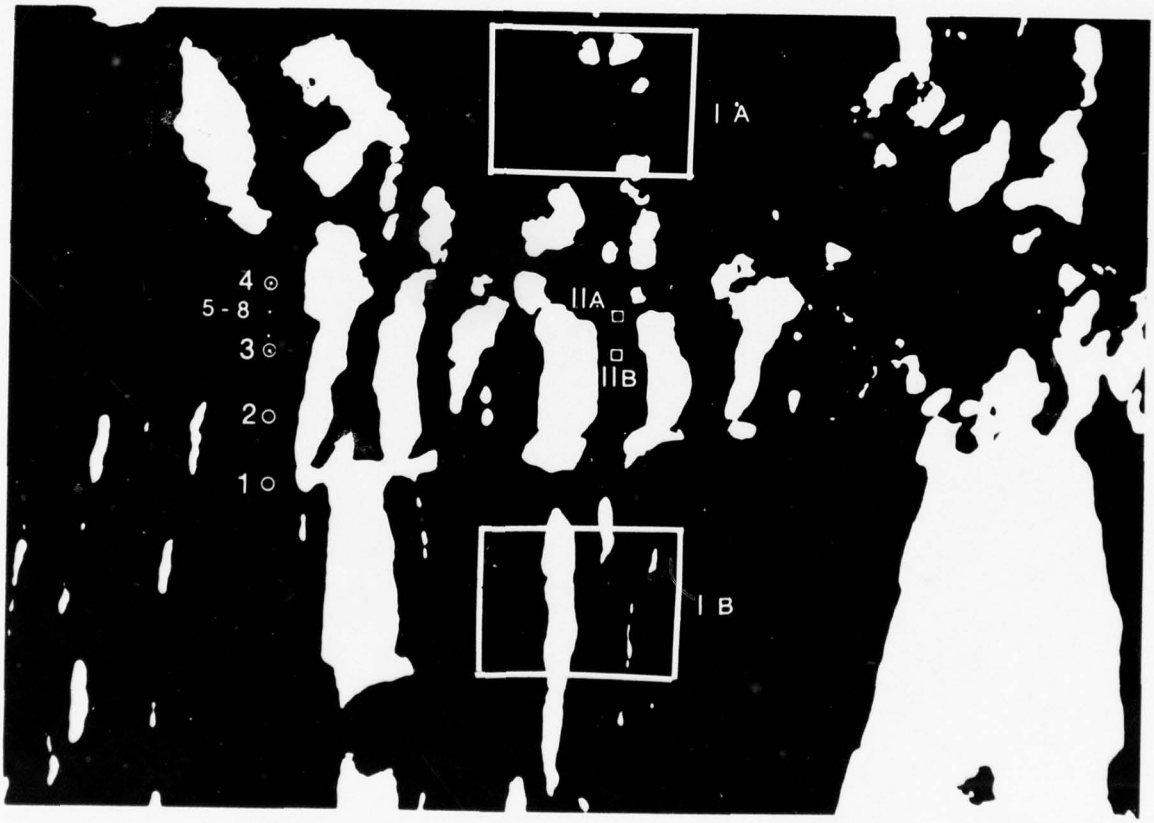

Fig. 4. Scanning transmission electron micrograph of bone-bioglass bonds. Area (I) is bioglass and area (II) is bone (see Fig. 5A for compositional analysis). Points represent point count analysis (see Fig. 5B).

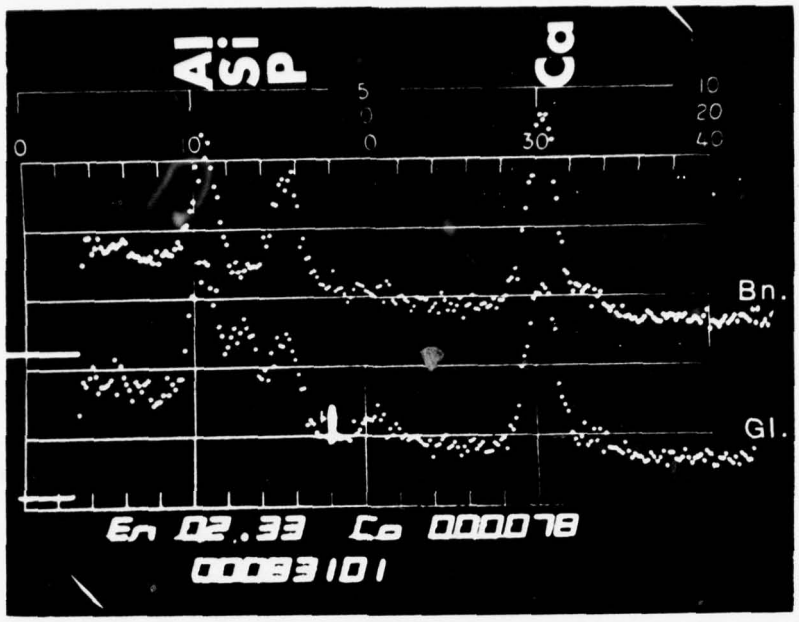

A

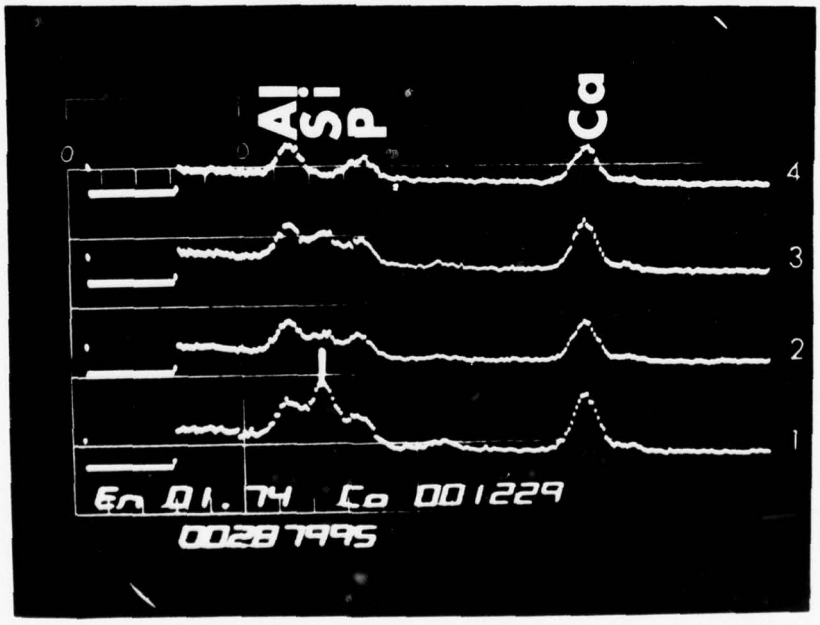

B

Fig. 5. (A) Energy dispersive X-ray spectra of areas (I) and (II) in Fig. 4. Peak assignments of Ca and P (from bone), Ca, P, Si (from bioglass) and Al (from sample holder) are indicated. (B) Similar to 5A but for region equivalent to points shown in Fig. 4. Peak assignments are the same.

High density apatite ceramics may also be promising as bioceramics (36-39) that form a bond with bone.

Potential applications of nearly inert, resorbable, and surface reactive bioceramics in total joint replacement are described in the following section. The final section delineates current problems associated with these potential applications.

III. POTENTIAL ORTHOPAEDIC APPLICATIONS

Dr. P. Boutin's implantations in France of more than 700 hip joints of high density 99% alumina bioceramics has pioneered the accelerating use of high density alumina in orthopaedic skeletal repair (7). The Boutin prosthesis is composed of a nearly inert high density alumina ball and socket joint. The ball component of the joint is attached by a mechanical self-locking joint to a titanium shaft to go into the femur. Both halves of the joint are cemented into place using polymethylmethacrylate (PMMA) bone cement. The purpose of the alumina joint over the standard prostheses composed of a metal ball with high density polyethylene or metal cups is to reduce the wear within the joint and to eliminate metallic or polymeric wear particles which can be toxic. A five year followup of 590 cases shows no mechanical failure of the alumina components after implantation (7).

The efforts of Drs. Griss and Heimke and co-workers (19,40) have been directed towards elimination of the use of PMMA bone cement as well as reduction of wear within the joint. They have achieved part of their objective by recently completing the design and implantation of more than 100 high density alumina joints in patients in both Germany and the U.S. The acetabular, component is mechanically screwed into the hip after preparation of a carefully tapped hope in the bone, or is fit into a square osteotomed cavity. PMMA is not used with either acetabular cup designs. Special surgical tools are required and are available. The femoral component in the Griss-Heimke hip continues to be a metal shaft and at present is cemented into place with PMMA. Thus, approximately one-third of the typical quantity of PMMA is required for this prostheses.

The Griss-Hemike animal research does not show promise for the use of a total alumina oxide femoral component. Although some successful tests have been completed in sheep, most femoral stems of fully dense alumina fracture after several months of use (41).

A further aspect of the Griss-Hemike study is the collaboration with the author's research team which has resulted in the fabrication of single and multiple layers of bioglass coatings on high density alumina total hip prostheses (42,43). Results from bone bonding studies in rats and dogs indicate that the bioglass coated alumina does bond to bone and prevents formation of a fibrous capsule (43,44). Total hip prostheses composed of bioglass coated alumina have shown the capability of establishing a direct chemical bond with the bone in sheep (42,44). Figure 6 shows results of a successful 3 month implant. Mechanical testing

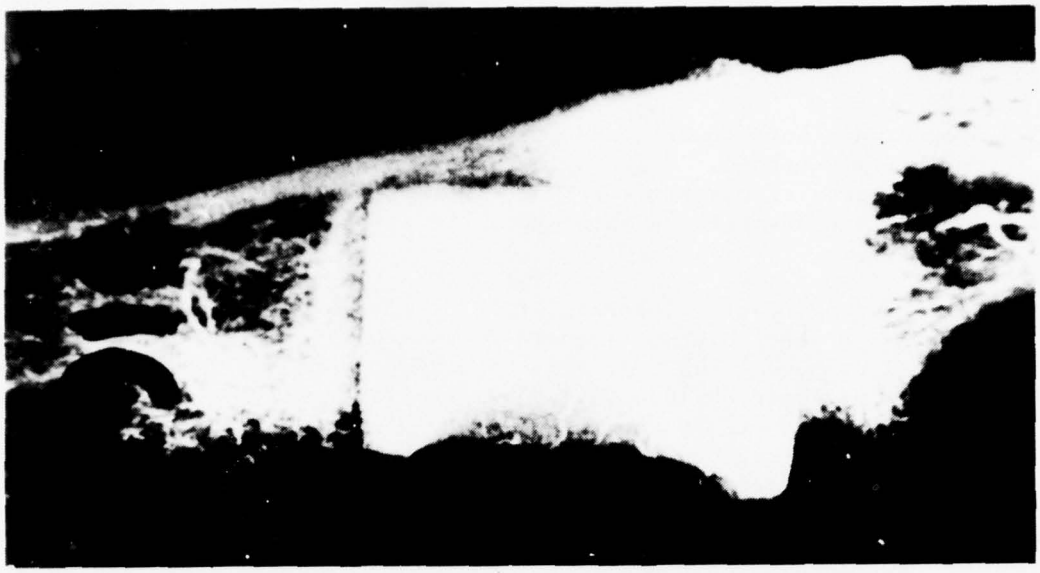

(A)

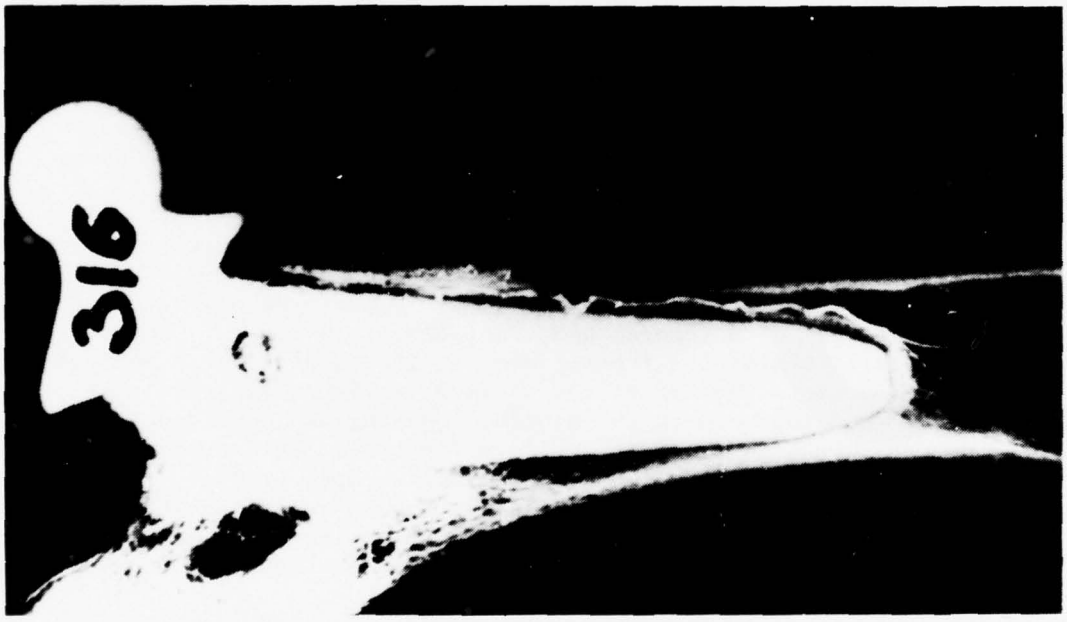

(B)

Fig. 6. Bioglass coated high density alumina total hip after 3 months implantation in a sheep (courtesy of P. Griss, G. Heimke, and J. Jentschura).

(A) Acetabular component firmly bonded into place with use of bone cement. Notice healthy blood supply (white lines).

(B) Femoral stem bonded into place by the bioglass coating. Notice new bone and blood capillaries at end of the implant.

showed that both femoral and acetabular components of the prostheses were firmly bonded. X-radiographic evidence showed new bone formation at the areas of maximum stress for both femoral and acetabular components and angiography shows good aterial supply to the bonded interface (42).

However, further testing of total hips of the bioglass coated dense alumina in sheep did not lead to successful implants. Fracture of the femoral component was typically observed. A recent analysis of the failure of these devices (44) shows that there is a tendency for separation of the bioglass coating from the alumina substrate. Bonding of the bone with regions of bioglass was observed but continuous bonding and stem fixation did not result due to failure at the glass-alumina interface.

Subsequent improvements of the bond at the bioglass-alumina diffusional interface have apparently eliminated this type of failure based upon the recent success of Smith using this type of implant for orthopaedic manipulation of the jaw in several monkeys (45). Loads from orthodontic appliances applied to the bioglass-coated alumina implants were sufficient to close the bony defects without movement of the implants, fracture of the devices, or failure of either the bioglass-alumina interface or bioglass-bone interface. However, even the best bioglass coated alumina tested to date also shows evidence of susceptibility to long term fatigue, although not as severe as uncoated alumina (46).

At the present time the most promising bioceramic system for joint reconstruction without use of PMMA is based upon bioglass coated surgical metal alloys. Evaluation of the biomaterials and device design involves use of a femoral head replacement in monkey. Short term immobilization of the femoral stem of the prosthesis is ensured by using a square cross section of the stem and a tight mechanical fit at surgery. Bonding between the bioglass coating and bone develops within several weeks to provide long term fixation. The animals are permitted to use the implanted limbs as they desire upon recovery from anesthesia. Visual inspection of the animals in the run indicates that full load bearing is applied within a couple days post-op. We feel this approach is essential for a mature interfacial chemical bond to develop between the coating and bone.

The first primates implanted were stumptail monkeys using 45S5F bioglass flame spray coated onto 316L surgical stainless steel devices. After 12-14 months the animals were sacrificed and the prostheses could not be forcibly extracted from the medullary canal (34,44). Metallic corrosion of the device was also prevented by use of the bioglass coating as shown using TEM histology of soft tissues adjacent to the head of the prosthesis (31).

In a subsequent experiment a somewhat smaller prosthesis of the same configuration (44) was implanted in Cynamologous monkeys (micaca fasicularis) using a similar surgical technique (31, 47).

After 6 months of use, the femoral head replacement was found to be almost totally surrounded with bone and was tight within the femoral stem, even after all the bone around the proximal end of the implant had been resected. Mechanical testing of the implant was conducted within 24 hours after sacrifice. At a force of 258 lb-f, the distal condyles were torn off the bone with no loosening of the implant. Three point bend tests causing fracture of the bone at 257 lb-f also did not loosen the implant. After the mechanical testing, the implant in its bony bed was sectioned with a diamond wafering saw for analytical evaluation of the bone-implant interface.

The 45S5F bioglass-coated femoral head of monkey hip prosthesis still attached to bone (B) after mechanical testing is shown in Fig. 7. A portion of the bone has been removed by osteotome to expose the implant surface (G). Fragments of bone are still attached to the exposed surface.

Fig. 7. Bioglass-coated femoral head of monkey hip prosthesis showing (B) attached bone and (G) osteotome-exposed implant surface (2X).

A scanning electron micrograph of a cross section of the implant and bone, Fig. 8a, shows three morphological regions: metal (M), bioglass coating (BG), and bone (B). Microporosity which can be seen at the bioglass-metal interface often occurs in flame spraying and can lead to destruction of the bioglass-metal bone in vivo if a sufficiently large number of such micropores are present. A fracture line of crack (C) runs along a portion of the bioglass-bone interface. As discussed below, it is likely that this is a drying crack between the bioglass and the interfacial bonding gel layer. No evidence of a fibrous capsule between the bone and the implant is present in this section. However, during sectioning of the femur and the implant stem, not all portions of the bone remained attached to the glass; this indicates that less than 100% of the interface is bonded at 6 months.

Energy dispersive X-ray (EDX) analysis of three regions 50 μm from each other across the bioglass-bone interface are given in Figs. 8b, 8c, and 8d. The EDX data show a decrease in concentration of Si and a variation in the Ca/P ratio across the interface from bioglass to bone. It is important to note that these compositional gradients occur across a region that is structurally contiguous and morphologically uniform. EDX analysis at various locations around this section of the implant-bone interface shows similar results.

Results similar to those obtained for the monkey femoral head prosthesis were obtained in just 10 days with bioglass-coated 316L stainless steel implants in rat tibiae. A 45S5 bioglass coating was applied to both sides of the steel implant by using a recently developed immersion coating process (Reports #7 and #8). This process eliminates most of the microvoids at the bioglass (BG)-stainless steel (SS) interface, as can be seen in Fig. 9a.

After ten days post-operative, the animal was sacrificed and the tibia removed. The implant resisted mechanical removal by a 30 N minipush-out test recently developed (Report #7). SEM evaluation of the bone-implant interface showed that 40-60% of the implant surface had achieved a bony union at the 10 day interval. An SEM of one of the bonded areas is shown in Fig. 9a and the corresponding EDX data across the contiguous junction are given in Figs. 9b, 9c, and 9d. The compositional gradients characteristic of the bioglass-bone interface are similar to those shown above for the monkey implant, indicating a decline in Si content across the interface from glass to bone.

Lack of control over the bioglass flame spray coating process led to a considerable number of failures of femoral head prostheses in monkeys due to corrosion between the metal and the bioglass coating resulting in spalling of the glass. Thus, motion of the metal stem in a shell of bioglass bonded bone occurred which is an unsatisfactory result.

The rapid immersion process for coating 45S5 bioglass onto 3316L surgical stainless steel has recently been extended to the coating of femoral head prostheses for the monkey model. The rapid immersion coating process eliminates most of the microporosity between the coating and the metal an results in a reliable coating that can be fabricated routinely including devices as large as the stem of Moore prostheses.

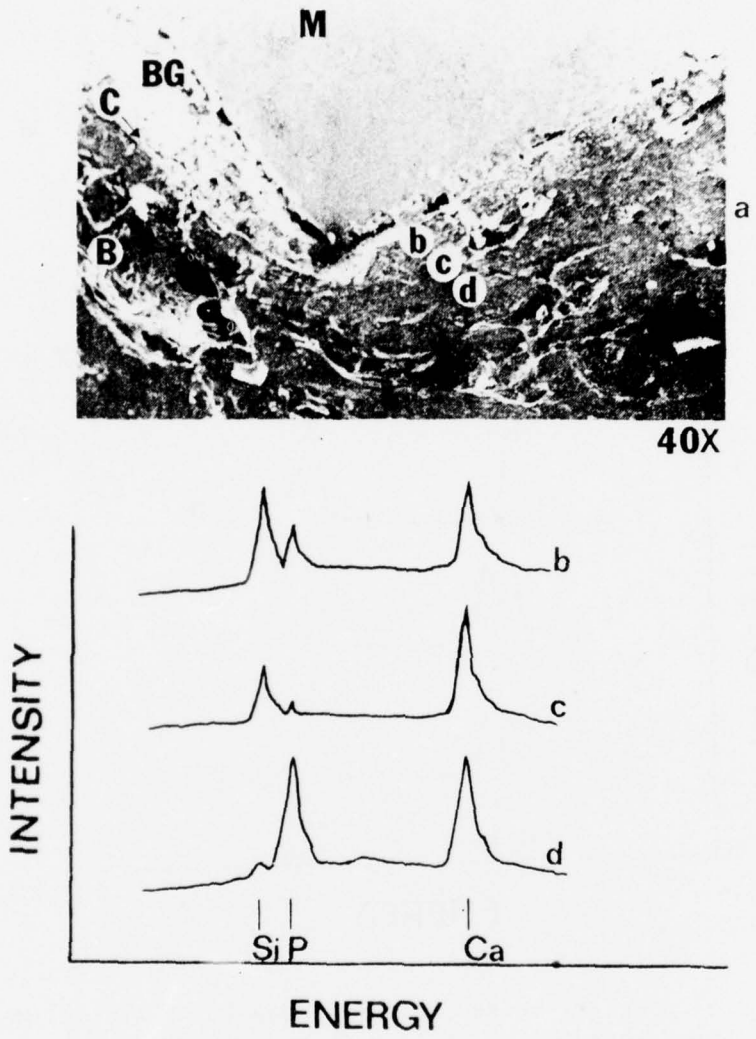

Fig. 8. (a) Cross-sectional view of a monkey hip implant and bone with the metal (M), bioglass coating (BG), and bone (B) indicated. Interfacial regions (b,c,d) are identified by corresponding EDX spectra.

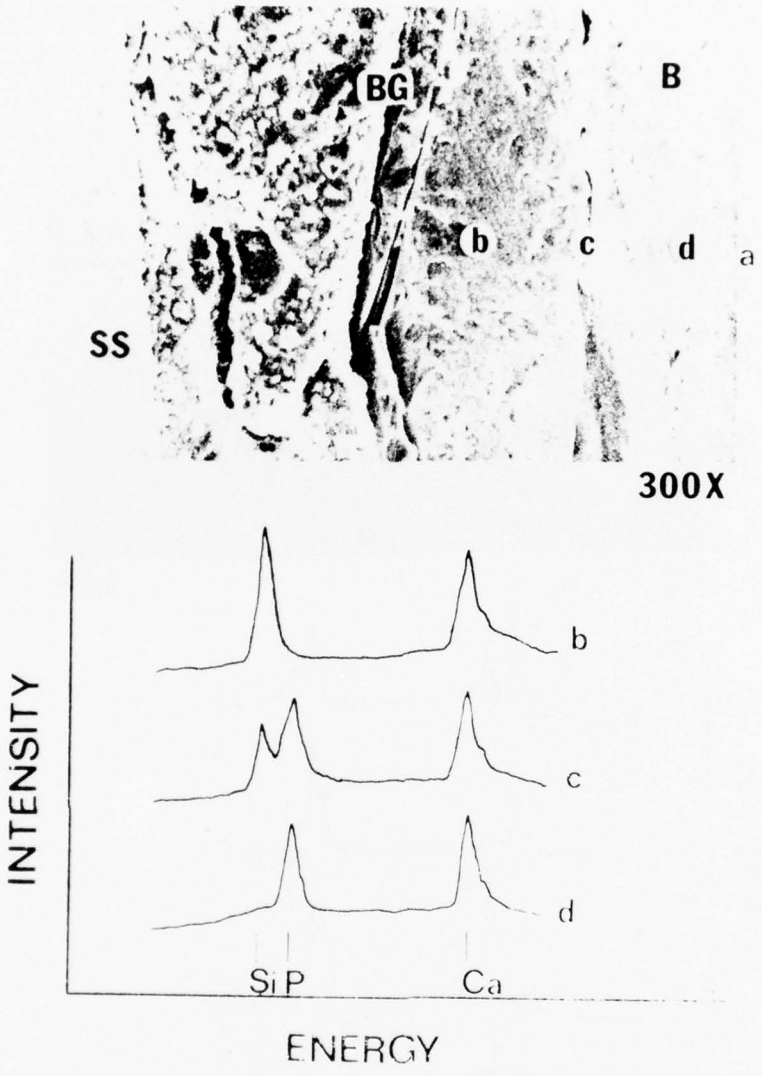

Fig. 9. (a) Bioglass-coated stainless steel rat tibiae implant with three interfacial regions (b,c,d) identified by corresponding EDX spectra.

The prime objective of the most recent experiments is to determine how rapid a strong mechanical interfacial bond is achieved with the bioglass coatings. Thus, the implants are tested eight weeks post-operatively uing a tensile pull out test of the device post sacrifice. The results recently reported (50) show that tensile loads as high as 137 lb force have been withstood by the femoral stem-bone interface before failure occurred. At this level of loading the bone-bioglass bond remained intact and the coating came off portions of the metal stem.

Thus the current status of the bioglass coated 316L stainless steel system is summarized: Bonding of the bioglass coating to the bone of the medullary canel occurs at least as early as eight weeks. The implant is functional within days after surgery. Tensile testing of the bonded stem results in an interfacial strength greater than the femur, 258 lb-f, if the coating does not separate from the metal. The flame spray coating process is not reliable at the present time. Debonding of the rapid immersion coating from the 316L surgical stainless steel is still observed, albeit at loads several times body weight.

The latest advance in achieving a highly reliable bioglss-metal interface on a high strength surgical alloy and still maintaining bioglass-bone bonding is the recently reported bioglass coated - Co, Cr alloy system (47). A series of bioglass compositions within the bone bonding region, Fig. 10, was optimized for coating on Vitallium(R), a Co-Cr surgical alloy. The optimal composition, designated 52S4.6 results in a very thin diffusional bonding zone between glass and metal, Fig. 11, that can be produced uniformly over the stem of femoral prostheses with a minimum of interfacial porosity or alteration of physical properties of the metal.

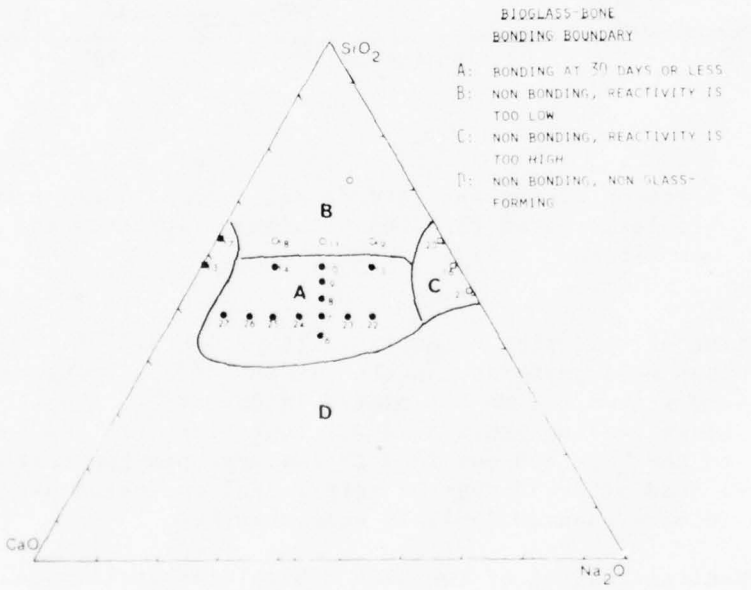

Fig. 10. Compositional range for bonding of rat bone to Bioglass in 30 days.

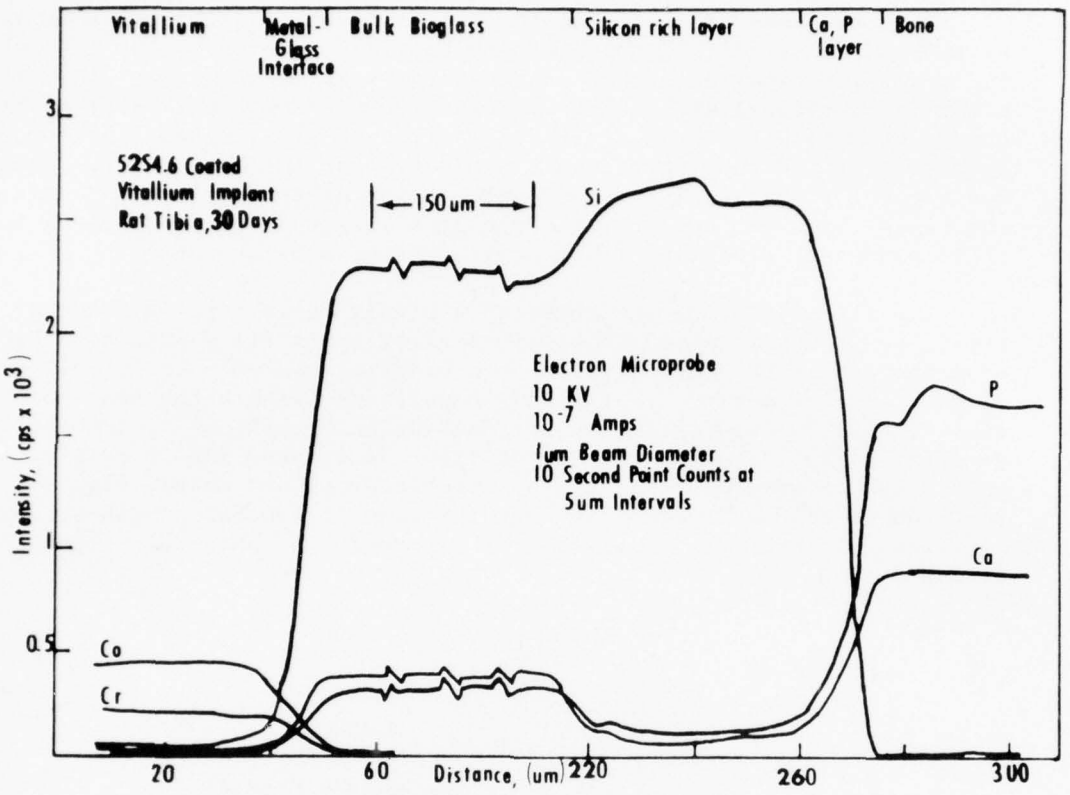

Fig. 11. Electron micrograph interfacial compositional profile of bioglass coated (52S4.6) vitallium implanted for 30 days in a rat tibia.

Testing of corrosion susceptibility of the 52S4.6 bioglass-Vitallium interface has been performed in the rat in the following manner. An implant 4 mm x 4 mm x 1 mm was placed in defects of the tibiae of rats with the glass coating exposed on all four sides of the implant. Exposure to the bone did not lead to failure upon application of a mechanical load after 30 days of interfacial corrosion has occurred. No failures in more than 20 implants were observed.

Mechanical testing of the 52S4.6 bioglass-Vitallium coatings using thermal shock methods also have shown large improvements in interfacial shear strength of the coating-metal interface over the bioglass coated-stainless steel system. Thus the required characteristics of a stable high strength metal-bioglass interface and a stable bioglass-bone interface appear to be achieved with the 52S4.6 bioglass coated-Vitallium prostheses.

Based upon these findings a series of monkey femoral head prostheses equivalent to the 316L stainless steel devices described above have been cast from Vitallium. Coating of the prostheses with the 52S4.6 bioglass formula is being completed and the implant mechanical testing will be conducted in future tests. If this series of tests is successful a longer term evaluation using the same models will follow.

A similar research objective is being pursued by a West German research team. The composition of their surface active glass-ceramic material (termed Ceravital) is similar to the 52S4.6 bioglass discussed above. Their studies of implants in rats, canines, and porcine models confirmed direct bonding of bone to the material. Nearly 50 humans have received tooth implants and mandibular ridge augmentations with the German surface active glass-ceramic material.

Metal total hip prostheses designed for canines coated with Ceravital surface active glass-ceramics are currently being tested by the W. German team. Their coating process involves enameling a ground coat and inert glass layer on the metal and a final fusion of surface active glass-ceramic granules within the inert glass layer. The surface active granules provide growth sites to bone when the device is implanted. Initial fixation is achieved with a close mechanical fit. Stable fixation by bone bonding is reported for an excess of 1 year post-op.

Surface active glass-ceramic granules of up to 70 volume percent have also been added by the same German research team to polymethylmethacrylate. The bio-active bone cement reduces the temperature rise during the in situ polymerization and apparently reduces free monomer transport within the circulatory system as well. Histology of the interface of the bio-active cement and bone shows that bone growth to the granules occurs wherever they are exposed to living bone at the cement interface.

Total hip components made of nearly inert Nucerite(R) glass-ceramic coated steel have been implanted by Englehardt and co-workers (48) using the PMMA cementing procedures. Preliminary results of this system also look encouraging at this time. However, there is no indication that elimination of a cementing media can be obtained with the use of the Nucerite(R) glass-ceramic coating.

Several other investigators are also proceeding to evaluate the potential for use of alumina ceramics in hip and knee joints. They include Semlitsch, et al. (49) and Eyring (50).

High density alumina long bone replacements using a non-cementing self-locking conical sleeve device has also undergone extensive tests in humans by a research team of M. Salzer and M. Plenk, et al. (49). Over 20 such prostheses have been utilized to restore the skeletal system for patients that have had to have surgical removal of long bones as a cancer treatment. Mechanical failure of the ceramic has not been observed for cases that now have been as long as 24 months. Stability of the alumina-bone interface also appears to be reasonable at this stage.

One of the longest histories of the use of ceramic implants is Professor Eyring's seven years of clinical studies in humans using high density alumina as a temporary spacer for osteotomies (50). The clinical studies were proceeded by a series of fibroblast tissue cultures, injection of alumina crystals in rabbit knees and implantation of small blocks of the alumina subcutaneously or intramuscularly in rats (50). All results showed extremely good biocompatibility with only a very small reactive membrane of a few μm thickness being formed. Implantation of a partial replacement of the knee of monkeys also preceded the human studies and recently total hip replacement has been performed successfully in dogs.

High density aluminum oxide spacers have been used by Eyring for opening wedge tibial, femoral or phalagenal osteogenomities 20 times in 14 patients without any untoward reactions (50). Use of the material obviates the need for a second operation to remove bone and the spacer saves considerable time and possible morbidity. Use of alumina spacers have also enabled Dr. Erying and co-workers to perfect a technique for a one stage femoral lengthening up to nearly two inches in seven patients with congenital or growth defects. Repeated osteogenomities have gained up to 5 inches in length for one patient.

Skeletal extensions such as needed for attachment of a permanently implanted artificial limb have also been explored using ceramic materials. A successful implanted limb was reported for humans and dogs by Dr. Mooney, et al. (52,53). Reasonable success was achieved for a short time. Dr. C. William Hall has been systematically exploring the many variables necessary to obtain long term success in permanently attached artificial limbs (54). He has achieved stable soft tissue interfacing by use of Nylon velour and silicone composite systems. Bioglass coatings applied to stainelss steel shafts have been used to achieve stability of the limb in contact with the bone in a goat model (54).

Plasma spray coated γ-alumina coatings of titanium alloy metals are showing reasonably long term (4 years) success in Italy (55) for total hip replacements. These implants are also used without PMMA and the surface active γ-alumina shows some evidence at the TEM level of forming bony attachment to the coating.

IV. CURRENT PROBLEMS IN APPLICATION OF BIOCERAMICS IN TOTAL JOINT REPLACEMENT

The objective of this section is to discuss briefly area of uncertainty that must be investigated before the three major types of bioceramics can be considered for large scale clinical applications.

First, there seems to be little potential for use of resorbable bioceramics in most types of total joint prostheses. The low mechanical strength of these highly porous materials and the severe deterioration of mechanical integrity with resorbtion pose an unsurmountable obstacle to use in any load bearing application.

Secondly, the increasing use of high density alumina in Europe in total hip prostheses means the long term physical behavior of this material must be examined closely. All brittle materials under tensile stresses are subject to slow crack growth of pre-existing flaws which leads to time dependent fatigue failure. The time to failure is always a function of the magnitude of the tensile stress applied, the distribution of pre-existing flaws, and an environmentally sensitive factor. Fracture mechanics theory is now developed to the point where all the necessary factors can be evaluated for a potential implant material such as high density alumina and lifetime predictions made (56-58).

Such a fracture mechanics study has been recently completed in the author's laboratory in collaboration with Prof. Ritter at the University of Massachusetts for a commercial high density alumina implant material with and without a bioglass coating (46). Both three point flexural tests using bars and biaxial flexural test configurations using thin discs were studied. The test environments included: liquid N_2 (where no environmental factors are present), air (80% RH), tris buffered water, and Ringer's solution. Various stress rates over a range from 500 psi/sec to 80,000 psi/sec were used in the dynamic fatigue test. Ten to fifteen samples were run for each data point. A definite environmentally dependent slope to the fracture strength of both coated and uncoated alumina was observed, see Fig. 12.

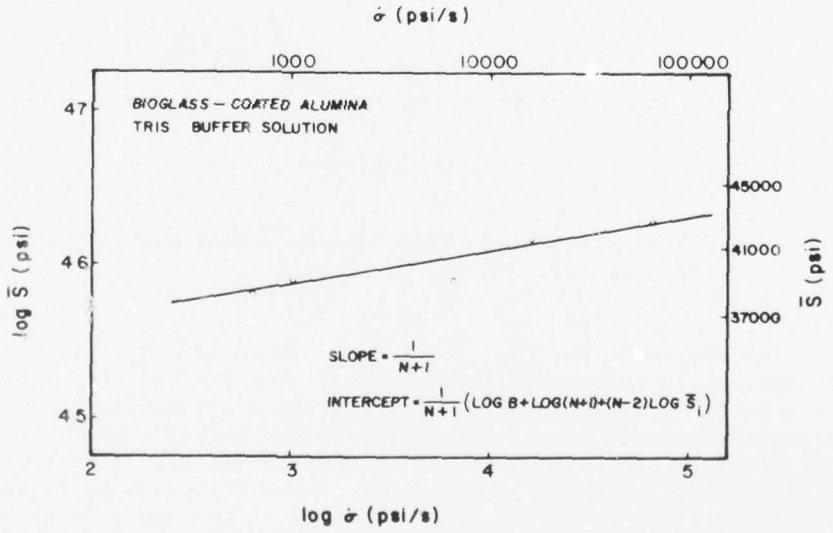

Fig. 12. Dynamic fatigue data of bioglass-coated alumina in a tris hydroxyaminomethane buffer solution.

Use of the dynamic fatigue data permitted calculation of design diagrams for the guaranteed lifetimes of the samples in a given environment, for a given applied tensile stress, and a given proof test applied to the samples. Figures 13 and 14 show the design diagrams obtained and Table I summarizes some of the relevant allowable tensile stresses that can be applied to this material to assure a minimum lifetime of 50 years. It is evident from the data that although the intrinsic strength of the material is in excess of 45,000 psi the material should not be used in an implant application where tensile stresses will exceed 15,000 psi.

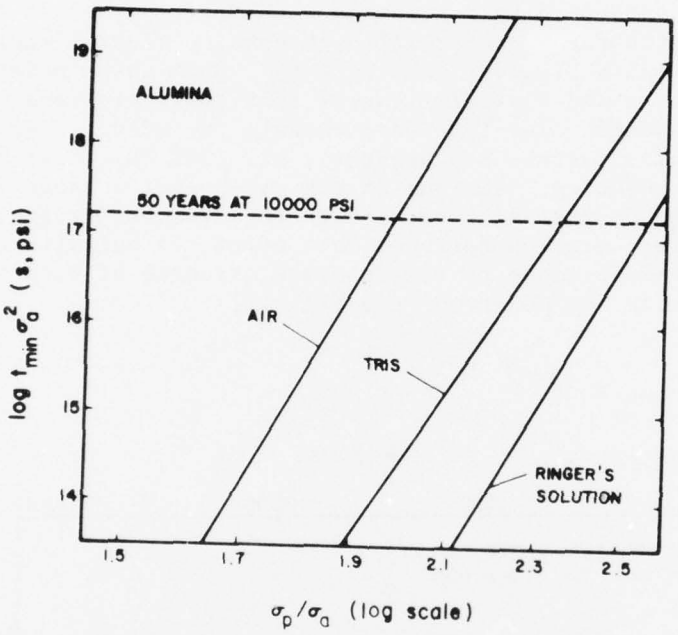

Fig. 13. Design diagram of lifetime predictions after proof testing for alumina.

The mechanism for this fatigue phenomena is not fully understood but appears to be related to H^+ ion exchange for Ca^{2+} ions which concentrate in the grain boundaries of the alumina during the firing stage of processing. Basic research in this area is sorely needed. Determining the relative magnitude of the environment sensitive parameters as a function of time in the in vivo environment must also be established. Relating purity levels and microstructure to the environment sensitivity is required. Autoclaving appears to accelerate this phenomena and the relative extent needs to be determined. Bioglass coatings apparently diminish the problem but the coatings must be optimized.

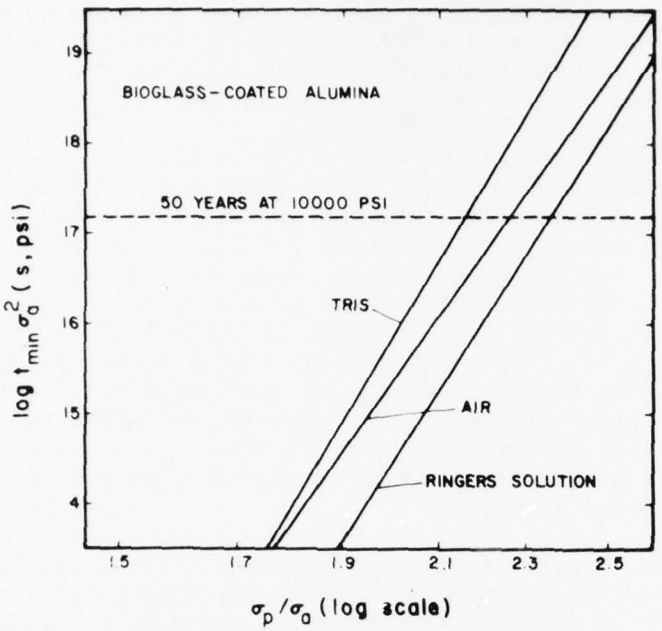

Fig. 14. Design diagram of lifetime predictions after proof testing for bioglass-coated alumina.

TABLE I

PROOF STRESS AND ALLOWABLE STRESS PREDICTIONS TO ASSURE A MINIMUM LIFETIME OF 50 YEARS

Material	Environment	σ_p (for σ_a = 10,000 psi)	σ_a (for σ_p = 30,000 psi)
Alumina	Air	19855 psi	14840 psi
Alumina	Tris	23603	13406
Alumina	Ringers	25806	11547
Bioglass-Coated Alumina	Air	22563	13091
Bioglass-Coated Alumina	Tris	21534	13722
Bioglass-Coated Alumina	Ringers	23590	12568

A recent study by Prof. Brown and students at the University of Illinois shows that the interfacial strength of plasma spray coatings of alumina on metal is also seriously degraded upon exposure to physiological environments. Long term effects of such deterioration must be established and the mechanisms determined or failures due to spalling of coatings from implant substrates may be predicted.

Long term fatigue studies of the various surface active glass and glass-ceramic coatings are also yet to be completed in either *in vitro* or *in vivo* tests. Because the coated metal system is a composite, the fracture mechanics testing is not simple and long term cyclic loading to determine fatigue limits similar to the procedures used for metals will probably have to be adopted. The stability and durability of the bioglass to bone bond appears to be satisfactory in all short term, <2 1/2 years, tests run so far. Only one baboon, with a functional bioglass graft replacing a mandibular resection has been observed for as long as six years. No problems are apparent at the bone-bioglass interface or the bioglass-gingival tissue interface, see Fig. 13. A series of long term primate femoral head replacements using the 52S4.6 bioglass coated Vitallium system seems indicated.

Since initial stabilization of the implant to be maintained in fixation with a surface active coating is by firm mechanical immobilization at the time of surgery, device design and surgical technique becomes critical and maybe even self limiting. A procedure where bioactive cement is applied in a small quantity only at a critical site at the area of the trochanter may serve as a compromise. A thorough reexamination of the biomechanics of the prostheses system to take maximal advantage of the bone-bonding coatings will obviously be required. The reported success of the recent Muller femoral stem which does not use PMMA indicates that a new generation of device design is possible. The success of the bone bonding coatings merged with device design and assurance of the elimination of a new type of fatigue problem may well indicate that a viable alternative to current procedures relying on *in situ* polymerization of PMMA may be possible.

REFERENCES

1. L. Smith, Arch. Surg., 87, 650 (1963).

2. G. Ross in "Use of Ceramics in Surgery," S.F. Hulbert and F.A. Young, eds., Gordon and Breach, New York (1970).

3. F.W. Rhinelander, "Microvascular and Histologic Effects of Implantation of Cerosium into Bone," a preliminary report submitted to Haeger Potteries, Dundee, Ill.

4. R.P. Welsh and Ian MacNab, J. Biomed. Mater. Res. Symp., 2, 231-249 (1971).

5. a. J.J. Klawitter and S.F. Hulbert, J. Biomed. Mater. Res. Symp., 2, 161-229 (1971).

   b. S.F. Hulbert and J.J. Klawitter, Mat. Res. Bull., 7, 1239-1246 (1972).

6. a. S.F. Hulbert, et al., J. Biomed. Mater. Res. Symp., 4, 1-23 (1973).

   b. S.F. Hulbert, S.J. Morrison and J.J. Klawitter, J. Biomed. Mater. Res., 6, 347-374 (1972).

7. P. Boutin, "Biomechanical Study of 590 Cases of Total Hip Arthroplasty by Means of an Alumina-Alumina Prosthesis (April 1970-April 1975)," presented at the 8th Annual Internation Biomaterials Symp. (1976).

8. J.C. Bokros, L.D. LaGrange and F.J. Schoen in "Chemistry and Physics of Carbon," P.L. Walker, ed., Vol. 9, Dekker, New York (1972) 103-171.

9. J.C. Bokros, et. al., "Carbon in Prosthetic Devices," ACS Symp. Series, No. 21, 237-265 (1975).

10. a. L.L. Hench and E.C. Ethridge in "Advances in Biomedical Engineering," J.H.U. Brown and J.F. Dickson, eds., Academic Press, N.Y. (1975) 36-139.

    b. L.L. Hench in "Annual Review of Materials Science," R.A. Huggins, R.H. Rube, R.W. Roberts, eds., Annual Reviews, Inc., Palo Alto, Calif. (1975) 279-300.

11. L.L. Hench in "Orthopedic Mechanics," D. Ghista, ed., Academic Press, in press (to be published in 1978).

12. S.D. Davis, J. Biomed. Mater. Res., 6, 425 (1972).

13. Flexi Escalas, et al., J. Biomed. Mater. Res., 10, 175-195 (1976).

14. A.F. Hegyeli and R. Johnson, J. Biomed. Mater. Res. Symp., 1, 1 (1971).

15. H. Kawahara in Proceedings of the Japan Society of Implant Dentistry, August 1975, 205-246.

16. H. Kawahara in Proceedings of the Japan Society of Implant Dentistry, August 1975, 187-205.

17. R.B. Leonard, et al., J. Biomed. Mater. Res. Symp., 4, 85-95 (1973).

18. a. E.W. White, et al., J. Biomed. Mats. Res. Symp., 6, 23-27 (1975).

    b. R.T. Chiroff, et al., J. Biomed. Mater. Res., 9, 29-45 (1975).

    c. E.W. White, et al., J. Biomed. Mater. Res., 9, 23-28 (1975).

19. a. P. Griss, et al., J. Biomed. Mater. Res. Symp., 4, 453-462 (1978).

    b. P. Griss, et al., J. Biomed. Mater. Res. Symp., 5, 39-48 (1974).

    c. P. Griss, B. Krempien, H.V. Andrian-Werburg, A. Orthop., 112, 1157-1161 (1974).

    d. P. Griss, et al., J. Biomed. Mater. Res., 9, 177-188 (1975).

20. a. J.T. Frakes, S.D. Brown and G.H. Kenner, Amer. Ceram. Soc. Bull., 53, 183-187 (1974).

    b. G.D. Schnittgrund, G.H. Kenner, and S.D. Brown, J. Biomed. Mater. Res. Symp., 4, 435-452 (1973).

21. a. S.F. Hulbert, J.J. Klawitter, C.D. Talbert and C.T. Fitts, in "Research in Dental and Medical Materials," K. Korostoff, ed., Plenum Press, New York (1969).

    b. S.F. Hulbert, et al., J. Biomed. Mater. Res., 4, 433 (1970).

22. G.A. Graves, et al., J. Biomed. Mater. Res. Symp., 2, 91-115 (1971).

23. a. T.D. Driskell, et al., J. Biomed. Mater. Res. Symp., 2, 345-361 (1971).

    b. T.D. Driskell, A.L. Heller, J.F. Koenig, "The Efficacy and Safety of Resorbable Tricalcium Phosphate Ceramic Implants," to be published.

24. M.P. Levin, L. Getter, and D.E. Cutright, J. Biomed. Mater. Res., 9, 183-195 (1975).

25. L.L. Hench, et al., J. Biomed. Mater. Res., 2, 117-141 (1971).

26. L.L. Hench and H.A. Paschall, J. Biomed. Mater. Res., 4, 25-42 (1973).

27. L.L. Hench, Medical Instrumentation, 1, 136-144 (1973).

28. L.L. Hench and H.A. Paschall, J. Biomed. Mats. Res., 5, 49-64 (1974).

29. G. Piotrowski, L.L. Hench, W.C. Allen and G.J. Miller, J. Biomed. Mater. Res. Symp., 9, 47-61 (1975).

30. A.E. Clark, L.L. Hench and H.A. Paschall, "The Influence of Surface Chemistry on Implant Interface Histology: A Theoretical Basis for Implant Materials Selection," J. Biomed. Mater. Res., 10, 161-174 (1976).

31. L.L. Hench, H.A. Paschall, W.C. Allen and G. Piotrowski, National Bureau of Standards Special Publication 415, 19-35 (1975).

32. A.E. Clark, Jr., C.G. Pantano, Jr., and L.L. Hench, J. Am. Ceram. Soc., 59, 37-39 (1976).

33. L.L. Hench, "Characterization of Glass Corrosion and Durability," J. Non-Crystalline Solids, 19, 27-39 (1975).

34. a. B.-A. Blencke, H. Bromer, E. Pfeil, and H.H. Kas, Implantate aus Glaskeramik in der Knockenchirurgie (Tierexperimentelle Untersuchunger). Langenbecks Arch. Klin, Chir., Chir. 116 bis 119, Forum (1973).

b. B.-A. Blencke, H. Bromer, E. Pfeil, Rasterelektronenmikroskopische Untersuchungen der Reaktion des Knochens auf glaskeramische Implantate, Z. Orthop. 112, 978-980 (1974).

35. V.V. Strunz, et. al., Dtsch. zahnarztl. Z. 31, 69-70 (1976).

36. H. Aoki, et al., 1975 Symp. on Biomats., Kyoto Univ., Ktoyo, Japan, August 29-30, 1975.

37. M. Jarcho, J.F. Kay, K.I. Gumaer, R.H. Doremus and H.P. Drobeck, "Tissue Cellular and Subcellular Events at a Bone-Ceramic Hydroxylapatite Interface," J. Bioengineering, 1, 79-92 (1970).

38. M. Jarcho, V. Jasty, K.I. Gumaer, J.F. Kay and R.H. Doremus, "Electron Microscopic Study of a Bone-Hydroxylapatite Implant Interface," Paper 71, Transactions 4th Annual Meeting of the Society for Biomaterials, San Antonio, Texas, April 29-March 2, 1978.

39. J.F. Kay, R.H. Doremus, and M. Jarcho, "Ion Micromilling of Bone-Implant Interfaces," Paper 114, Transactions 4th Annual Meeting of the Society for Biomaterials, San Antonio, Texas, April 29-March 2, 1978.

40. P. Griss and G. Jentschura, "Clinical Experience with Two Composite Ceramic-Metal Hip Prostheses," presented at the 2nd Annual Meeting of the Society for Biomaterials, Philadelphia, April 9-13, 1976.

41. P. Griss, Private Communication.

42. P. Griss, D.C. Greenspan, G. Heimke, B. Krempien, R. Buchinger, L.L. Hench and G. Jentschura, "Evaluation of a Bioglass Coated Al_2O_3 Total Hip Prosthesis in Sheep," J. Biomed. Maters. Res., 10, No. 4, 511-518 (1976).

44. L.L. Hench, C.G. Pantano, P.J. Buscemi and D.C. Greenspan, "Analysis of Bioglass Fixation of Hip Prostheses," J. Biomed. Maters. Res., 11, No. 2, 267-281 (1977).

45. J.R. Smith, "Bone Dynamics Associated with a Controlled Loading of Bioglass Coated Alumina-Oxide Endosteal Implants," Masters Thesis, University of Washington, 1977.

46. J.E. Ritter, Jr., D.C. Greenspan, R.A. Palmer, and L.L. Hench, "Use of Fracture Mechanics Theory in Lifetime Predictions for Alumina and Bioglass-Coated Alumina," accepted for publication by J. Biomed. Materials Research, 1978.

47. D.E. Clark, M.C. Madden and L.L. Hench, "Development of Bioglass Coatings for Vitallium Prosthetic Devices," U.S. Army Report No. 8, "An Investigation of Bonding Mechanisms at the Interface of a Prosthetic Material," December 1977, pp. 68-77.

48. a. Engelhardt, Komitowski, Heipertz, Zeitz, and Hoffman, "Histological Findings Concerning the Reaction of Implants with Selected Ceramic Coatings," presented at the 2nd Annual Meeting of the Society for Biomaterials, April 9-13, 1976, Philadelphia.

    b. A. Engelhardt, M. Salzer, A. Zeibig, and H. Locke, J. Biomed. Mater. Res., 6, 227-232 (1975).

49. M. Selitsch, M. Lehmann, E. Doerre, and H.G. Willert, "New Prospects for a Longer Service Life of Artificial Hip Joints Using a Polyethylene/Al_2O_3 Ceramic/Metal Combination," presented at the 2nd Annual Meeting of the Society for Biomaterials, April 9-13, 1976, Philadelphia.

50. E.J. Eyring, "High Density Aluminum Oxide--Orthopedic Uses," presented at the 2nd Annual Meeting of the Society for Biomaterials, April 9-13, 1976, Philadelphia.

51. H. Plenk, Jr., H. Locke, G. Punzet, M. Salzer and K. Sweymuller, "Attachment of Ceramic Endoprostheses to the Exterior of Long Bones without the use of Bone Cement, II. Histomorphometrical Analysis of Bone Reactions," presented at the 2nd Annual Meeting of the Society for Biomaterials, April 9-13, 1976, Philadelphia.

52. C.L. Stanitski and V. Mooney, J. Biomed. Mater. Res. Symp., 4, 97-108 (1973).

53. V. Mooney, et al., J. Biomed. Mater. Res. Symp., 2, 143-159 (1971).

54. C.W. Hall, W. Mallow, and F. Hose, "Progress Toward A Permanent Skeletal Extension," presented at the 2nd Annual Meeting of the Society for Biomaterials, April 9-13, 1976, Philadelphia.

55. L. Cini, F. Gasparini, S. Mitchieli, A. Pizzoferrato, and S. Sandrolini-Cortesi, "Impianti dentari metallici riverstiti di ceramica, Min. Stom., 24, 75-90, (1975).

56. S.M. Weiderhorn, "Subcritical Crack Growth in Ceramics," in Fracture Mechanics of Ceramics, Vol 2, ed. by R.C. Bradt, D.P.H. Hasselman, and F.F. Lange, Plenum Press, New York, 1974.

57. J.E. Ritter, Jr. and J.A. Meisel, J. Am. Ceram. Soc., 59, 478 (1976).

58. J.E. Ritter, Jr., "Engineering Design and Fatigue Failure of Brittle Materials," Fracture Mechanics of Ceramics, Vol. 4, edited by R.C. Bradt, D.P.H. Hasselman, and F.F. Lange, Plenum Press, New York, 1978.

H. FUTURE DEVELOPMENTS AND APPLICATIONS OF BIOMATERIALS: AN OVERVIEW

by

L.L. Hench

ABSTRACT

It is recommended that the emphasis of biomaterials research and development for the future should be to achieve improved reliability. Use of increasing numbers of implants per year coupled with decreasing long term (> 5 years) success rates are resulting in progressively larger numbers of reparative implant operations. This trend can be altered by emphasizing three areas of R&D: 1) Studies of composite biomaterial systems offering unique combinations of biological surface behavior and substrate mechanical performance; 2) Investigate mechanisms of interfacial reactions so that long term responses of the host-implant can be predicted; 3) Develop long term predictive relationships for biomaterials reliability based upon interfacial reactions, biomechanics, fracture mechanics, fatigue testing, and retrieval analysis.

Brief examples of efforts to develop understanding in these three areas are described using bioglass coated metal and bioglass coated alumina implants.

INTRODUCTION

During the last 15 years there has been dramatic change in the field of biomaterials. Change in the clinical importance of prosthetic devices, change in the demands placed upon biomaterials used in devices, and change in the research approach required to acheive further improvements in biomaterials and device performance. The field has grown to where it is estimated that 2-3 x 10^6 prosthetic devices per year are presently being implanted in the U.S. and Europe. Short term, < 5 years, success rates of 85-98% reported for most prostheses are so encouraging that there exists a large driving force from both the clinician and patient for prostheses to be used in even larger numbers in the future: 1) a broadening range of symptom severity for a patient to be a candidate for prostheses; 2) use of prostheses in progressively younger patients; 3) an increase in number of clinicians who feel confident to use implants; and 4) use of prostheses in new clinical applications. Each of the above factors imposes increased severity in the performance demands on the biomaterials used in the prostheses. Thus, a prime, if not overriding, emphasis of biomaterials R&D for the future in to achieve improved reliability.

To emphasize long term reliability is a major change for a field that has tended to concentrate upon very short term (< 2 years) screening of large numbers of new types of biomaterials. Previously, the dominant theme in the biomaterials literature has been short term

studies of mechanical performance or tissue response to different material composition, microstructure, porosity, surface finish or chemistry, and sample configuration. The motivation for such studies often appears to be that they are easy to design, the materials easy to fabricate in small configurations and quantities, the small animals are easy to maintain, and the costs are low.

In contrast, design and implementation of long term (> 2 years) investigations of functional devices is difficult and costly. Design and fabrication of devices for animals that will provide the desired function is complicated. Surgical techniques and post-op maintenance of animals with functional devices is usually significantly more difficult than equivalent human requirements. Decisions regarding number of devices per animal, number of animals per time period, duration sequence, and method for time dependent monitoring of function usually involve considerable compromise with respect to the financial investment available. Post sacrifice evaluation protocol also requires a compromise because mechanical testing destroys the tissue-material interface. Thus, it is difficult to achieve data needed for both the engineer and histologist in statistical quantity. The extent of data and even type of data necessary to satisfy regulatory requirements is also often uncertain.

It is especially important to plan now for long term reliability research because there is increasing evidence that the long term (> 5 years) success rates for many prosthetic devices is considerably less than 75%. Specific data on long term success rates is difficult to compile and assess because of several factors: 1) patient follow-up is progressively more difficult with increasing time; 2) changes in biomaterials specifications, device design, surgical technique, and post-op maintenance make it difficult to correlate results over long periods of time; 3) the largest fraction of devices have been implanted during the last five years; and 4) many of the long term implants have been a result of extremely careful patient selection, meticulous surgical technique and conservative post-operative care and, therefore, do not necessarily represent the majority of cases being performed today.

Decreasing long term success rates coupled with an increasing number of implants per year will obviously result in a progressively larger and larger fraction of reparative operations on progressively older patients. Such reparative operations are generally more difficult technically, less amenable to use of generalized procedures and devices, and are complicated by more extensive tissue damage associated with the implant failure. These factors coupled with the increased age of the patient and negative psychological consequences of a previous implant failure all serve to reduce the probability of success in reoperative cases. It is also apparent that reoperative cases generally require the services of the more specialized and capable implant surgery teams and can consume a progressively larger fraction of their time and facilities. Saturation of highly competent implant teams is a very real possibility in the next decade. Consequently, reduction of the need for reoperative surgery by emphasis on improved reliability of the implant-tissue system seems to be of paramount importance.

Therefore, increasing demands for improved long term reliability of biomaterials and implant devices versus the difficulty and costs of studying long term performance require at this time a close re-examination of the approaches taken in biomaterials research and development.

RESEARCH AND DEVELOPMENT EMPHASIS

1) One of the primary areas that should be emphasized in biomaterials R&D is that of composite materials systems. It has become clear that the rigorous mechanical and biological requirements of most devices cannot be satisfied with a single material. Composites designed for simultaneous satisfaction of biological surface compatibility and performance with stable mechanical behavior of the bulk structure offer high promise for long term reliability. Thin film ULTI carbon coatings of flexible cardiovascular components recently described by Bockros, et al. in a Biomaterials Symposium at UCLA December 29, 1978, serve as an excellent example of the use of coatings technology to modify the surface performance of a variety of materials without changing the mechanical characteristics. Bioglass coatings on surgical metal alloys or on high strength alumina ceramics also illustrate combinations of a controlled biological interface with high strength substrate performance.

2) The second area that is recommended for intensive investigation is the study of mechanisms of interfacial reactions. Either the interface between tissue and implant surface or the interface between phases in a composite, such as a coating and substrate, are potential weak links in the long term reliability of functional devices. Only by a thorough study of the kinetics and mechanisms of interfacial reactions will it be possible to determine why failure occurs. Knowledge of failure mechanisms is essential in designing devices that minimize failure conditions. Likewise, prediction of reliability of a biomaterial/device under function requires understanding the modes of failure of the tissue-implant system.

In the past only minimal effort has been applied to studying the complex combinations needed to elucidate mechanisms of failure. It is difficult to establish cause and effect relationships operative over the long term, but without emphasizing mechanistic studies it will not be possible to proceed past the stage of trial and error experiments in patient populations.

3) It is proposed that the ultimate objective of the present generation of biomaterials R&D be directed towards developing a comprehensive theory of predictive relationships for the long term performance of the implant-host system. Components for achieving such relationships include: a) mechanisms and kinetics of interfacial reactions; b) use of biomechanics techniques, such as finite element stress analysis, to describe the anticipated stress-tissue cycles to be applied to functional devices and define reasonable safety margins of stress; c) expand and apply appropriate fracture mechanics theories for brittle materials to predict the expected lifetimes of implants loaded to given stress

levels; d) collaborate with the fracture mechanics R&D community to extend lifetime predictive theories to include visoelastic materials such as bone and polymeric materials, plastically deforming metallic components, and combinations thereof with variable degrees of interfacial attachment between the materials and between materials and tissue; e) develop accelerated fatigue tests of simple sample configurations and devices that are representative of in-vivo conditions; f) establish methods to correlate predictive relationships with implant retrieval analyses.

EXAMPLES OF RELIABILITY RELATED RESEARCH

Recent studies of controlled surface reactive glasses have been directed along the lines recommended above. Extensive efforts have been made to achieve reliable composite materials comprised of either bioglass coated surgical metal alloys or bioglass coated high density alumina. The processing steps involved and the systems design approach taken in achieving the coated materials are described elsewhere (1-4).

Coatings of 45S5 Bioglass on 316L stainless steel femoral head replacements tested in monkeys have been shown to result in formation of a bond with bone at the coating-bone interface (5). Likewise, coatings of 45S5 Bioglass on high purity alumina (6) have resulted in an interfacial bone-coating bond (7).

Mechanical testing of the bone-coating implant substrate has shown that interfacial bond strength between bone and coating can be equivalent to the fracture strength of natural bone (8,9). However, failure either within the bioglass or at the bioglass-substrate interface may limit the strength of the composite system (8,9).

Figures 1 and 2 illustrate the type of mechanical test used to establish that the strength of the bulk 45S5 Bioglass was a limiting factor in load bearing applications. A functional, load bearing segmental bone replacement was used in a monkey femoral model. An intermedullary nail, Figure 1, provided alignment and stabilization of the device during healing. The sequence of radiographs of Figure 1 illustrate progressive stages of healing and callous remodeling of one of the monkey femora containing the 45S5 segmental bone replacement. After remodeling was completed via radiography, the IM nail was removed post sacrifice, any residual callous superficial to the implant was excised and the bone-implant system was tested to failure in torsion (10). Figure 2 shows a failure mode that established the unacceptable reliability of the bulk 45S5 Bioglass material for use as a functional, load bearing orthopaedic device. The implant-bone interface was never observed to fail, even under interfacial stresses in excess of 10,000 psi. However, as in the example of Figure 2, numerous implants failed at stresses less than that of either the bone or the bonding interface (10). Thus, establishing that the "weak link" in the reliability of the new biomaterial was bulk strength of the glass, it was apparent that developing composites using coatings of the controlled surface reactive glasses on substrates of significantly higher mechanical strength was the only means of achieving the required long term performance of the

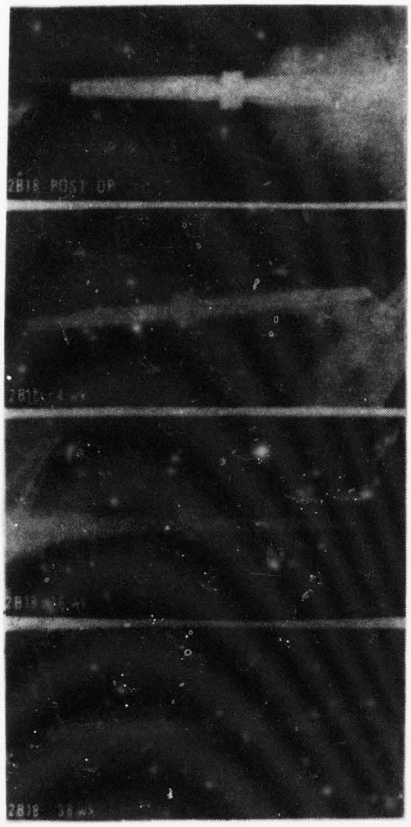

Fig. 1. X-rays of time sequence of segmental bone replacement of 45S5 Bioglass in monkey femur.

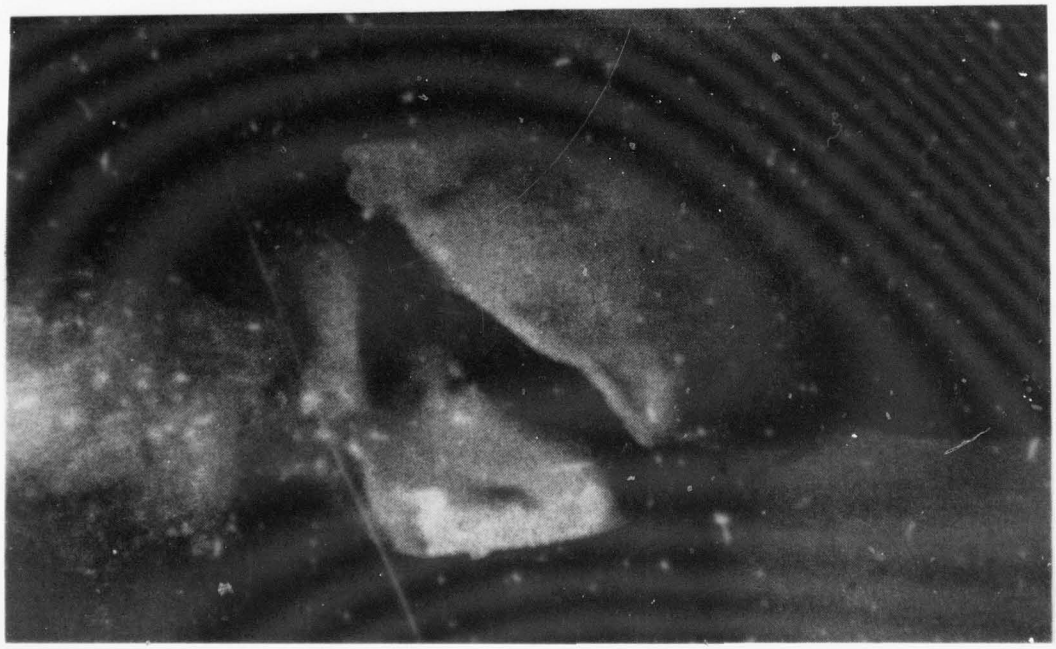

Fig. 2. Torsional fracture of monkey femur - 45S5 Bioglass segmental bone replacement.

AD-A077 052 FLORIDA UNIV GAINESVILLE F/G 6/5
AN INVESTIGATION OF BONDING MECHANISMS AT THE INTERFACE OF A PR--ETC(U)
DEC 78 L L HENCH , R W PETTY , G PIOTROWSKI DAMD17-76-C-6033
UNCLASSIFIED NL

3 OF 3
AD A077052

END
DATE FILMED
12-79
DDC

prostheses. Similar types of mechanical testing of the bioglass coated implant systems are now in progress using both canine segmental and monkey femoral head replacement models.

An illustration of the type of testing that can be employed to evaluate the long term chemical stability of an interface bonded to bone is presented in Figures 3 and 4. Figure 3 shows a scanning electron micrograph of a 45S5 Bioglass implant bonded to a rat tibia after one year. The bonding interface is labeled as I, osteocytes are labeled O, the bulk bioglass as G and an electron microprobe trace across the interface is labeled M. The compositional analysis of the bonded interface obtained by the electron microprobe is shown in Figure 4 (10). Compositional regions characteristic of bulk bioglass, silica-rich amorphous gel, the calcium-phosphate rich layer that bonds with mucopolysaccharides and collagen and finally bone are evident in Figure 4.

Use of this technique to follow the change in interfacial compositions as a function of time show that the bonding interface matures during a period of 3-6 months and undergoes little change thereafter for periods of more than 2 years. Consequently, this type of time dependent analysis can be used to achieve an understanding of the reliability of bonding interfaces.

Fig. 3. Scanning electron micrograph of bonded interface between 45S5 Bioglass and rat tibia after 1 year. (190X)

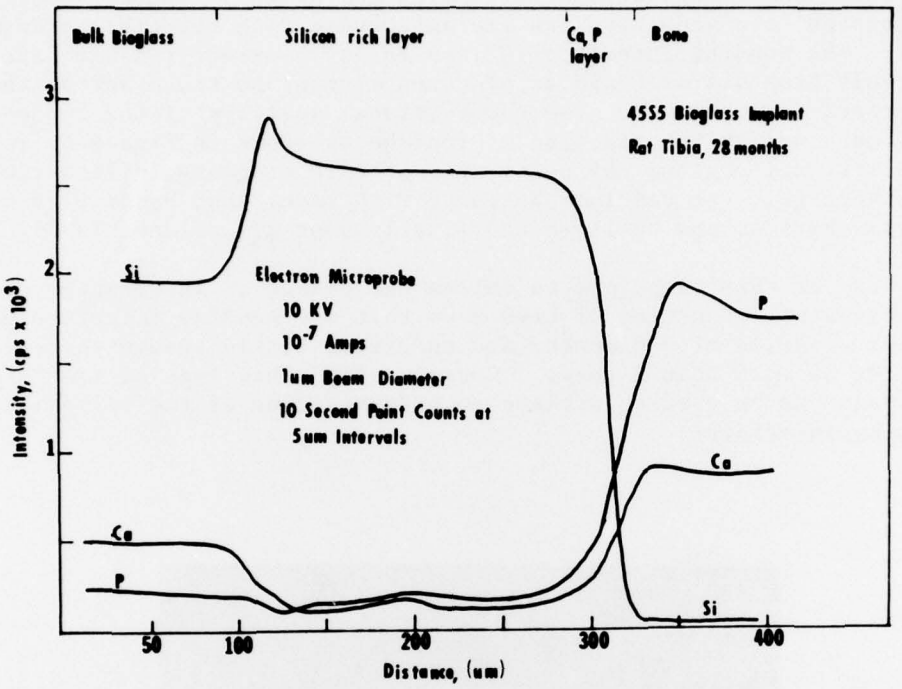

Fig. 4. Electron microprobe compositional analysis of the bonded interface shown in Figure 3.

REFERENCES

1. L.L. Hench, "The Processing of Bioceramics," Ceramurgia International, Vol. VII, No. 5 (1977) 252-266.

2. L.L. Hench and D.C. Greenspan, "Bioglass Coated Al_2O_3 Ceramics," U.S. Patent Application #4,103,002, July 1978.

3. L.L. Hench and P.J. Buscemi, "A Method of Bonding a Bioglass to Metal and Product Produced Thereby," U.S. Patent Application #798,671.

4. L.L. Hench, "Development of a New Biomaterial--Prosthetic Device," Orthopedic Mechanics: Procedures and Devices, (D.H. Ghista and R. Roaf, eds.) Academic Press, Inc., London (1978) 287-316.

5. L.L. Hench, C.G. Pantano, Jr., P.J. Buscemi and D.C. Greenspan, "Analysis of Bioglass Fixation of Hip Prostheses," J. Biomed. Maters. Res., 11, No. 2 (1977) 267-281.

6. D.C. Greenspan and L.L. Hench, "Chemical and Mechanical Behavior of Bioglass Coated Alumina," J. Biomed. Maters. Res., 10, No. 4 (1976) 503-509.

7. P. Griss, D.C. Greenspan, G. Heimke, B. Krempien, R. Buchinger, L.L. Hench and G. Jentschura, "Evaluation of a Bioglass Coated Al_2O_3 Total Hip Prosthesis in Sheep," J. Biomed. Maters. Res., 10, No. 4 (1976) 511-518.

8. L.L. Hench, "Bioceramics," Science of Ceramics, 9 (1977) 193-211.

9. G. Piotrowski, L.L. Hench, W.C. Allen and G.J. Miller, "Mechanical Studies of the Bone-Bioglass Interfacial Bond," J. Biomed. Maters. Res., 9 [6] (1975) 47-61.

10. M.S. Harrell, M.A. Keane, W.A. Acree, S.R. Bates, A.E. Clark and L.L. Hench, "Thickness of Bioglass Bonding Layers," 4th Annual Meeting of the Society for Biomaterials, San Antonio, Texas, Abstract No. 8, (1978) 111.

DISTRIBUTION LIST

Commanding General U.S. Army Medical Research and Development Command ATTN: MEDDH-SI Washington, D.C. 20314	4
Defense Documentation Center ATTN: DDCIR Cameron Station Alexandria, Virginia 22314	12
Commanding Officer U.S. Army Combat Development Command Medical Service Agency Brooke Army Medical Center Fort Sam Houston, Texas 78231	1
National Institute of Dental Research Dental Materials Science Bethesda, Maryland 20014	1
NASA Materials Science Division Washington, D.C. 20546	1
Army Research Office - Durham Metallurgy and Ceramics Division Durham, North Carolina 27709	1
National Institutes of Health Division of Orthopaedics Bethesda, Maryland 20014	1
Defense Ceramic Information Center Battelle Memorial Institute 505 King Avenue Columbus, Ohio 43201	1
National Institutes of Health National Institute of General Medical Sciences Bethesda, Maryland 20014	1
Colonel Simon Civjan, DC Dental Detachment Ft. Leonard Wood, Missouri 65473	1
Air Force Office of Scientific Research Chief, Chemistry Division Bolling Air Force Base, D.C. 20332	1